การพัฒนาวิธีวิเคราะห์แบบไม่ใช้เซลล์เพื่อคัดกรองสารที่มีฤทธิ์ยับยั้งนิวรามินิเดส ของไวรัสไข้หวัดนก

นางสาว จรินรัตน์ คงกำเหนิด

วิทยานิพนธ์นี้เป็นส่วนหนึ่งของการศึกษาตามหลักสูตรปริญญาวิทยาศาสตรดุษฎีบัณฑิต
สาขาวิชาเภสัชเวท ภาควิชาเภสัชเวทและเภสัชพฤกษศาสตร์
คณะเภสัชศาสตร์ จุฬาลงกรณ์มหาวิทยาลัย
ปีการศึกษา 2553

DEVELOPMENT OF NON-CELL BASED ASSAYS FOR SCREENING OF INHIBITORS AGAINST AVIAN INFLUENZA NEURAMINIDASE

Miss Jarinrat Kongkamnerd

A Dissertation Submitted in Partial Fulfillment of the Requirements
for the Degree of Doctor of Philosophy Program in Pharmacognosy
Department of Pharmacognosy and Pharmaceutical Botany
Faculty of Pharmaceutical Sciences
Chulalongkorn University
Academic year 2010

Thesis Title	DEVELOPMENT OF NON-CELL BASED ASSAYS FOR SCREENING OF INHIBITORS AGAINST AVIAN INFLUENZA NEURAMINIDASE
By	Miss Jarinrat Kongkamnerd
Field of Study	Pharmacognosy
Thesis Advisor	Associate Professor Wanchai De-Eknamkul, Ph.D.
Thesis Co-Advisor	Assistant Professor Wanchai Assavalapsakul, Ph.D.

Accepted by the Faculty of Pharmaceutical Sciences, Chulalongkorn University in Partial Fulfillment of the Requirements for the Doctoral Degree

..... Dean of the Faculty of Pharmaceutical Sciences

(Associate Professor Pintip Pongpech, Ph.D.)

THESIS COMMITTEE

..... Chairman

(Professor Kittisak Likhitwitayawuid, Ph.D.)

..... Thesis Advisor

(Associate Professor Wanchai De-Eknamkul, Ph.D.)

..... Thesis Co-Advisor

(Assistant Professor Wanchai Assavalapsakul, Ph.D.)

..... Examiner

(Assistant Professor Suchada Sukrong, Ph.D.)

..... External examiner

(Orawan Monthakantirat, Ph.D.)

จรินรัตน์ คงกำเหนิด : การพัฒนาวิธีวิเคราะห์แบบไม่ใช้เซลล์เพื่อคัดกรองสารที่มีฤทธิ์ยับยั้งนิวรามินิเดสของไวรัสไข้หวัดนก (DEVELOPMENT OF NON-CELL BASED ASSAYS FOR SCREENING OF INHIBITORS AGAINST AVIAN INFLUENZA NEURAMINIDASE) อ. ที่ปรึกษาวิทยานิพนธ์หลัก : รศ.ดร. วันชัย ดีเอกนามกูล, อ. ที่ปรึกษาวิทยานิพนธ์ร่วม : ผศ. ดร. วันชัย อัศวลาภสกุล, 130 หน้า.

การคัดกรองสารที่มีฤทธิ์ยับยั้งนิวรามินิเดสของไวรัสไข้หวัดนกโดยทั่วไป ยังจำกัดเฉพาะในห้องปฏิบัติการชีวนิรภัยระดับ 3 เนื่องจากต้องนำนิวรามินิเดสที่ได้จากการเพาะเชื้อไวรัสไข้หวัดนกซึ่งเป็นเชื้อก่อโรคชนิดรุนแรงมาใช้ในการทดสอบ ดังนั้นจึงมีความจำเป็นในการพัฒนาวิธีวิเคราะห์ที่มีความปลอดภัยและสามารถใช้ในห้องปฏิบัติการทั่วไป เพื่อคัดกรองสารที่มีฤทธิ์ยับยั้งนิวรามินิเดสของไวรัสไข้หวัดนกได้อย่างสะดวกและมีประสิทธิภาพ งานวิจัยครั้งนี้จึงมีการประยุกต์ใช้รีคอมบิแนนท์เอนไซม์นิวรามินิเดส 2 ชนิด จากเชื้อไข้หวัดนกสายพันธุ์ H7N1 และ H7N3 รวมทั้งนิวรามินิเดสของเชื้อ H5N1 ที่ได้จากการทำให้เชื้อไข้หวัดนกอ่อนแรงลง เป็นแหล่งของเอนไซม์สำหรับใช้คัดกรองสาร โดยวิธีการวิเคราะห์ดังกล่าวอาศัยคุณสมบัติการเรืองแสงของผลิตภัณฑ์ที่เกิดจากปฏิกริยาระหว่างสารตั้งต้นและเอนไซม์ วิธีนี้ถือเป็นวิธีที่มีความไวสูงโดยมีความสามารถวัดผลิตภัณฑ์ที่เกิดขึ้นในระดับนาโนโมลาร์ โดยวิธีการวิเคราะห์ที่พัฒนาขึ้นได้ถูกนำมาใช้ทดสอบกับอนุพันธ์ของ oseltamivir ที่ถูกสังเคราะห์ขึ้น 5 ชนิดและสารฟลาโวนอยด์ 35 ชนิดที่สกัดได้จากพืชสมุนไพรไทย *Dalbergia parviflora และ Belamcanda chinensis* ผลการวิจัยพบว่าสารสังเคราะห์ PMC-35 ให้ฤทธิ์ในการยับยั้งเอนไซม์นิวรามินิเดสของ H7N3 ได้ดีกว่า oseltamivir ส่วน PMC-36 ให้ฤทธิ์ในการยับยั้งเอนไซม์นิวรามินิเดสของ H7N1 ได้ดีที่สุด สำหรับเอนไซม์นิวรามินิเดสของ H5N1 นั้นพบว่า PMC-35 และ PMC-36 ให้ผลในการยับยั้งได้ใกล้เคียงกับ oseltamivir ในสารกลุ่มฟลาโวนอยด์นั้น พบว่าฤทธิ์ในการยับยั้งเอนไซม์นิวรามินิเดสอยู่ในระดับไมโครโมลาร์ แต่เป็นที่น่าสนใจว่าโครงสารของฟลาโวนอยด์สามารถรบกวนการวัดผลการวิเคราะห์ ส่งผลให้การรายงานฤทธิ์ในการยับยั้งนิวรามินิเดสอาจสูงกว่าความเป็นจริงได้ ดังนั้นหากต้องคัดกรองสารที่มีฤทธิ์ยับยั้งนิวรามินิเดสของไวรัสไข้หวัดนกในสารกลุ่มนี้ ควรมีการทดสอบ หา Quenching effect ร่วมด้วยเพื่อให้ผลการทดสอบมีความถูกต้องมากยิ่งขึ้นสำหรับสารในกลุ่มนี้

ภาควิชา เภสัชเวทและเภสัชพฤกษศาสตร์ ลายมือชื่อนิสิต จรินรัตน์ คงกำเหนิด

สาขาวิชา เภสัชเวท ลายมือชื่อ อ.ที่ปรึกษาวิทยานิพนธ์หลัก

ปีการศึกษา 2553 ลายมือชื่อ อ.ที่ปรึกษาวิทยานิพนธ์ร่วม

4976559033 : MAJOR PHARMACOGNOSY
KEYWORDS : AVIAN INFLUENZA VIRUS / NEURAMINIDASE / NON-CELL BASED ASSAYS

JARINRAT KONGKAMNERD: DEVELOPMENT OF NON-CELL BASED ASSAYS FOR SCREENING OF INHIBITORS AGAINST AVIAN INFLUENZA NEURAMINIDASE. THESIS ADVISOR: ASSOC. PROF. WANCHAI DE-EKNAMKUL, Ph.D., THESIS CO-ADVISOR: ASST. PROF. WANCHAI ASSAVALAPSAKUL, Ph.D., 130 pp.

A screening for avian influenza neuraminidase inhibitors is presently limited to be operated only in the biosafety level-3 laboratory. This is due to the use of high virulence strains of avian influenza virus as a direct source of neuraminidase enzymes in the screening assay. It is, therefore, necessary to develop new screening methods with high safety and efficiency for being used in a general laboratory in order to speed up the seach for new neuraminidase inhibitors. In this research work, two recombinant neuraminidases obtained from H7N1, H7N3, and a viral neuraminidase from inactivated H5N1 were used as the safe enzyme sources for screening. This assay is based on the use of florescence method which is highly sensitive with the limit of detection at the level of as low as nanomolar scale. Various compounds, including 5 synthetic oseltamivir analogs and 35 naturally occurring flavonoids from Thai medicinal plants: *Dalbergia parviflora* and *Belamcanda chinensis* were tested for their potential inhibitory activities. The results showed that the analog PMC-35 exhibited higher inhibitory activity against H7N3 neuraminidase than oseltamivir, the analog PMC-36, on the other hand, exhibited its highest activity against that of H7N1 whereas both analogs gave similar activity to oseltamivir in inhibiting H5N1 neuraminidase. For the natural flavonoids, the inhibitory activity on the neuraminidases appeared to be weaker in micromolar level range. However, it was found, interestingly, that the structures of flavonoids themselves had a quenching effect on the observed inhibitory activity which leads to the overestimated inhibitory efficacy of some compounds. Thus, it is necessary to determine the degree of quenching of each flavonoid in order to obtain accurate inhibitory values of this group of natural products.

Department: Pharmacognosy and Pharmaceutical botany Student's signature

Field of Study: Pharmacognosy Advisor's Signature

Academic Year: 2010 Co-Advisor's Signature

ACKNOWLEDGEMENTS

I am cordially delighted to express my appreciation to my advisor Associate Professor Dr. Wanchai De-Eknamkul, my co-advisor in Italy Dr. Paolo Pengo and my co-advisor Assistant Professor Dr. Wanchai Assavalapsakul for their great understandings, excellent counsels, encouragements, guidance and supporting throughout this thesis. Without their kindness and understanding, this work could not have been accomplished.

My thankfulness is also expressed to Dr Giorgio Fassina and all members in Xeptagen S.p.A., for valuable comments and many chemical reagents and also their great friendships I had received.

I would like to thank Pharmaceutical Research Instrument Center, Faculty of Pharmaceutical Sciences, Chulalongkorn University, for supporting the instruments throughout this study.

In addition, I also would like to express my deeply indebted and special appreciation to Professor Dr. Kittisak Likhitwitayawuid, Assistant Professor Dr. Suchada Sukrong and Dr. Orawan Monthakantirat, serving as the members of the doctor committees, for their helpful suggestions and valuable comments.

Eventually, the highest gratitude is expressed to my mother and father for their love, understanding, helping, supporting and encouragement with care which enable me to carry out this study successfully whereas I have spent almost my whole time with this thesis rather than with them.

This work was partially supported by the grants from ICS-UNIDO (subprogram CHM/08/1 Combinatorial Chemistry and Molecular Design), Embassy of Italy in Thailand and Graduate school of Chulalongkorn University.

CONTENTS

Page

LIST OF TABLES

Page

LIST OF FIGURES

Page

Page

LIST OF SCHEMES

LIST OF ABBREVIATIONS AND SYMBOLS

α	= alpha
°C	= Degree Celsius
µl	= microliter
µg	= microgram
µM	= micromolar
nM	= nanomolar
mM	= millimolar
nm	= nanometer
pM	= picomolar
τ_0	= Lifetime of the fluorophore in the absence of quencher
4-MU	= 4-methylumbelliferone
BSA	= Bovine serum albumin
C. perfringens	= *Clostridium perfringens*
$CaCl_2$	= Calcium chloride
CH_3CN	= Acetonitrile
DCM	= Dichloromethane
DMF	= Dimethylformamide
DMSO	= Dimethyl sulfoxide
EtOH	= Ethanol
Et_3SiH	= Triethylsilane
I	= Fluorescence intensities in the presence of quencher
I_0	= Fluorescence intensities in the absence of quencher
HCl	= Hydrochloric acid
hr	= hour(s)
IC_{50}	= 50% inhibitory activity
IR	= Infrared
K_m	= Michealis constant
K_i	= Inhibition constant
K_{sv}	= Stern-Volmer quenching constant
K_q	= Bimolecular quenching constant
$KHCO_3$	= Potassium bicarbonate
KOH	= Potassium hydroxide

min	= Minute
M	= Molar
MES	= 2-N-morpholino-ethanesulfonic acid
MS	= Mass spectrometry
MsCl	= Methanesulfonyl chloride
MUNANA	= 4-methylumbelliferyl-α-D-N-acetylneuraminic acid
NA	= Neuraminidase
$NAHB(Oac)_3$	= Sodium triacetoxyborohydride
$NaHCO_3$	= Sodium bicarbonate
NaN_3	= Sodium azide
NH_4Cl	= Ammonium chloride
NMO	= 4-methylmorpholine 4-oxide
NMR	= Nuclear Magnetic Resonance
Q	= The concentration of quencher
rt	= Room temperature
rv	= Recombinant virus
$SOCl_2$	= Thionyl chloride
PBS	= Phosphate-buffered saline
Pme_3	= Trimethylphosphine
p-TSA	= p- toluene sulfonic
TEA	= Triethylamine
THF	= Tetrahydrofuran
$TiCl_4$	= Titanium tetrachloride
UV	= Ultraviolet

CHAPTER I

INTRODUCTION

Avian influenza is an infectious disease of birds that is caused by influenza virus type A strains. Avian influenza H5 and H7 subtypes are classified as highly pathogenic since there is a high possibility to mutate from mild strain by a wild bird into highly lethal strain in poultry. Human can be infected with highly pathogenic avian influenza virus by close contact with infected poultry or with objects contaminated by their feces. The outbreaks of avian influenza A (H5N1) in Southeast Asia in 2003 are the largest and most severe on record. In the same year, 4 dead humans infected with highly pathogenic avian influenza virus H5N1 have been reported to World Health Organization (WHO). Up to date, 516 human cases in 15 countries around the world have been documented while 306 cases died. In Thailand, 17 deaths from 25 infected cases have been reported (WHO, 2011). Avian influenza virus H5N1 and the problem of its possible reassortment in suitable "mixing vessels" generating new viral strains highly infective for humans is a main concern for the public health. Although so far the cumulative number of confirmed patients is incomparable to the recently emerged H1N1 'swine' influenza, the scientific community agrees that the emergence of a new highly pathogenic H5N1 influenza pandemic is more a real concern (Eichelberger *et al.*, 2008, Russell *et al.*, 2006, Taylor *et al.*, 2010)

Currently, anti-influenza medications consist of two classes of drugs: matrix (M2) protein inhibitors (amantadine and rimantadine) and neuraminidase inhibitors (oseltamivir and zanamivir) (Moscona, 2005). M2 protein inhibitors are specifically active against influenza A; they interfere with the viral uncoating process through a direct interaction with the matrix (M2) protein, which functions as a channel for hydrogen ions (De Clercq, 2006). Neuraminidase inhibitors prevent the removal of the sialic acid (*N*-acetylneuraminic acid) residue from the Glycopeptides receptor by the viral neuraminidase, which would otherwise allow the virus particles to be released from the infected cell thus spreading to neighbouring cells (De Clercq, 2004). As a class,

neuraminidase inhibitors are effective against all neuraminidase subtypes and, therefore, against all strains of influenza. This is a key point in epidemic and pandemic preparedness and an important advantage over the M2 protein inhibitors which are effective only against sensitive strains of influenza A (Moscona, 2005). Among all antiviral drugs, oseltamivir is the only recommended antiviral to treat patients infected with avian influenza (H5N1) including chemoprophylaxis in high-risk exposure populations (Schunemann *et al.*, 2007). An alarming oseltamivir resistance associated to the N294S mutation in neuraminidase has been recently detected in an influenza A (H5N1) infected patient in Egypt prior to oseltamivir treatment (Earhart *et al.*, 2009). Oseltamivir-resistant influenza A (H5N1) with H274Y mutation has also been reported in Vietnamese patients during treatment (de Jong *et al.*, 2005, Le *et al.*, 2005). These findings stress the importance of developing and investigating new putative neuraminidase inhibitors.

Recently, X-ray crystallographic studies of neuraminidase from type A influenza viruses has been revealed that these structures can be divided in two different classes, known as group-1 (comprising N1, N4, N5, N8) and group-2 neuraminidases (comprising N2, N3, N6, N7, N9), according to distinctive structural features near the oseltamivir binding site (Russell *et al.*, 2006). Since currently available neuraminidase inhibitors were targeted against the structures of group-2 neuraminidases, the discovery of the "150-cavity" in group-1 neuraminidases prompted the design the novel neuraminidase inhibitors in order to improve the efficiency of current antiviral treatments. Besides the synthesized compounds, many studies have reported that natural occurring products such as flavonoids also showed potent neuraminidase inhibitory activity (Jeong *et al.*, 2009, Liu *et al.*, 2008a, 2008b, Mercader and Pomilio, 2010, Miki *et al.*, 2007, Nguyen *et al.*, 2010a, 2010b, Ryu *et al.*, 2008, Ryu *et al.*, 2010b, Ryu *et al.*, 2009b). Since Thailand has plenty of medicinal plants containing flavonoids, screening for neuraminidase inhibitory activity among these flavonoids would be interesting in order to understand the structure-activity relationship.

So far, the neuraminidases used in the screening of potential antivirals have been obtained from several sources. Many of them rely on the cumbersome use of the influenza virus preparations (Eichelberger *et al.*, 2008, Guo, 2006, Liu *et al.*, 2008a, 2008b, Miki *et al.*, 2007, Song *et al.*, 2005). Nonetheless, this procedure is risky, costly and inconvenient to set-up the screening assay. Many studies aimed to screen putative neuraminidase inhibitor have used a commercially available neuraminidase as an alternative source, for instance from *Clostridium perfringens* (Ryu *et al.*, 2008, 2009a, Ryu *et al.*, 2009b) or secreted recombinant neuraminidase form H1N1 expressed in baculovirus (Jeong *et al.*, 2009). This source is costly for applying in medium to high throughput screening. Recently, a recombinant influenza A virus H5N1 neuraminidase has been expressed in *Pichia pastoris* (Yongkiettrakul *et al.*, 2009). This system is cost-effective expression of functional enzymes since yeast can be rapidly grown on simple growth media and high levels of secreted recombinant proteins (Verma *et al.*, 1998). However, insect cells are a higher eukaryotic system than yeast. The relatively new stable transformation system, in addition to the already well established baculovirus mediated gene expression in insects, produces high amounts of the foreign protein of interest while allowing it to retain its functional activity (Verma *et al.*, 1998).

To fulfill these aims, it is necessary to have cost-effective sources of neuraminidase to set up an enzyme-based assay system with medium to high throughput screening capacity. The assay system has to be reliable and accurate to assess the potency of novel inhibitors from both synthetic and natural sources. In this research, a non-cell based neuraminidase inhibition assay using 3 different neuraminidase sources from inactivated avian influenza virus A/Turkey/Turkey/1/2005 (H5N1) and the crude preparation of recombinant neuraminidases NA1 A/Turkey/Italy/99 from (H7N1) and NA3 from A/ty/Italy/8000/02 (H7N3) expressed in baculovirus have been set-up. The neuraminidase inhibitory activity of synthesized compounds designed by in-silico analysis (Rungrotmongkol *et al.*, 2009) and a series of natural occurring flavonoids extracted from *Dalbergia parviflora* (Umehara *et al.*, 2008) and *Belamcanda chinensis* (Monthakantirat *et al.*, 2005) was then investigated. Moreover, the structure-activity relationship of the obtained inhibitors from both sources was also explored.

CHAPTER II

LITERATURE REVIEW

2.1 Avian influenza virus

Influenza viruses are enveloped virus with a segmented-single negative stranded RNA belonging to the family *Orthomyxoviridae*. There are three types of influenza viruses: A, B, and C which can be distinguished on the basic of antigenic differences between their nucleocapsid (NP) and matrix (M) proteins. Only influenza A viruses are further classified by subtype based on the two main surface glycoproteins, hemagglutinin (HA) and neuraminidase (NA). Other important characteristics that distinguish influenza A, B and C are firstly, influenza A viruses infect naturally a wide variety of avian species, human and several other mammalian species, including swine and horses, while Influenza B and C viruses appears to mainly infect only humans. In addition, the surface glycoproteins of influenza A viruses (HA and NA) exhibit much greater amino acid sequence variability than their counterparts in the influenza B viruses. Influenza C viruses have only a single multifunctional glycoprotein, the hemagglutinin-esterase-fusion protein (HEF). Moreover, although influenza A, B, and C viruses possess similar proteins, each virus type has distinct mechanisms for encoding proteins. Furthermore, Influenza A and B viruses each contain eight distinct RNS segments whereas influenza C viruses contain seven segments (Knipe and Howley, 2007).

The nucleocapsid of influenza virus is composed of nucleoprotein (NP) enclosing a segmented RNA genome associated with an RNA polymerase (P) complex (PA, PB1, and PB2). The envelope is lined on the inside by matrix protein (M1) and is spanned by a small number of ion channels composed of tetramer of protein M2. There are two kinds of peplomers: rod shape hemagglutinin (HA) molecules, which are homotrimers of a class I membrane glycoprotein, and mushroom-shaped neuraminidase (NA) molecules, which are tetramers of a class II membrane protein (White and Fenner, 1994). The structural diagram of influenza virus is shown in **Figure 1**.

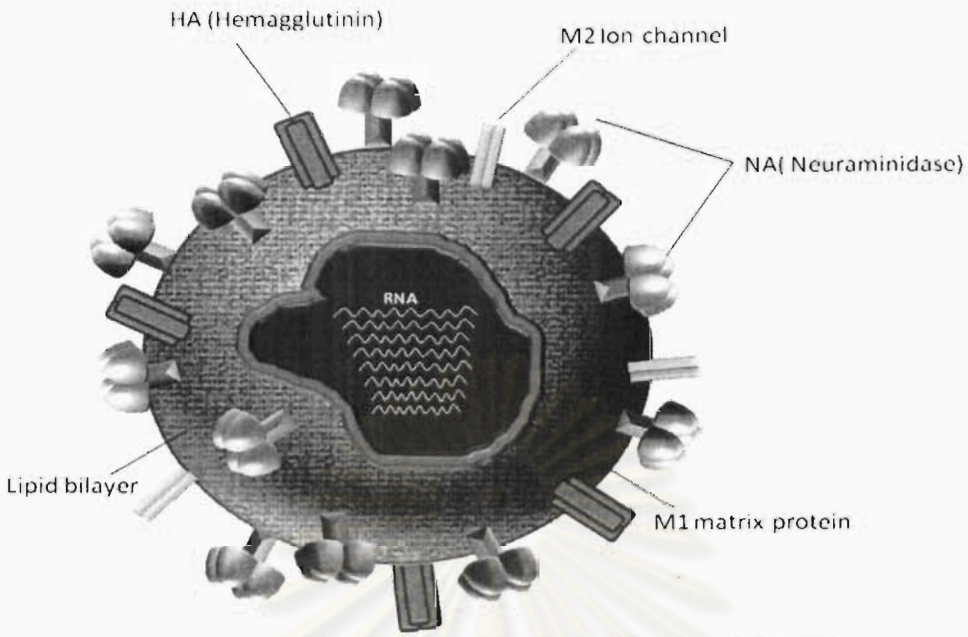

Figure 1 Structural diagram of the Influenza virus

Human influenza strains preferentially bind to sialic acid residues linked to galactose by the α 2,6 linkage, while avian and equine influenza strains recognize sialic acid linked to galactose by α 2,3 linkage (Connor *et al.*, 1994, Gambaryan *et al.*, 1997, Matrosovich *et al.*, 1997, Rogers *et al.*, 1983, Rogers and Paulson, 1983, Rogers and D'Souza, 1989). Correspondingly, human respiratory epithelial cells predominantly contain α 2,6 sialic acid–galactose linkages, while the host cells in birds and horses mainly contain α 2,3 linkages (Couceiro *et al.*, 1993, Ito *et al.*, 1998, Matrosovich *et al.*, 2004) Respiratory epithelial cells in the pig contain both α 2,3- and α 2,6 linkages, which explains why this animal is susceptible to both human and avian influenza viruses (Ito *et al.*, 1998). Because of this trait, the pig is widely regarded as a potential source of new pandemic strains, since it could serve as a non-selective host in which mixed infection of avian and human strains efficiently occurs, potentially resulting in new reassortant viruses, or in which purely avian strains can adapt to human receptor recognition (de Jong and Hien, 2006).

The replication cycles of human (H1N1, H2N2 and H3N2) and avian (H5N1) influenza viruses follow a similar 'scenario' (De Clercq, 2006) (**Figure 2**). After binding to sialic acid receptors, influenza virions are internalized by receptor mediated

endocytosis. The low pH in the endosomes triggers the fusion of the viral and endosomal membranes, and the influx of H+ through the M2 channel releases the viral RNA genes in the cytoplasm ('uncoating'). The RNA replication and transcription steps [which require repeated cycles of (-)RNA <-> (+)RNA polymerization reactions] occur in the nucleus. The translation of viral mRNA to proteins could be prevented by interferon and small interfering (si)RNAs. Packaging and budding of virions occur at the cytoplasmic membrane, by neuraminidase in order to release newly formed virions from the infected cells (De Clercq, 2004).

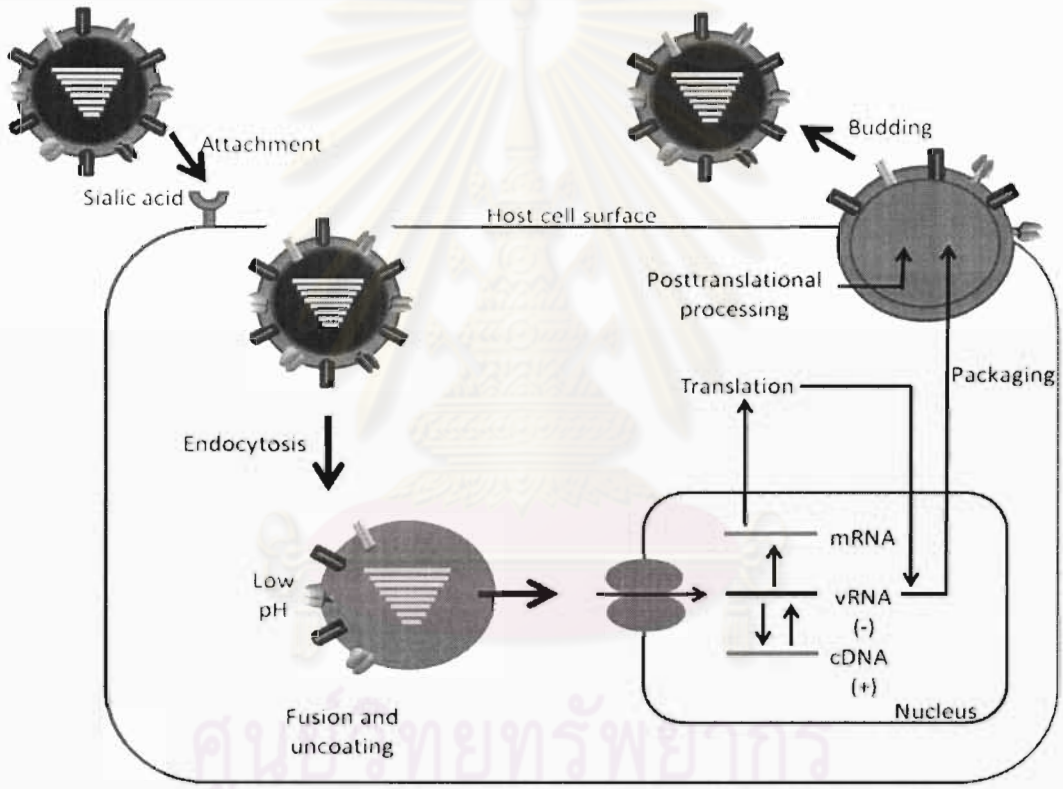

Figure 2 Influenza A virus replication cycle

2.2 Neuraminidase screening methods

Several methods have been developed for the determination of neuraminidase activity as well as for NA inhibition assays: a colorimetric thiobarbituric acid (TBA) method which is based on the reaction with TBA resulting in a red color complex (Aymard-Henryn *et al.*, 1973, Romero *et al.*, 1997, Skehel and Schild, 1971). A fluorometric method using Amplex Red (FL-AR) which uses fetuin as substrate and

involves oxidation of Amplex Red to resofurin for fluorescent detection (Molecular Probes, The Netherlands), a fluorometric method with 2-*O*-(4-methylumbelliferyl)-*N*-acetylneuraminic acid (MU-NANA) as a substrate, i.e. FL-MU-NANA method (Barnett *et al.*, 2000, Gubareva *et al.*, 1997, Gubareva *et al.*, 2002) and chemiluminescent method using a 1,2-dioxetane derivative of neuraminic acid (Buxton *et al.*, 2000).

The TBA assay is the most common method and widely used as a neuraminidase inhibition test of allantoic fluids, e.g. for the characterization of influenza A viruses by WHO International Influenza Centres (Nayak and Reichl, 2004). This colorimetric assay employs fetuin, a large natural glycoprotein containing sialic acid (N-acetylneuraminic; NANA), as a neuraminidase enzyme substrate. In the presence of neuraminidase, the NANA released by enzymatic cleavage of fetuin is converted to β-formol pyruvic acid by periodate oxidation process, whose ultimate product is pigmented and can be analyzed by a spectrophotometer (Aymard-Henryn *et al.*, 1973). This assay does not require expensive chemicals and equipment, it is time-consuming and sensitive to interference in the complex culture media used in animal cell culture (Nayak and Reichl, 2004).

Attractive options are fluorometric assays, which are simpler and less time consuming but more expensive. Most assays in use, however, are based on the substrate 4-methylumbelliferyl-α-D-N-acetylneuraminic acid (MUNANA) (Potier *et al.*, 1979). In these assays, fluorescent 4-methylumbelliferone (4-MU) is quantified after cleavage from MU-NANA. Assays based on MU-NANA have been used for the detection of neuraminidase activity in clinical isolates and the characterization of neuraminidase susceptibility towards inhibitors (Buxton *et al.*, 2000, Gubareva *et al.*, 2002, McSharry *et al.*, 2004, Rameix-Welti *et al.*, 2006, Rameix-Welti *et al.*, 2008, Song *et al.*, 2010, Wetherall *et al.*, 2003, Woods *et al.*, 1993, Yen *et al.*, 2007).

Another alternative is the use of a chemiluminescent method, which has a distinct advantage over other assays because of its high sensitivity. Additionally, it is a suitable method for the screening of clinical isolates for influenza virus diagnosis. However, this method is of limited use in monitoring virus replication in animal cell culture as it shows

interference due to the quenching effects of phenol red added as pH indicator in many tissue culture media (Buxton *et al.*, 2000). In this assay, 1,2-dioxetane derivative of neuraminic acid, is used as a chemiluminogenic substrates. After the enzymatic cleavage of the substrate, an optical energy as light emission can be detected.

2.3 Natural products with neuraminidase inhibitory activity

Several natural occurring products have been investigated for the neuraminidase inhibitory activity. However, flavonoids have been found to be a relevant inhibitor among these natural products. The lists of natural compounds which are reported for their inhibitory activity are shown in **Tables 1-4**.

Table 1 Flavonoids with neuraminidase inhibitory activity

Chemical compounds	IC_{50} ± SD (Strains)	References
Abyssinone VI [1] 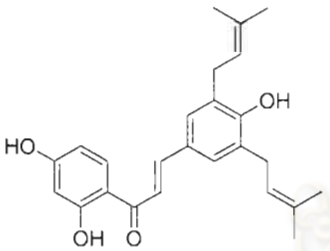	26.44 ± 0.42 μg/ml (H1N1) 24.56 ± 0.44 μg/ml (H9N2)	(Nguyen *et al.*, 2010a)

Table 1 (continued)

Chemical compounds	IC_{50} ± SD (Strains)	References
Apigenin [2] 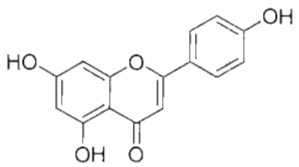	17.4 ± 0.5 μM (*C. perfringens*) 33.4 ± 7.0 μM (rvH1N1) 8.55 ±1.45 μg/ml (A/PR/8/34 (H1N1)) 31.6 ± 0.9 μM (A/PR/8/34 (H1N1)) 7.81 ± 1.70 μg/ml (A/PR/8/34 (H1N1)) 28.9 ± 0.7 μM (A/Jinan/15/ 90(H3N2)) 12.35 ± 3.71 μg/ml (A/PR/8/34 (H1N1)) 45.7 ± 2.3 μM (B/Jiangsu/10/2003)	(Jeong *et al.*, 2009, Liu *et al.*, 2008a, 2008b)
Apiin [3] 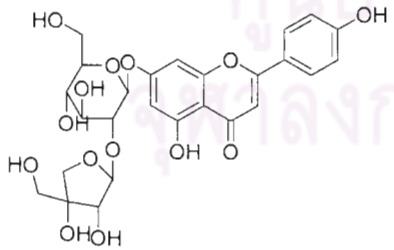	14.63 ± 4.38 μg/ml (A/PR/8/34 (H1N1)) 25.34 ± 5.82 μg/ml (A/Jinan/15/ 90(H3N2)) 28.49 ± 5.40 μg/ml (B/Jiangsu/10/2003)	(Liu *et al.*, 2008a)

Table 1 (continued)

Chemical compounds	IC_{50} ± SD (Strains)	References
Astragalin [4] 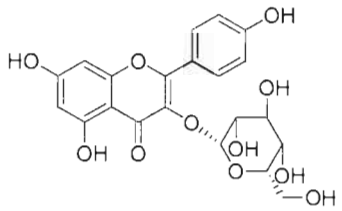	29.4 ± 1.2 μM (*C. perfringens*) 38.4 ± 6.3 μM (rvH1N1)	(Jeong *et al.*, 2009)
Calopocarpin [5] 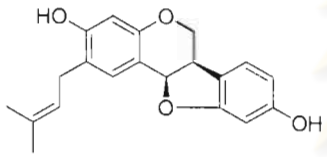	1.57 ± 0.06 μM (*C. perfringens*) 7.55 ± 2.23 μM (*V. cholera*)	(Nguyen *et al.*, 2010b)
Catechin [6] 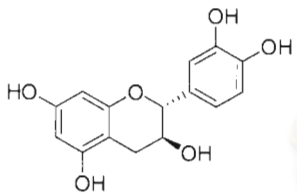	>100 μM (A/PR/8/34 (H1N1)) >100 μM (A/Jinan/15/90(H3N2)) >100 μM (B/Jiangsu/10/2003)	(Liu *et al.*, 2008b)
Chrysin [7] 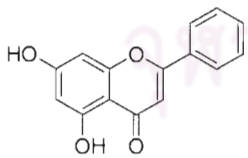	45.7 ± 1.9 μM (A/PR/8/34 (H1N1)) 33.36 ± 3.8 μM (A/Jinan/15/ 90(H3N2)) 52.9 ± 2.5 μM (B/Jiangsu/10/2003)	(Liu *et al.*, 2008b)

Table 1 (continued)

Chemical compounds	IC_{50} ± SD (Strains)	References
Cosmosiin [8] 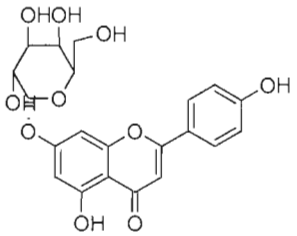	39.3 ± 3.3 μM (*C. perfringens*) 46.9 ± 1.0 μM (rvH1N1)	(Jeong *et al.*, 2009)
Corylin [9] 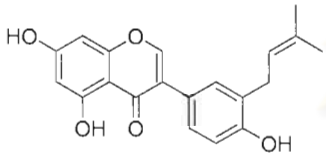	>50 μg/ml (H1N1) >50 μg/ml (H9N2)	(Nguyen *et al.*, 2010a)
Crystacarpin [10] 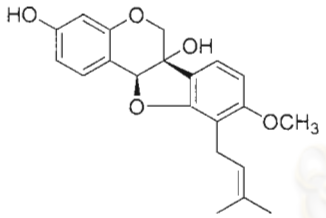	2.28 ± 0.31 μM (*C. perfringens*) 22.03 ± 2.24 μM (*V. cholera*)	(Nguyen *et al.*, 2010b)
Cudraflavanone A [11] 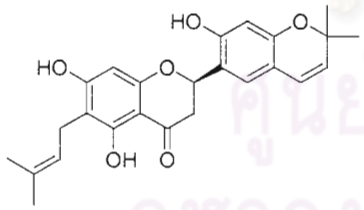	1.53 ± 0.8 μM (*C. welchii*)	(Ryu *et al.*, 2009b)
Cudraflavanone D [12] 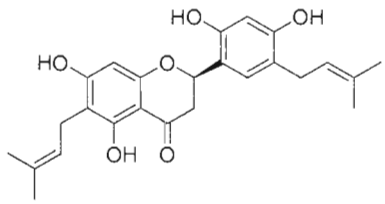	10.74 ± 2.4 μM (*C. welchii*)	(Ryu *et al.*, 2009b)

Table 1 (continued)

Chemical compounds	IC_{50} ± SD (Strains)	References
Cudraflavone A [13] 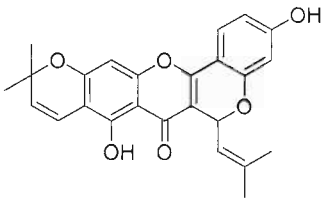	29.01 ± 1.9 μM (*C. welchii*)	(Ryu *et al.*, 2009b)
Cudraflavone B [14] 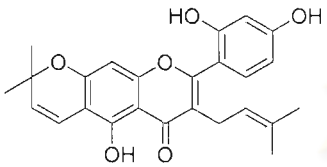	10.14 ± 3.0 μM (*C. welchii*)	(Ryu *et al.*, 2009b)
Cycloartocarpetin [15] 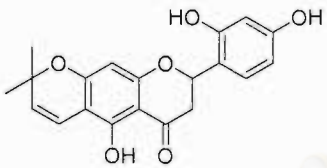	6.01 ± 0.2 μM (*C. welchii*)	(Ryu *et al.*, 2009b)
Daidzein [16] 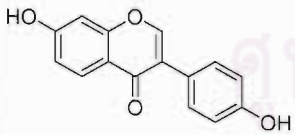	37.1 ± 0.6 μM (A/PR/8/34 (H1N1)) 26.6 ± 0.3 μM (A/Jinan/15/ 90(H3N2)) 46.8 ± 1.9 μM (B/Jiangsu/10/2003)	(Liu *et al.*, 2008b)
Demethylmedicarpin [17] 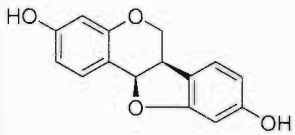	6.39 ± 0.40 μM (*C. perfringens*) 29.54 ± 1.94 μM (*V. cholera*)	(Nguyen *et al.*, 2010b)

Table 1 (continued)

Chemical compounds	IC_{50} ± SD (Strains)	References
Dinatin [18] 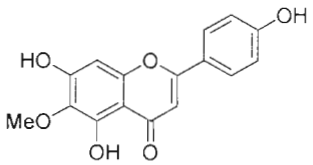	46.3 ± 4.4 μM (A/PR/8/34 (H1N1)) 26.0 ± 0.5 μM (A/Jinan/15/ 90(H3N2)) 33.2 ± 0.4 μM (B/Jiangsu/10/2003)	(Liu *et al.*, 2008b)
Echinantin [19] 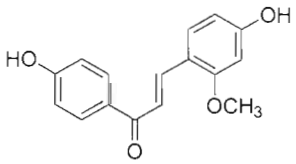	5.80 ± 0.30 μg/ml (H1N1) 5.70 ± 0.55 μg/ml (H9N2) 2.49 ± 0.14 μg/ml $(H1N1)^{WT}$ 2.19 ± 0.06 μg/ml $(H1N1^{H274Y})$	(Dao *et al.*, 2011)
Epicatechin [20] 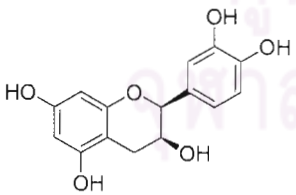	>100 μM (A/PR/8/34 (H1N1)) >100 μM (A/Jinan/15/ 90(H3N2)) >100 μM (B/Jiangsu/10/2003)	(Liu *et al.*, 2008b)
Erysenegalensein M [21] 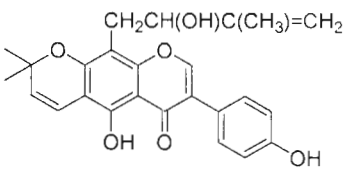	>50 μg/ml (H1N1) >50 μg/ml (H9N2)	(Nguyen *et al.*, 2010a)

Table 1 (continued)

Chemical compounds	IC_{50} ± SD (Strains)	References
Erystagallin A [22] 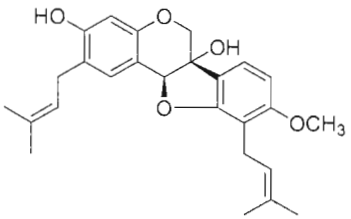	2.04 ± 0.08 μM (*C. perfringens*) 27.74 ± 0.40 μM (*V. cholera*)	(Nguyen *et al.*, 2010b)
Erysubin D [23] 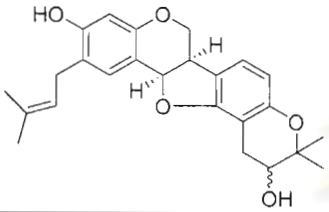	26.39 ± 1.94 μM (*C. perfringens*) 26.39 ± 1.78 μM (*V. cholera*)	(Nguyen *et al.*, 2010b)
Erysubin E [24] 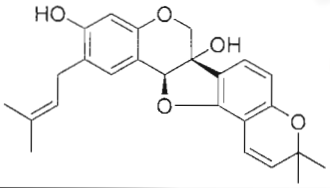	1.30 ± 0.12 μM (*C. perfringens*) 19.48 ± 1.94 μM (*V. cholera*)	(Nguyen *et al.*, 2010b)
Erythraddison A [25] 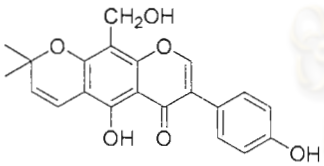	>50 μg/ml (H1N1) >50 μg/ml (H9N2)	(Nguyen *et al.*, 2010a)
Erythribyssin D [26] 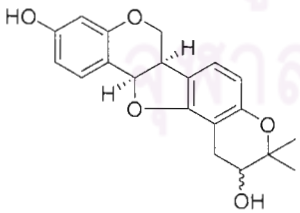	77.10 ± 2.17 μM (*C. perfringens*) 46.20 ± 5.89 μM (*V. cholera*)	(Nguyen *et al.*, 2010b)
Erythribyssin L [27] 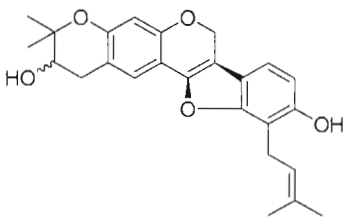	2.79 ± 0.33 μM (*C. perfringens*) 27.14 ± 2.29 μM (*V. cholera*)	(Nguyen *et al.*, 2010b)

Table 1 (continued)

Chemical compounds	IC_{50} ± SD (Strains)	References
Erythribyssin M [28] 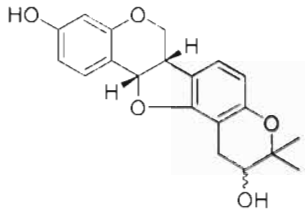	205.40 ± 4.03 μM (*C. perfringens*) 77.73 ± 11.01 μM (*V. cholera*)	(Nguyen *et al.*, 2010b)
Erythribyssin O [29] 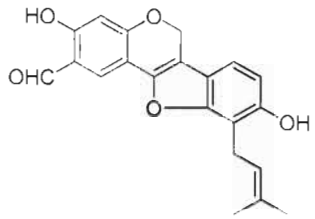	1.32 ± 0.16 μM (*C. perfringens*) 0.35 ± 0.02 μM (*V. cholera*)	(Nguyen *et al.*, 2010b)
Eryvarin D [30] 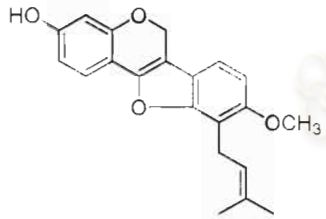	2.09 ± 0.08 μM (*C. perfringens*) 3.30 ± 0.53 μM (*V. cholera*)	(Nguyen *et al.*, 2010b)
Formononetin [31] 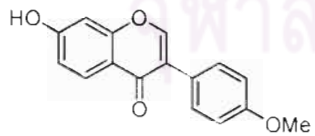	>100 μM (A/PR/8/34 (H1N1)) >100 μM (A/Jinan/15/ 90(H3N2)) >100 μM (B/Jiangsu/10/2003)	(Liu *et al.*, 2008b)

Table 1 (continued)

Chemical compounds	IC_{50} ± SD (Strains)	References
Galuteolin [32] 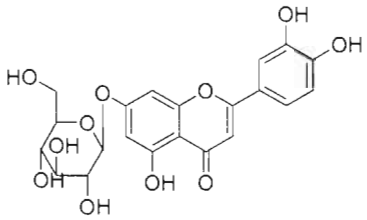	21.23 ± 2.97 μg/ml (A/PR/8/34 (H1N1)) 47.4 ± 0.5 μM (A/PR/8/34 (H1N1)) 23.42 ± 3.51 μg/ml (A/PR/8/34 (H1N1)) 52.2 ± 1.8 μM (A/Jinan/15/ 90(H3N2)) 26.26 ± 5.27 μg/ml (A/PR/8/34 (H1N1)) 58.6 ± 2.7 μM (B/Jiangsu/10/2003)	(Liu *et al.*, 2008a, Liu *et al.*, 2008b)
Genistein [33] 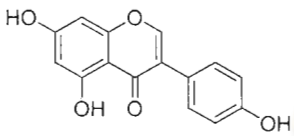	77.1 ± 5.1 μM (A/PR/8/34 (H1N1)) 134.4 ± 11.5 μM (A/Jinan/15/ 90(H3N2)) 83.3 ± 9.0 μM (B/Jiangsu/10/2003)	(Liu *et al.*, 2008b)
Glyasperin C [34] 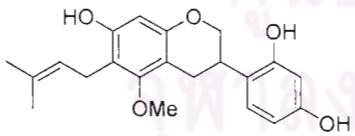	20% at 200 μM (rvH1N1 A/Bervig_Mission/1/18)	(Ryu *et al.*, 2010b)
Glyasperin D [35] 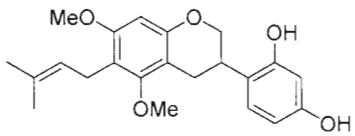	20% at 200 μM (rvH1N1 A/Bervig_Mission/1/18)	(Ryu *et al.*, 2010b)

Table 1 (continued)

Chemical compounds	IC_{50} ± SD (Strains)	References
Gossypetin [36] 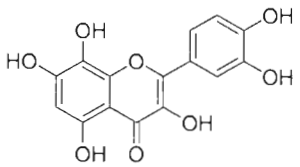	0.8 ± 0.1 μM (*C. perfringens*) 2.6 ± 1.1 μM (rvH1N1)	(Jeong *et al.*, 2009)
Herbacetin [37] 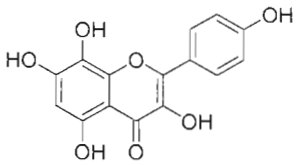	1.4 ± 0.2 μM (*C. perfringens*) 8.9 ± 1.4 μM (rvH1N1)	(Jeong *et al.*, 2009)
Hesperidin [38] 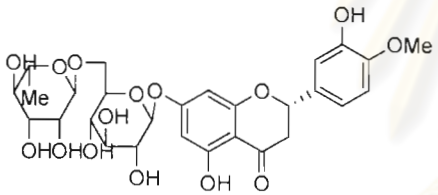	>100 μM (A/PR/8/34 (H1N1)) >100 μM (A/Jinan/15/ 90(H3N2)) >100 μM (B/Jiangsu/10/2003)	(Liu *et al.*, 2008b)
Isoliquiritigenin [39] 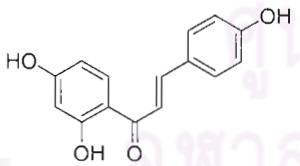	8.41 ± 0.39 μg/ml (H1N1) 9.69 ± 0.37 μg/ml (H9N2) 3.48 ± 0.19 μg/ml $(H1N1)^{WT}$ 3.42 ± 0.12 μg/ml $(H1N1^{H274Y})$ 9.0 ± 0.7 μM (rvH1N1 A/ Bervig_Mission/1/18)	(Dao *et al.*, 2011, Ryu *et al.*, 2010b)

Table 1 (continued)

Chemical compounds	IC_{50} ± SD (Strains)	References
2'-Methoxyisoliquiritigenin [40] 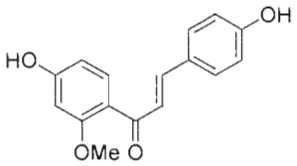	24.3 ± 2.2 μM (rvH1N1 A/Bervi g_Mission/1/18)	(Ryu *et al.*, 2010b)
Isoliquiritin [41] 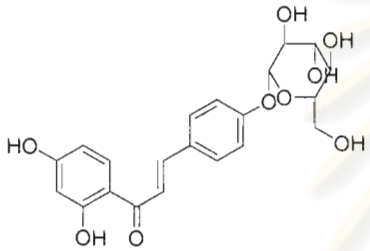	124.0 ± 2.3μM (rvH1N1 A/Bervi g_Mission/1/18)	(Ryu *et al.*, 2010b)
Isoliquiritin apioside [42] 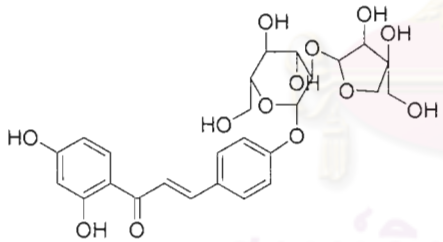	12.9 ± 1.2μM (rvH1N1 A/Bervi g_Mission/1/18)	(Ryu *et al.*, 2010b)
Isoneorautenol C [43] 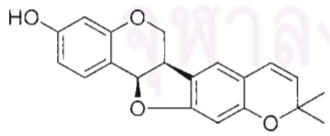	14.12 ± 0.19 μM (*C. perfringens*) 64.75 ± 6.19 μM (*V. cholera*)	(Nguyen *et al.*, 2010b)

Table 1 (continued)

Chemical compounds	IC_{50} ± SD (Strains)	References
Kaempferol [44] 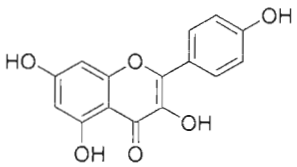	8.0 ± 1.0 μM (*C. perfringens*) 11.2 ± 1.0 μM (rvH1N1) 58.6 ± 0.6 μM (A/PR/8/34 (H1N1)) 38.1 ± 0.3 μM (A/Jinan/15/ 90(H3N2)) 46.4 ± 0.8 μM (B/Jiangsu/10/2003)	(Jeong *et al.*, 2009, Liu *et al.*, 2008b)
Kanzonol C [45] 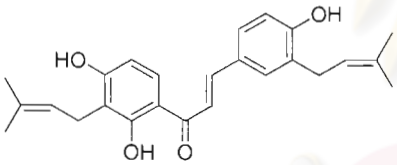	75.38 ± 2.47 μg/ml (H1N1) 52.96 ± 1.33 μg/ml (H9N2)	(Dao *et al.*, 2011)
Kumatakenin [46] 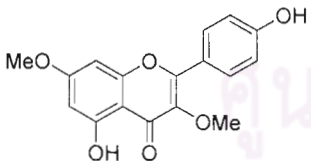	36.4 ± 6.9 μM (rvH1N1 A/Bervig_Mission/1/18)	(Ryu *et al.*, 2010b)
Kurarinol [47] 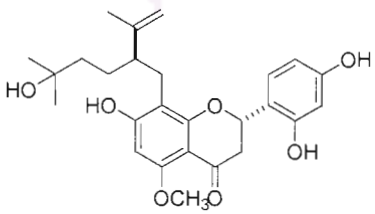	17.0 ± 1.6 μM (*C. perfringens*)	(Ryu *et al.*, 2008)

Table 1 (continued)

Chemical compounds	IC_{50} ± SD (Strains)	References
Kurarinone [48] 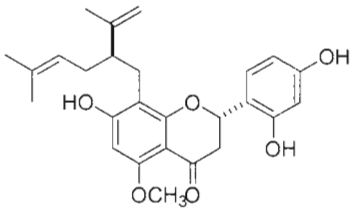	15.1 ± 2.0 μM (*C. perfringens*)	(Ryu *et al.*, 2008)
Kushenol A [49] 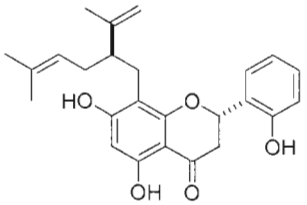	14.8 ± 1.5 μM (*C. perfringens*)	(Ryu *et al.*, 2008)
Kushenol T [50] 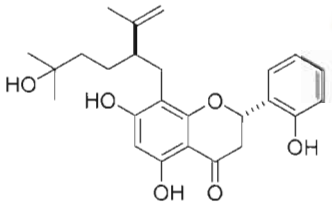	12.1 ± 2.4 μM (*C. perfringens*)	(Ryu *et al.*, 2008)
Leachianone A [51] 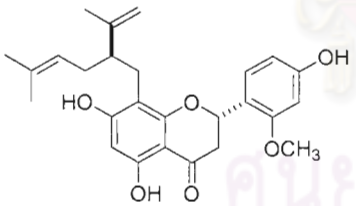	20.1 ± 0.8 μM (*C. perfringens*)	(Ryu *et al.*, 2008)
Licoagrochalcone A [52] 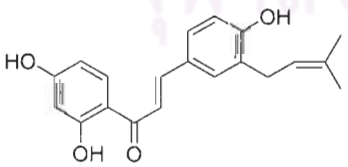	51.59 ± 2.77 μg/ml (H1N1) 56.92 ± 2.15 μg/ml (H9N2) 21.51 ± 0.25 μg/ml (H1N1) 20.03 ± 0.35μg/ml (H9N2)	(Dao *et al.*, 2011, Nguyen *et al.*, 2010a)

Table 1 (continued)

Chemical compounds	IC_{50} ± SD (Strains)	References
Licochalcone A [53] 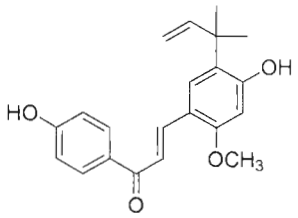	19.09 ± 1.10 µg/ml (H1N1) 17.98 ± 0.97 µg/ml (H9N2) 5.42 ± 0.40 µg/ml $(H1N1)^{WT}$ 4.20 ± 0.57 µg/ml $(H1N1^{H274Y})$	(Dao *et al.*, 2011)
Licochalcone D [54] 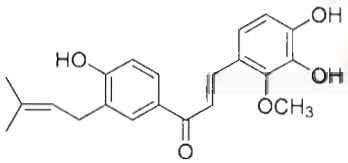	28.62 ± 1.67 µg/ml (H1N1) 35.21 ± 3.10 µg/ml (H9N2)	(Dao *et al.*, 2011)
Licochalcone G [55] 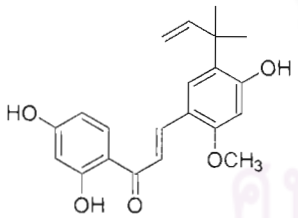	37.68 ± 2.17 µg/ml (H1N1) 42.11 ± 2.12 µg/ml (H9N2)	(Dao *et al.*, 2011)
Licoflavonol [56] 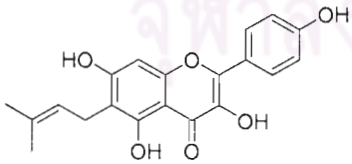	20.6 ± 0.9 µM (rvH1N1 A/Bervig_Mission/1/18)	(Ryu *et al.*, 2010b)

Table 1 (continued)

Chemical compounds	IC_{50} ± SD (Strains)	References
Licorisoflavan A [57] 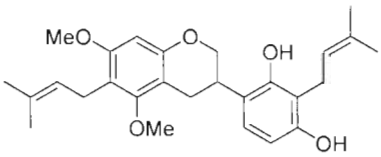	30% at 200 μM (rvH1N1 A/Bervig_Mission/1/18)	(Ryu *et al.*, 2010b)
Linocinamarin [58] 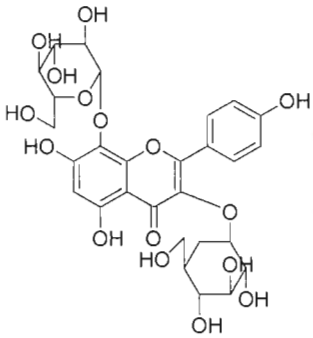	39.1 ± 5.5 μM (*C. perfringens*) 44.2 ± 3.9 μM (rvH1N1)	(Jeong *et al.*, 2009)
Liquiritigenin [59] 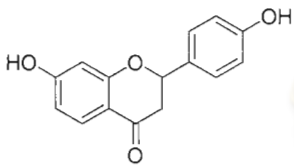	46.8 ± 3.3 μM (rvH1N1 A/Bervig_Mission/1/18)	(Ryu *et al.*, 2010b)
Liquiritin [60] 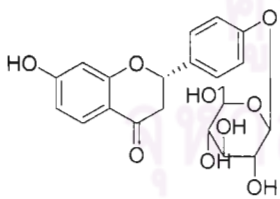	>100 μM (A/PR/8/34 (H1N1)) >100 μM (A/Jinan/15/ 90(H3N2)) >100 μM (B/Jiangsu/10/2003) 82.3 ± 0.1μM (rvH1N1 A/Bervig _Mission/1/18)	(Liu *et al.*, 2008b, Ryu *et al.*, 2010b)

Table 1 (continued)

Chemical compounds	IC_{50} ± SD (Strains)	References
Liquiritin apioside [61] 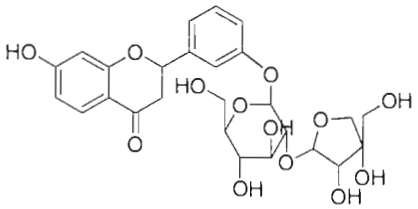	18.2 ± 2.0 μM (rvH1N1 A/Bervig_Mission/1/18)	(Ryu *et al.*, 2010b)
Luteolin [62] 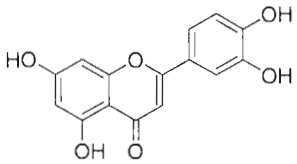	4.3 ± 0.1 μM (*C. perfringens*) 11.0 ± 0.7 μM (rvH1N1) 9.64 ± 1.83 μg/ml (A/PR/8/34 (H1N1)) 33.7 ± 0.7 μM (A/PR/8/34 (H1N1)) 9.34 ± 2.80 μg/ml (A/PR/8/34 (H1N1)) 32.6 ± 0.1 μM (A/Jinan/15/ 90(H3N2)) 15.26 ± 3.20 μg/ml (A/PR/8/34 (H1N1)) 53.3 ± 5.1 μM (B/Jiangsu/10/2003)	(Jeong *et al.*, 2009, Liu *et al.*, 2008a, 2008b)

Table 1 (continued)

Chemical compounds	IC_{50} ± SD (Strains)	References
Luteolin 3'-glucuronyl acid methyl ester [63] 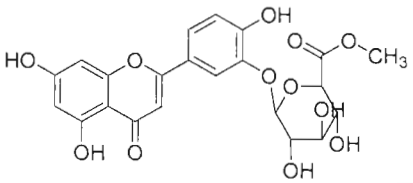	21.16 ± 6.34 µg/ml (A/PR/8/34 (H1N1)) 24.28 ± 6.28 µg/ml (A/Jinan/15/ 90(H3N2)) 24.44 ± 5.35 µg/ml (B/Jiangsu/10/2003)	(Liu *et al.*, 2008a)
Maackiain [64] 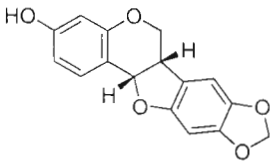	3.2 ± 1.1 µM (*C. perfringens*)	(Ryu *et al.*, 2008)
Myricetin [65] 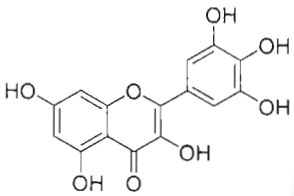	82.6 ± 8.9 µM (A/PR/8/34 (H1N1)) 46.2 ± 3.9 µM (A/Jinan/15/ 90(H3N2)) 75.4 ± 6.7 µM (B/Jiangsu/10/2003)	(Liu *et al.*, 2008b)
Naringenin [66] 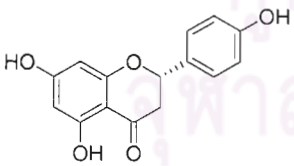	52.2 ± 1.6 µM (A/PR/8/34 (H1N1)) 87.7 ± 5.9 µM (A/Jinan/15/ 90(H3N2)) >100 µM (B/Jiangsu/10/2003)	(Liu *et al.*, 2008b)
Neorautenol [67] 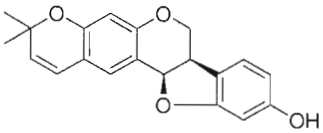	19.82 ± 0.88 µM (*C. perfringens*) 53.11 ± 3.98 µM (*V. cholera*)	(Nguyen *et al.*, 2010b)

Table 1 (continued)

Chemical compounds	IC_{50} ± SD (Strains)	References
Nicotiflorin [68] 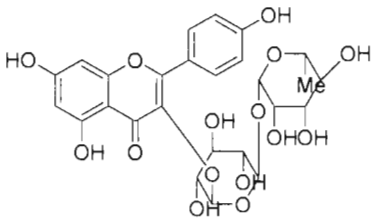	55.5 ± 2.2 μM (*C. perfringens*) 31.7 ± 3.0 μM (rvH1N1)	(Jeong *et al.*, 2009)
Norkurarinol [69] 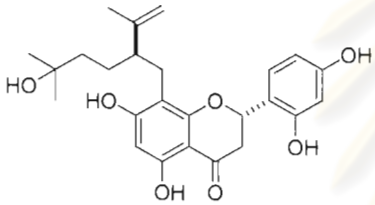	18.3 ± 1.2 μM (*C. perfringens*)	(Ryu *et al.*, 2008)
Ononin [70] 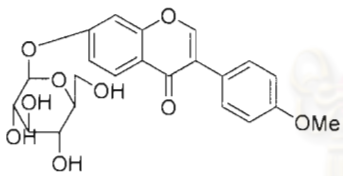	30% at 200 μM (rvH1N1 A/Bervig_Mission/1/18)	(Ryu *et al.*, 2010b)
Phaseolin [71] 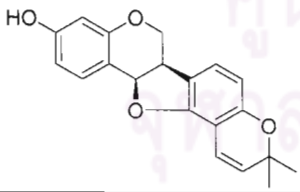	33.55 ± 2.07 μM (*C. perfringens*) 31.40 ± 1.55 μM (*V. cholera*)	(Nguyen *et al.*, 2010b)
5'-Phenylbutein [72] 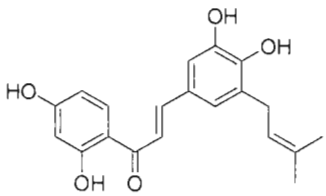	25.87 ± 2.03 μg/ml (H1N1) 35.50 ± 1.43 μg/ml (H9N2) 21.93 ± 0.44 μg/ml (H1N1) 20.47 ± 0.48 μg/ml (H9N2)	(Dao *et al.*, 2011, Nguyen *et al.*, 2010a)

Table 1 (continued)

Chemical compounds	IC_{50} ± SD (Strains)	References
Pterocarpin [73] 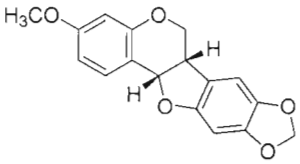	1.4 ±0.36 μM (*C. perfringens*)	(Ryu *et al.*, 2008)
Quercetin [74] 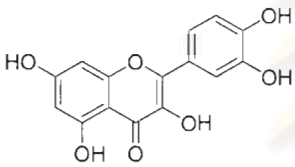	1.7±0.6 μM (*C. perfringens*) 2.2±0.3 μM (rvH1N1) 58.4 ± 3.8 μM (A/PR/8/34 (H1N1)) 87.6 ± 5.5 μM (A/Jinan/15/ 90(H3N2)) 67.5 ± 2.6 μM (B/Jiangsu/10/2003)	(Jeong *et al.*, 2009, Liu *et al.*, 2008b)
Rhamnocitrin [75] 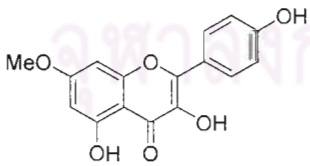	51.5 ± 6.1 μM (A/PR/8/34 (H1N1)) 83.9 ± 4.4 μM (A/Jinan/15/ 90(H3N2)) 62.0 ± 7.2 μM (B/Jiangsu/10/2003)	(Liu *et al.*, 2008b)

Table 1 (continued)

Chemical compounds	IC_{50} ± SD (Strains)	References
Rhodiolinin [76] 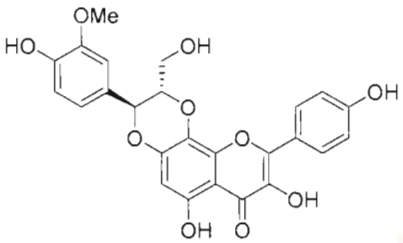	6.1 ± 2.2 μM (*C. perfringens*) 10.3 ± 0.2 μM (rvH1N1)	(Jeong *et al.*, 2009)
Rhodionin [77] 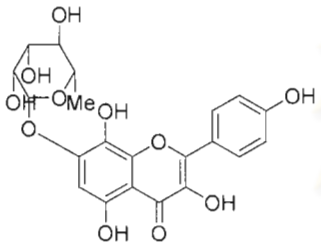	40.6 ± 3.7 μM (*C. perfringens*) 32.2 ± 3.2 μM (rvH1N1)	(Jeong *et al.*, 2009)
Rhodiosin [78] 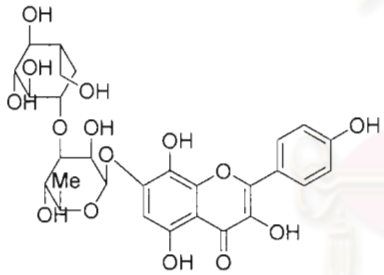	56.9 ± 8.6 μM (*C. perfringens*) 56.5 ± 0.5 μM (rvH1N1)	(Jeong *et al.*, 2009)
Rutin [79] 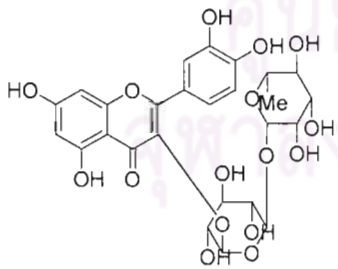	30.9 ± 2.5 μM (*C. perfringens*) 34.4 ± 5.0 μM (rvH1N1) 52.2 ± 1.6 μM (A/PR/8/34 (H1N1)) 87.7 ± 5.9 μM (A/Jinan/15/ 90(H3N2)) >100 μM (B/Jiangsu/10/2003)	(Jeong *et al.*, 2009, Liu *et al.*, 2008b)

Table 1 (continued)

Chemical compounds	IC_{50} ± SD (Strains)	References
Scutellarin [80] 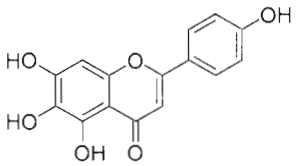	50.6 ± 0.9 μM (A/PR/8/34 (H1N1)) 47.3 ± 1.3 μM (A/Jinan/15/ 90(H3N2)) 59.9 ± 3.8 μM (B/Jiangsu/10/2003)	(Liu *et al.*, 2008b)
Sophoraflavanone G [81] 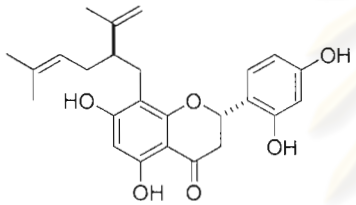	13.5 ± 1.08 μM (*C. perfringens*)	(Ryu *et al.*, 2008)
Sophorapterocarpan A [82] 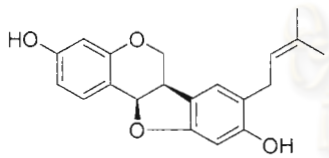	2.01 ± 0.16 μM (*C. perfringens*) 11.59 ± 3.17 μM (*V. cholera*)	(Nguyen *et al.*, 2010b)
Sophoricoside [83] 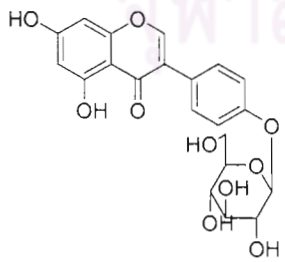	>100 μM (A/PR/8/34 (H1N1)) >100 μM (A/Jinan/15/ 90(H3N2)) >100 μM (B/Jiangsu/10/2003)	(Liu *et al.*, 2008b)

Table 1 (continued)

Chemical compounds	IC_{50} ± SD (Strains)	References
Sulphuretin [84]	29.6 ± 0.5 μM (A/PR/8/34 (H1N1)) 27.7 ± 0.8 μM (A/Jinan/15/ 90(H3N2)) 51.2 ± 5.7 μM (B/Jiangsu/10/2003)	(Liu *et al.*, 2008b)
Trifolrhizin [85]	237 ± 25.1 μM (*C. perfringens*)	(Ryu *et al.*, 2008)
Vitexin [86]	46.5 ± 0.6 μM (A/PR/8/34 (H1N1)) 45.1 ± 1.3 μM (A/Jinan/15/ 90(H3N2)) 49.6 ± 3.1 μM (B/Jiangsu/10/2003)	(Liu *et al.*, 2008b)
Wighteone [87]	>50 μg/ml (H1N1) >50 μg/ml (H9N2)	**(Nguyen *et al.*, 2010a)**
Isowighteone [88]	>50 μg/ml (H1N1) >50 μg/ml (H9N2)	(Nguyen *et al.*, 2010a)

Table 1 (continued)

Chemical compounds	IC_{50} ± SD (Strains)	References
2-((E)-4'-hydroxyphenylidene) -6-hydroxy-2,3-dihydrobenzofuran-3-one [89] 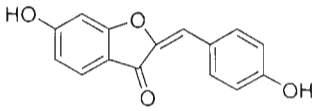	22.0 ± 0.7 μM (A/PR/8/34 (H1N1)) 22.1 ± 0.3 μM (A/Jinan/15/ 90(H3N2)) 22.9 ± 0.5μM (B/Jiangsu/10/2003)	(Liu *et al.*, 2008b)
2-((E)-4'- hydroxyphenylidene) -4,6-dihydroxy-2,3-dihydrobenzofuran-3-one [90] 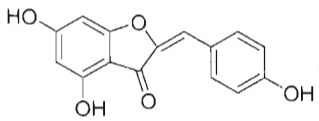	25.6 ± 1.1 μM (A/PR/8/34 (H1N1)) 22.3 ± 0.6 μM (A/Jinan/15/ 90(H3N2)) 25.4 ± 1.0 μM (B/Jiangsu/10/2003)	(Liu *et al.*, 2008b)
2-((E)- phenylidene)-6-hydroxy-2,3 -dihydrobenzofuran-3-one [91] 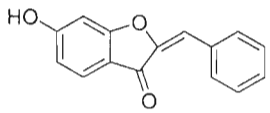	72.0 ± 3.5 μM (A/PR/8/34 (H1N1)) 73.3 ± 7.9 μM (A/Jinan/15/ 90(H3N2)) 86.6 ± 6.1μM (B/Jiangsu/10/2003)	(Liu *et al.*, 2008b)
2',5,7-trihydroxy-4',5'-(2,2-dimethylchromeno)-8-(3-hydroxy-3-methylbutyl) flavanone [92] 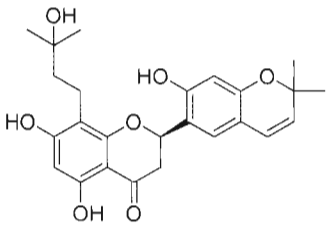	0.38 ± 0.1 μM (*C. welchii*)	(Ryu *et al.*, 2009b)

Table 2 Stilbenes with neuraminidase inhibitory activity

Chemical compounds	IC_{50} ± SD	References
(+)-Ampelopsin [93] 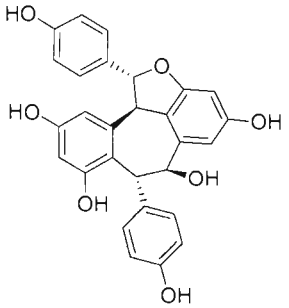	234.61 ± 25.07 μM A/PR/8/34(H1N1) 215.30 ± 23.84 μM Novel H1N1(WT) 261.60 ± 29.18 μM H274Y mutant	(Nguyen *et al.*, 2011)
Amurensin G [94] 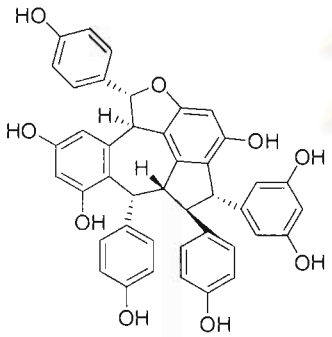	38.15 ± 4.30 μM A/PR/8/34(H1N1) 42.01 ± 4.78 μM Novel H1N1(WT) 42.47 ± 4.80 μM H274Y mutant	(Nguyen *et al.*, 2011)
Amurensin K [95] 	48.44 ± 4.59 μM A/PR/8/34(H1N1) 14.43 ± 1.67 μM Novel H1N1(WT) 34.03 ± 3.63 μM H274Y mutant	(Nguyen *et al.*, 2011)
Erythraddison B [96] 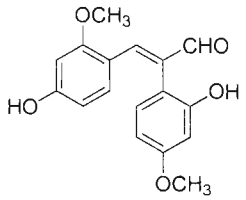	8.80 ± 0.34 μg/ml (H1N1) 7.19 ± 0.40 μg/ml (H9N2)	(Nguyen *et al.*, 2010a)

Table 2 (Continued)

Chemical compounds	IC_{50} ± SD	References
Licocoumarone [97] 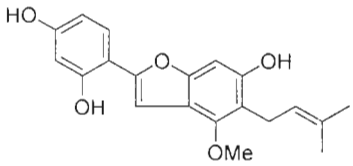	27.8 ± 0.7 μM (rvH1N1 A/ Bervig_Mission/1/18)	(Ryu *et al.*, 2010b)
Napalensinol B [98] 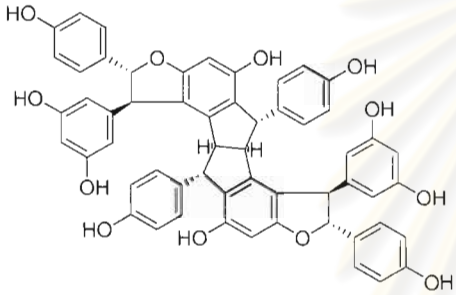	40.26 ± 3.65 μM A/PR/8/34(H1N1) 52.30 ± 6.04 μM Novel H1N1(WT) 30.42 ± 2.51 μM H274Y mutant	(Nguyen *et al.*, 2011)
Piceid [99] 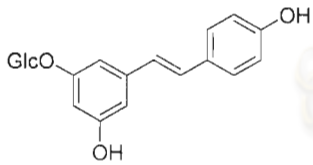	110.79 ± 10.78 μM A/PR/8/34(H1N1) 110.25 ± 11.72 μM Novel H1N1(WT) 150.81 ± 15.40 μM H274Y mutant	(Nguyen *et al.*, 2011)
trans-ε-Viniferin [100] 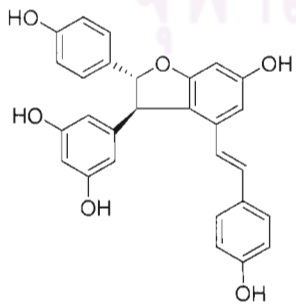	88.54 ± 8.21 μM A/PR/8/34(H1N1) 129.32 ± 12.92 μM Novel H1N1(WT) 173.79 ± 21.05 μM H274Y mutant	(Nguyen *et al.*, 2011)

Table 2 (Continued)

Chemical compounds	IC_{50} ± SD	References
(+)-Viniferol C [101]	8.94 ± 1.06 μM A/PR/8/34(H1N1) 38.52 ± 4.41 μM Novel H1N1(WT) 61.16 ± 6.06 μM H274Y mutant	(Nguyen *et al.*, 2011)
trans-Vitisin B [102]	41.68 ± 4.57 μM A/PR/8/34(H1N1) 66.73 ± 7.70 μM Novel H1N1(WT) 23.89 ± 2.76 μM H274Y mutant	(Nguyen *et al.*, 2011)

Table 3 Xanthones with neuraminidase inhibitory activity

Chemical compounds	IC_{50} ± SD	References
Cudratricusxanthone [103]	0.245 ± 0.03 μM (*C. perfringens*)	(Ryu *et al.*, 2009a)

Table 3 (continued)

Chemical compounds	IC_{50} ± SD	References
Cudratricusxanthone F [104] 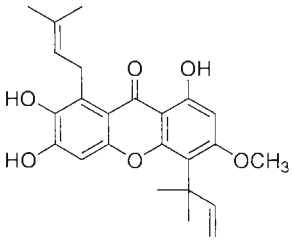	1.271 ± 0.21 μM (*C. perfringens*)	(Ryu *et al.*, 2009a)
Cudraxanthone [105] 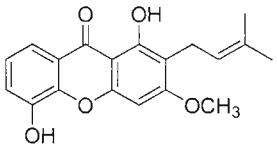	65.7 ± 2.1 μM (*C. perfringens*)	(Ryu *et al.*, 2010a)
Cudraxanthone D [106] 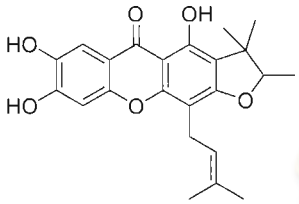	0.278 ± 0.08 μM (*C. perfringens*)	(Ryu *et al.*, 2009a)
Cudraxanthone L [107] 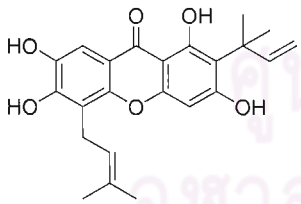	0.228 ± 0.01 μM (*C. perfringens*)	(Ryu *et al.*, 2009a)
Cudraxanthone M [108] 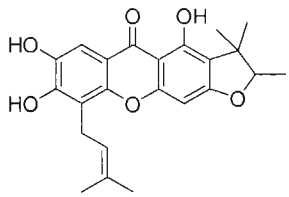	0.186 ± 0.04 μM (*C. perfringens*)	(Ryu *et al.*, 2009a)

Table 3 (continued)

Chemical compounds	IC_{50} ± SD	References
Garcinone D [109] 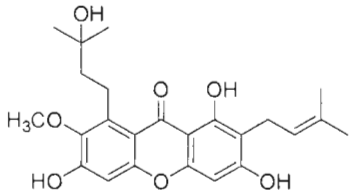	5.7 ± 0.8 μM (*C. perfringens*)	(Ryu *et al.*, 2010a)
Gartanin [110] 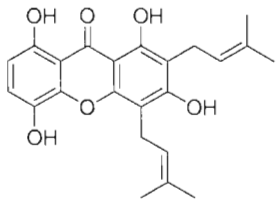	2.9 ± 0.3 μM (*C. perfringens*)	(Ryu *et al.*, 2010a)
8-deoxygartanin [111] 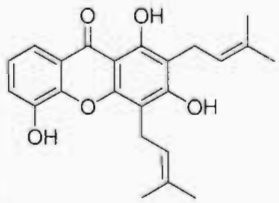	29.2 ± 0.7 μM (*C. perfringens*)	(Ryu *et al.*, 2010a)
Macluraxanthone [112] 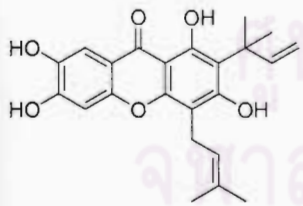	0.186 ± 0.02 μM (*C. perfringens*)	(Ryu *et al.*, 2009a)
Mangostanol [113] 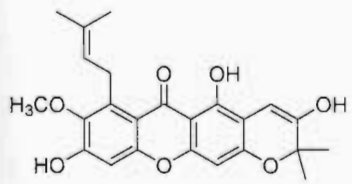	21.5 ± 0.4 μM (*C. perfringens*)	(Ryu *et al.*, 2010a)

Table 3 (continued)

Chemical compounds	IC_{50} ± SD	References
Mangostenone F [114] 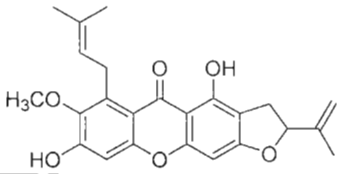	24.8 ± 0.6 μM (*C. perfringens*)	(Ryu *et al.*, 2010a)
Mangostenone G [115] 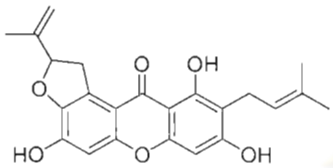	14.6 ± 0.8 μM (*C. perfringens*)	(Ryu *et al.*, 2010a)
α-mangostin [116] 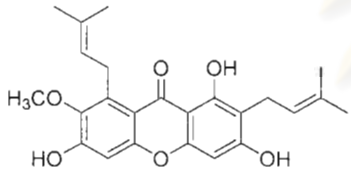	12.2 ± 1.2 μM (*C. perfringens*)	(Ryu *et al.*, 2010a)
β-mangostin [117] 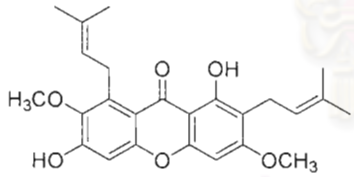	60.7 ± 1.5 μM (*C. perfringens*)	(Ryu *et al.*, 2010a)
γ-mangostin [118] 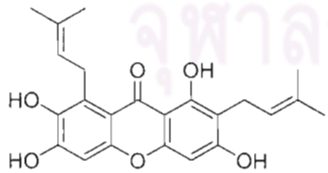	2.2 ± 0.4 μM (*C. perfringens*)	(Ryu *et al.*, 2010a)
Smeathxanthone A [119] 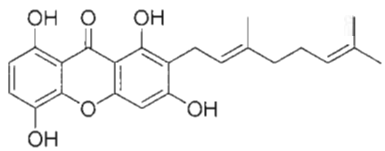	0.27 ± 0.05 μM (*C. perfringens*)	(Ryu *et al.*, 2010a)

Table 3 (continued)

Chemical compounds	IC_{50} ± SD	References
1,3,6,7-Tetrahydroxy-2-(3-methylbut-2-enyl)-8-(2-methylbut-3-en-2-yl)-9H-xanthen-9-one **[120]** 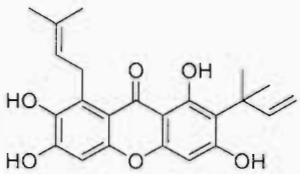	0.080 ± 0.01 μM (*C. perfringens*)	(Ryu *et al.*, 2009a)
1,3,7-Trihydroxy-4-(1,1-dimethyl-2-propenyl)-5,6-(2,2 dimethylchromeno) xanthone **[121]** 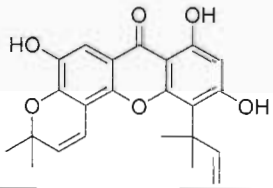	33% at 200 μM (*C. perfringens*)	(Ryu *et al.*, 2009a)
9-Hydroxycalabaxanthone **[122]** 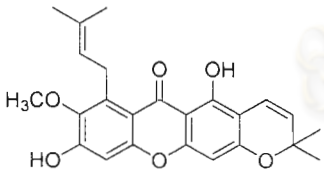	20.1 ± 1.1 μM (*C. perfringens*)	(Ryu *et al.*, 2010a)

Table 4 Miscellaneous compounds with neuraminidase inhibitory activity

Chemical compounds	Class	IC_{50} ± SD	References
Calyceramide A [123] 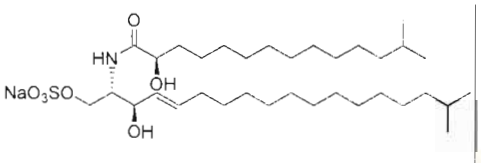	Ceramide	0.4 µg/ml (*C. perfringens*)	(Nakao *et al.*, 2001)
Calyceramide B [124] 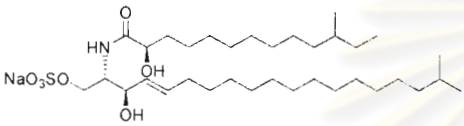	Ceramide	0.2 µg/ml (*C. perfringens*)	(Nakao *et al.*, 2001)
Calyceramide C [125] 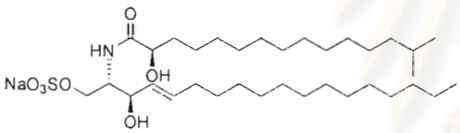	Ceramide	0.8 µg/ml (*C. perfringens*)	(Nakao *et al.*, 2001)
Glycyrin [126] 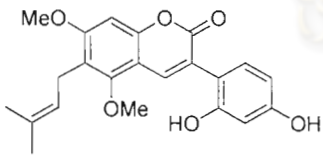	Coumarins	10% at 200 µM (rvH1N1 A/Bervig _Mission/1/18)	(Ryu *et al.*, 2010b)
Glycyrol [127] 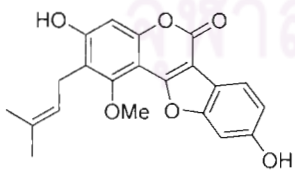	Coumarins	3.1 ± 1.0 µM (rvH1N1 A/Bervig _Mission/1/18)	(Ryu *et al.*, 2010b)
Isoglycyrol [128] 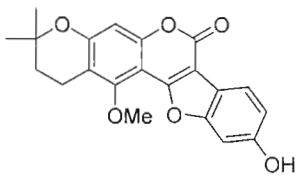	Coumarins	92.4 ± 0.7 µM (rvH1N1 A/Bervig _Mission/1/18)	(Ryu *et al.*, 2010b)

Table 4 (continued)

Chemical compounds	Class	IC_{50} ± SD	References
Licopyranocoumarin [129] 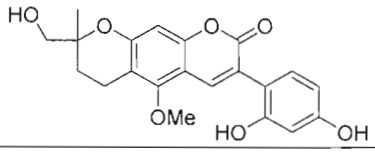	Coumarins	10% at 200 μM (rvH1N1 A/ Bervig _Mission/1/18)	(Ryu *et al.*, 2010b)
Nobiloside [130] 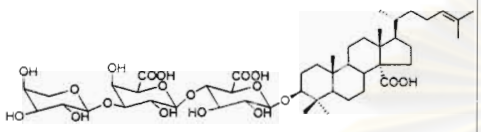	Triterpe-noidal saponin	0.46 μg/ml (*C. perfringens*)	(Takada *et al.*, 2002)

2.4 Fluorescence Quenching

Fluorescence quenching refers to any process that decreases the fluorescence intensity of a sample. A variety of molecular interactions can result in quenching. These include excited-state reactions, molecular rearrangements, energy transfer, ground-state complex formation, and collisional quenching (Lakowicz, 2006).

Fluorescence quenching has been widely studied both as a fundamental phenomenon, and as a source of information about biochemical systems. These biochemical applications of quenching are due to the molecular interactions that result in quenching. Both static and dynamic quenching requires molecular contact between the fluorophore and quencher. In the case of collisional quenching, the quencher must diffuse to the fluorophore during the lifetime of the excited state. Upon contact, the fluorophore returns to the ground state, without emission of a photon. In general, quenching occurs without any permanent change in the molecules, that is, without a photochemical reaction. In static quenching a complex is formed between the fluorophore and the quencher, and this complex is nonfluorescent (Lakowicz, 2006).

For either static or dynamic quenching to occur the fluorophore and quencher must be in contact. The requirement of molecular contact for quenching results in the

numerous applications of quenching. For example, quenching measurements can reveal the accessibility of fluorophores to quenchers. Consider a fluorophore bound either to a protein or a membrane. If the protein or membrane is impermeable to the quencher, and the fluorophore is located in the interior of the macromolecule, then neither collisional nor static quenching can occur. For this reason quenching studies can be used to reveal the localization of fluorophores in proteins and membranes, and their permeabilities to quenchers. Additionally, the rate of collisional quenching can be used to determine the diffusion coefficient of the quencher (Lakowicz, 2006).

2.4.1 Quenchers of fluorescence

A wide variety of substances act as quenchers of fluorescence. One of the best-known collisional quenchers is molecular oxygen (Kautsky, 1939), which quenches almost all known fluorophores. Depending upon the sample under investigation, it is frequently necessary to remove dissolved oxygen to obtain reliable measurements of the fluorescence yields or lifetimes. The mechanism by which oxygen quenches has been a subject of debate. The most likely mechanism is that the paramagnetic oxygen causes the fluorophore to undergo intersystem crossing to the triplet state. In fluid solutions the long-lived triplets are completely quenched, so that phosphorescence is not observed. Aromatic and aliphatic amines are also efficient quenchers of most unsubstituted aromatic hydrocarbons. For example, anthracene fluorescence is effectively quenched by diethylaniline (Knibbe *et al.*, 1968). For anthracene and diethylaniline the mechanism of quenching is the formation of an excited charge-transfer complex. The excited-state fluorophore accepts an electron from the amine. In non polar solvents fluorescence from the excited charge-transfer complex (exciplex) is frequently observed, and one may regard this process as an excited state reaction rather than quenching. In polar solvents the exciplex emission is often quenched, so that the fluorophore–amine interaction appears to be that of simple quenching. While it is now known that there is a modest through-space component to almost all quenching reactions, this component is short range (<2 Å), so that molecular contact is a requirement for quenching.

Another type of quenching is due to heavy atoms such as iodide and bromide. Halogenated compounds such as trichloroethanol and bromobenzene also act as collisional quenchers. Quenching by the larger halogens such as bromide and iodide may be a result of intersystem crossing to an excited triplet state, promoted by spin–orbit coupling of the excited (singlet) fluorophore and the halogen (Kasha, 1952). Since emission from the triplet state is slow, the triplet emission is highly quenched by other processes. The quenching mechanism is probably different for chlorine-containing substances. Indole, carbazole, and their derivatives are uniquely sensitive to quenching by chlorinated hydrocarbons and by electron scavenger (Steiner and Kirby, 1969) such as protons, histidine, cysteine, NO_3^-, fumarate, Cu^{2+}, Pb^{2+}, Cd^{2+}, and Mn^{2+}. Quenching by these substances probably involves a donation of an electron from the fluorophore to the quencher. Additionally, indole, tryptophan, and its derivatives are quenched by acrylamide, succinimide, dichloroacetamide, dimethylformamide dimethylformamide, pyridinium hydrochloride, imidazolium hydrochloride, methionine, Eu^{3+}, Ag^+, and Cs^+. Quenchers of protein fluorescence have been summarized in several insightful reviews(Eftink and Ghiron, 1981, Eftink, 1991a, Eftink, 1991b). Hence a variety of quenchers are available for studies of protein fluorescence, especially to determine the surface accessibility of tryptophan residues and the permeation of proteins by the quenchers.

Additional quenchers include purines, pyrimidines, N-methylnicotinamide and N-alkyl pyridinium, and picolinium salts (Davis, 1973, Shinitzky and Rivnay, 1977). For example, the fluorescence of flavin adenine dinucleotide (FAD) and reduced nicotinamide adenine dinucleotide (NADH) are both quenched by the adenine moiety. Flavin fluorescence is quenched by both static and dynamic interactions with adenine (Spencer and Weber, 1972), whereas the quenching of dihydronicotinamide appears to be primarily dynamic (Scott *et al.*, 1970). These aromatic substances appear to quench by formation of charge-transfer complexes. Depending upon the precise structure involved, the ground-state complex can be reasonably stable. As a result, both static and dynamic quenching are frequently observed. A variety of other quenchers are known. These are summarized in **Table 5**, which is intended to be an overview and not a

complete list. Known collisional quenchers include hydrogen peroxide, nitric oxide (NO), nitroxides, BrO_4^-, and even some olefins.

Because of the variety of substances that act as quenchers, one can frequently identify fluorophore–quencher combinations for a desired purpose. It is important to note that not all fluorophores are quenched by all the substances listed above. This fact occasionally allows selective quenching of a given fluorophore. The occurrence of quenching depends upon the mechanism, which in turn depends upon the chemical properties of the individual molecules. Detailed analysis of the mechanism of quenching is complex. In this chapter we will be concerned primarily with the type of quenching, that is, whether quenching depends on diffusive collisions or formation of ground state complexes.

2.4.2 Theory of collisional quenching

Collisional quenching of fluorescence is described by the Stern-Volmer equation:

$$I_0 / I = 1 + K_q \tau_0 [Q] = 1 + K_D [Q]$$

In this equation I_0 and I are the fluorescence intensities in the absence and presence of quencher, respectively; K_q is the bimolecular quenching constant; τ_0 is the lifetime of the fluorophore in the absence of quencher, and Q is the concentration of quencher. The Stern-Volmer quenching constant is given by $K_D = K_q \tau_0$. If the quenching is known to be dynamic, the Stern-Volmer constant will be represented by K_D Otherwise this constant will be described as K_{sv}. Quenching data are usually presented as plots of I_0 / I versus $[Q]$. This is because I_0 / I is expected to be linearly dependent upon the concentration of quencher. A plot of I_0 / I versus $[Q]$ yields an intercept of one on the *y*-axis and a slope equal to K_D. Intuitively, it is useful to note that K_D^{-1} is the quencher concentration at which $I_0 / I = 2$ or 50% of the intensity is quenched. A linear Stern- Volmer plot is generally indicative of a single class of fluorophores, all equally accessible to quencher. If two fluorophore populations are

present, and one class is not accessible to quencher, then the Stern-Volmer plots deviate from linearity toward the *x*-axis. This result is frequently found for the quenching of tryptophan fluorescence in proteins by polar or charged quenchers. These molecules do not readily penetrate the hydrophobic interior of proteins, and only those tryptophan residues on the surface of the protein are quenched (Lakowicz, 2006) .

It is important to recognize that observation of a linear Stern-Volmer plot does not prove that collisional quenching of fluorescence has occurred. Static quenching also results in linear Stern-Volmer plots. Static and dynamic quenching can be distinguished by their differing dependence on temperature and viscosity, or preferably by lifetime measurements. Higher temperatures result in faster diffusion and hence larger amounts of collisional quenching. Higher temperature will typically result in the dissociation of weakly bound complexes, and hence smaller amounts of static quenching (Lakowicz, 2006).

Table 5 Quenchers of Fluorescence (Lakowicz, 2006)

Quenchers	Typical fluorophore
Acrylamide	Tryptophan, pyrene, and other fluorophores
Amines	Anthracene, perylene
Amines	Amines Carbazole
Amine anesthetics	Perylene, anthroyloxy probes
Bromobenzene	Many fluorophores
Carbon disulfide Laser dyes	perylene
Carboxy groups	Indole
Cesium (Cs+)	Indole
Chlorinated compounds	Indoles and carbazoles
Chloride	Quinolinium, SPQ

Table 5 (continued)

Quenchers	Typical fluorophore
Cobalt (Co2+)	NBD, PPO, Perylene (Energy transfer for some probes)
Dimethylformamide	Indole
Disulfides	Tyrosine
Ethers	9-Arylxanthyl cations
Halogens	Anthracene, naphthalene, carbazole
Halogen anesthetics	Pyrene, tryptophan
Hydrogen peroxide	Tryptophan
Iodide	Anthracene
Imidazole, histidine	Tryptophan
Indole	Anthracene, pyrene, cyanoanthracene
Methylmercuric chloride	Carbazole, pyrene
Nickel (Ni2+)	Perylene
Nitromethane and nitro compounds	Polycyclic aromatic hydrocarbon
Nitroxides	Naphthalene, PAH, Tb3+, anthroyloxy probes
NO (nitric oxide)	Naphthalene, pyrene
Olefins	Cyanonaphthalene 2,3- dimethylnaphthalene, pyrene
Oxygen	Most fluorophores
Peroxides	Dimethylnaphthalene
Picolinium nicotinamide	Tryptophan, PAH
Pyridine	Carbazole
Silver (Ag+)	Perylene
Succinimide	Tryptophan
Sulfur dioxide	Rhodamine B
Thallium (Tl+)	Naphthylamine sulfonic acid
Thiocyanate	Anthracene, 5,6-benzoquinoline

CHAPTER III

MATERIALS AND METHODS

3.1 Materials

3.1.1 Neuraminidase sources

All neuraminidases from H7N3 (A/ty/Italy/8000/02LPAI), H7N1 (A/Turkey/Italy/4426/2000 LPAI) and inactivated influenza H5N1 (A/turkey/turkey/1/2005) used in this research were obtained from OIE, FAO and National Reference Laboratory for Avian Influenza and Newcastle Disease, Istituto Zooprofilattico Sperimentale delle Venezie, Padua, Italy.

3.1.1.1 Recombinant neuraminidase N3

Recombinant neuraminidase (N3) antigen was expressed using a Bac-to-Bac baculovirus expression system (Invitrogen Life Technologies) according to the manufacturer's instructions. The complete N3 ORF of the LPAI isolate A/ty/Italy/8000/02 (H7N3) was amplified, ligated into pFast-Bac donor plasmid and cloned in *E.coli* DH5α competent cells. Recombinant pFast-Bac containing the correct insert was cloned in *E.coli* DH10Bac cells containing the shuttle vector (bacmid) for the site-specific recombination. HighFive cells were transfected with the recombinant bacmid obtained; 72 hours post-transfection the supernatant containing the recombinant baculovirus particles was collected (Cattoli *et al.*, 2006, 2003).

3.1.1.2 Recombinant neuraminidase N1

Cloning and expression of gene N1 gene: Viral RNA from H7N1 4426/V00LPAI strain was extracted and the gene coding for the neuraminidase was amplified by RT-PCR using the forward primer 5'-GCC CGC GGC CGC CAG GAG TTT AAA ATG AAT CCA AAT C-3' and the reverse primer 5'-GCG CGC GGC CGC CTA CTT GTC AAT GGT GAA TGG C-3', both with a *Not* I site included (underlined). The expected product

consisted of approximately 1.4 kb. The cDNA produced was gel purified and sequenced to confirm the identity of the amplicon (Cattoli *et al.*, 2006, 2003).

The N1 amplified gene was then expressed using the Bac-to-Bac® baculovirus expression system (Invitrogen Life technologies) according to the manufacturer's instructions. Briefly, cDNA was *Not* I digested, ligated in a *Not* I-cleaved pFast-Bac donor plasmid and cloned in *E. Coli* DH5α competent cells. Colonies containing the correct insert were selected and the recombinant pFast-Bac subsequently extracted. *E. Coli* DH10Bac cells, containing the baculovirus shuttle vector (bacmic), were pFast-Bac transformed and the recombinant bacmid were isolated and used for transfection of HighFive® cells. Recombinant baculovirus particles were collected from cell cultures after 72 hours and were titrated by plaque assay. Expression of the gene of interest was confirmed by western blot (Cattoli *et al.*, 2006, 2003).

3.1.1.3 Inactivated avian influenza virus H5N1

Viral solution of A/turkey/Turkey/1/2005 (H5N1) was treated with beta-propiolactone at the appropriate dilution. The mixture was incubated for 3 hours at 37°C and stored at 4°C until use.

3.1.2 Oseltamivir analogs

Five oseltamivir analogs were synthesized by Centro Interdipartimentale Studi biomolecolari e Industriali applicati (CISI), Milan, Italy. Their synthesis was achieved through the adaptation of some published experimental protocols (Federspiel *et al.*, 1999, Rohloff *et al.*, 1998) and implied at first the preparation of a common, key amino-azide intermediate 15 (**Scheme 1**). Key intermediate **15** was acylated (**PMC 31** and **32**), acylated and reduced (**PMC33-35**), or acylated, reduced and alkylated (**PMC-36**) to provide respectively the six carboxylate esters **16**, **17**, **19**, **21**, **24** and **26**. The six esters were hydrolyzed with KOH to give the six potassium carboxylates **PMC 31-36** (**Scheme 2**).

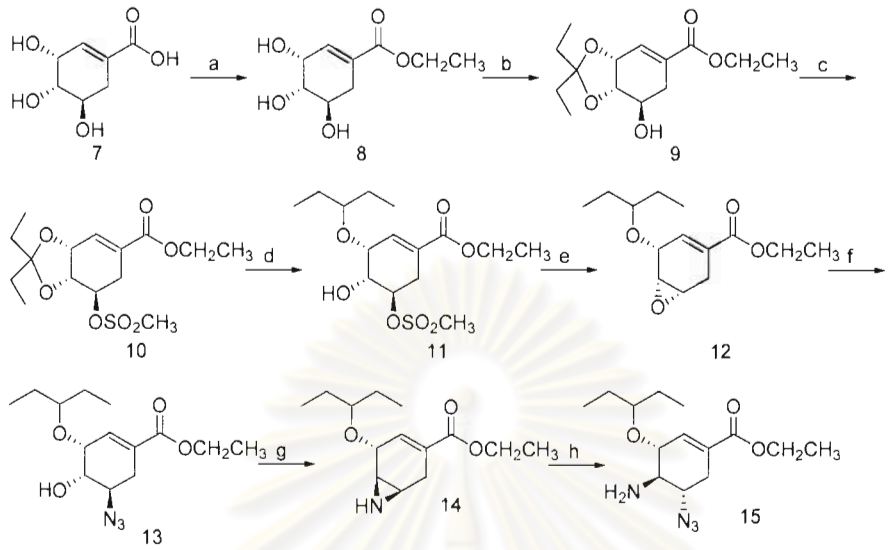

Scheme 1 (a) Ethanol, $SOCl_2$, reflux 3 hr. (b) 3-pentanone, p-TSA, toluene, 100°C, MW, 15 min (c) MsCl, TEA, DCM, rt, 2 hr. (d) Et_3SiH, $TiCl_4$, DCM, -35°C, 1 hr. (e) $KHCO_3$, H_2O, EtOH, 60°C, 1 hr. (f) NaN_3, NH_4Cl, H_2O, EtOH, 68°C, 14 hr. (g) Pme_3, THF, CH_3CN, 25°C, 10 min. (h) NaN_3, NH_4Cl, DMF, 70°C, overnight.

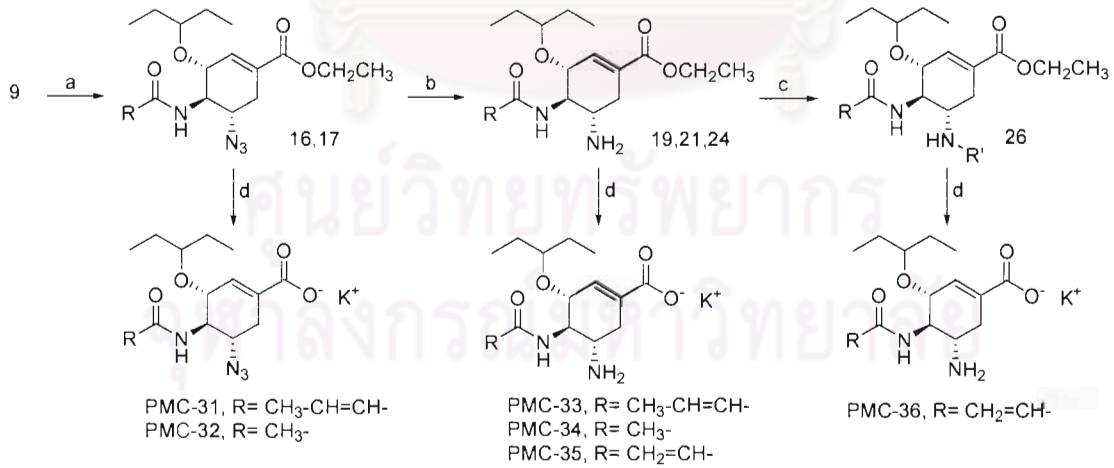

Scheme 2 (a) Acyl chloride, NMO, DCM, rt. (b) Pme_3, DCM, 1M HCl, rt. (c) aldehyde, DCM, then $NAHB(Oac)_3$, 0°C to rt. (d) 1M aq. KOH, dioxane, 4 to 23 hrs, rt.

3.1.3 Flavonoids

Thirty three flavonoids were extracted and isolated from *Dalbergia parviflora* Roxb. and *Belamcanda chinensis* (L.). The methanol extract of these plants were isolated using several chromatographic techniques. Their flavonoids structures were determined from their UV, IR, NMR and MS data (Monthakantirat *et al.*, 2005, Umehara *et al.*, 2008). Daidzein (**1**) and Quercetin (**20**) were purchased from Sigma. Oxyresveratrol (**36**) was obtained from Professor Dr. Kittisak Likhitwitayawuid. The chemical structures of 36 flavonoids used in this experiment were demonstrated in **Table 6-10** and **Figure 3**.

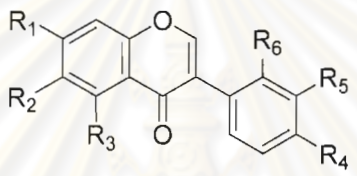

Table 6 Chemical structures of Isoflavones used in the experiment

No.	Chemical names	R1	R2	R3	R4	R5	R6
1	Daidzein	OH	H	H	OH	H	H
2	Genistein	OH	H	OH	OH	H	H
3	Calycosin	OH	H	H	OMe	OH	H
4	Biochanin A	OH	H	OH	OMe	H	H
5	Tectorigenin	OH	OMe	OH	OH	H	H
6	3'-*O*-Methylorobol	OH	H	OH	OH	OMe	H
7	Khrinone C	OH	H	OH	OMe	OH	OMe
8	Theralin	OH	H	OH	OH	H	OMe
9	2'-Methoxybiochanin A	OH	H	OH	OMe	H	OMe
10	Cajanin	OMe	H	OH	OH	H	OH
11	Irilin D	OH	OMe	OH	OH	OH	H

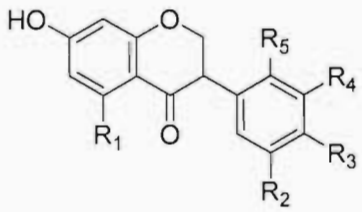

Table 7 Chemical structures of Isoflavanones used in the experiment

No.	Chemical names	R1	R2	R3	R4	R5
12	(3*R*)-7,3'Dihydroxy-4'-methoxyisoflavanone	H	H	OMe	OH	H
13	(3*S*)-Sativanone	H	H	OMe	H	OMe
14	(3*RS*)-Violanone	H	H	OMe	OH	OMe
15	Dalparvin B	H	H	OMe	OMe	OH
16	Dalparvin	H	OH	OMe	H	OMe
17	Secundiflorol H	OH	H	OMe	OH	OMe
18	(3*RS*)-Onogenin	H	$O-CH_2-O$		H	OMe
19	Dalparvin A	OH	OH	OH	H	OMe

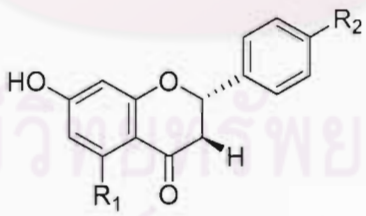

Table 8 Chemical structures of Flavanones used in the experiment

No.	Chemical names	R1	R2
21	(2*S*)- Liquiritigenin	H	OH
22	(2*S*)-Pinocembrin	OH	H
23	Alpinetin	OMe	H
24	(2*S*)-Naringenin	OH	OH

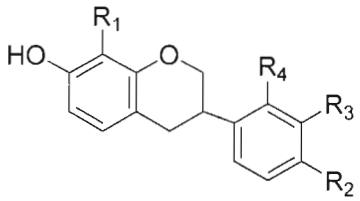

Table 9 Chemical structures of Isoflavans used in the experiment

No.	Chemical names	R1	R2	R3	R4
25	Duartin	OMe	OMe	OH	OMe
26	(3*R*)(+)-Mucronulatol	H	OMe	OH	OMe
27	(3*S*)-8-Demethylduartin	OH	OMe	OH	OMe
28	(3*RS*)-3'-Hydroxy-8-methoxyvestitol	OMe	OMe	OH	OH
29	Sativan	H	OMe	H	OMe

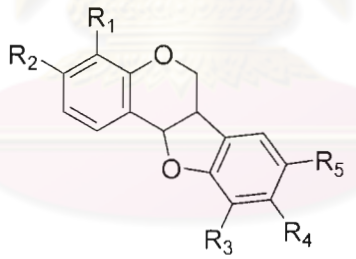

Table 10 Chemical structures of Pterocarpans used in the experiment

No.	Chemical names	R1	R2	R3	R4	R5
30	(6αR, 11αR)-3,8-Dihydroxy-9-methoxy pterocarpan	H	OH	H	OMe	OH
31	Melilotocarpan D	OH	OMe	OH	OMe	H

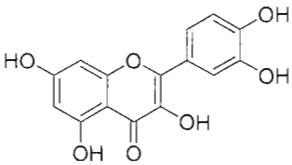

Quercetin (20)

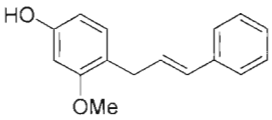

Obustyrene (32)

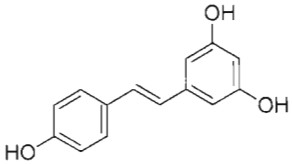

Resveratrol (33)

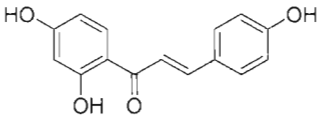

Isoliquiritigenin (34)

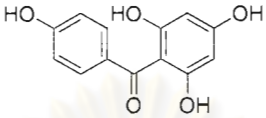

Iriflophenone (35)

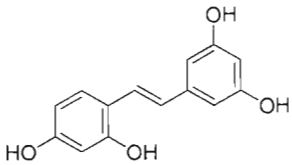

Oxyresveratrol (36)

Figure 3 Chemical structures of other flavonoids and miscellaneous compounds used in the experiment

3.2 Chemicals and reagents

- Oseltamivir free acid (Toronto Research Chemical Inc)
- 2´-(4-methylumbelliferyl)-α-D-acetyl neuraminic acid (MUNANA) (Gold-Biotechnology Inc)
- 4-Methylumbelliferone (4-MU) (Alfa Aesar GmbH & Co KG.)
- 2-N-morpholino-ethanesulfonic acid (MES) (Sigma)
- Calcium chloride (Sigma Aldrich)
- Daidzein (Sigma)
- DMSO (Sigma)
- Ethanol (Sigma)
- Quercetin(Sigma)
- Glycine (Sigma)
- Methanol (Sigma)

3.3 Instruments

- Victor^3 multilabel counter (Perkin Elmer)
- Vortex mixer (Scientific Industries)
- Refrigerated centrifuge (Beckman Coulter)
- Incubator (Memmert)
- pH meter (Eutech)

3.4 Methods

3.4.1 Establishment of *in vitro* neuraminidase inhibition assay set-up

3.4.1.1 Determination of signal to noise ratio for fluorogenic substrate, MUNANA, and 4-MU.

3.4.1.1.1 MUNANA

A serial dilution of MUNANA was carried out in a microtitre plate. For this, 100 µl of 2 mM MUNANA in 33 mM MES pH 6.5 containing 4 mM $CaCl_2$ were added and thoroughly mixed into the first well containing 100 µl of 33 mM MES pH 6.5 containing 4 mM $CaCl_2$. 100 µl of this solution were transferred to the second well containing 100 µl of 33 mM MES pH 6.5 containing 4 mM $CaCl_2$ in the same vertical lane obtaining a two-fold diluted solution of MUNANA. The 2-fold dilution process was continued up to the seventh well, with the eighth well used as blank (no inhibitor was added). At the end of the dilution process each well contained 100 µl of solution. The fluorescence intensity was recorded at excitation wavelength 355 nm and emission wavelength 460 nm.

3.4.1.1.2 4-MU

A serial dilution of 4-MU was carried out in a microtitre plate. For this, 5 µl of 0.57 mM 4-MU in ethanol were added and thoroughly mixed into the first well containing 195 µl of 33 mM MES pH 6.5 containing 4 mM $CaCl_2$. 100 µl of this solution were transferred to the second well containing 100 µl of 33 mM MES pH 6.5 containing 4 mM $CaCl_2$ in the same vertical lane obtaining a two-fold diluted solution of MUNANA. The 2-fold dilution process was continued up to the seventh well, with the eighth well used as blank (no inhibitor was added). At the end of the dilution process each well contained 100 µl of solution. Then, 100 µl of 0.1 M Glycine pH 10.7 containing 25% ethanol were added into every well. The fluorescence intensity was recorded at excitation wavelength 355 nm and emission wavelength 460 nm.

3.4.1.2 Effect of pH on fluorescence intensity of 4-MU

Ten microlitres of 0.57 mM 4-MU in ethanol were diluted in 90 µl of 6 different buffers: 0.1 M Glycine pH 2.5, 0.1 M Sodium acetate pH 4, 33 mM MES pH 6.5 containing 4 mM $CaCl_2$, PBS pH 7.2, 0.1 M Glycine pH 10.7 and 0.1 M $NaHCO_3$ pH 12.2. The fluorescence intensity was recorded at excitation wavelength 355 nm and emission wavelength 460 nm.

3.4.2 Determination of neuraminidase activity

Lyophilized of both recombinant neuraminidases H7N1 and H7N3 were dissolved in 0.5 ml of double distilled water. Stock solutions of these recombinant neuraminidases and inactivated H5N1 virus solution were prepared by diluting the supernatants in 33 mM MES pH 6.5 containing 4 mM $CaCl_2$. The N1 containing supernatant was diluted ten-fold, while the N3 supernatant and inactivated H5N1 virus solution were diluted eighty-fold.

To measure the neuraminidase activity, a 25 µl aliquot of these solutions were mixed with 90 µl of 33 mM MES pH 6.5 containing 4 mM $CaCl_2$ and incubated at 37 ^{o}C with 25 µl of 500 µM MUNANA in a transparent, medium binding ELISA plate (GREINER). After a given incubation time, the reaction was terminated by adding 100 µl of 0.1 M Glycine pH 10.7 containing 25% ethanol. The fluorescence of each reaction mixture was then recorded by using the Victor^3 multilabel counter (Perkin Elmer) with setting excitation and emission wavelengths at 355 and 460 nm respectively. A standard curve of 4-methylumbelliferone (4-MU) was established by plotting the observed fluorescence intensity versus the concentration of 4-MU.

3.4.2.1 Determination of total protein concentration

Bradford solution (Sigma-Aldrich) was diluted 1:2 with Milli Q water. 195µl of this solution was dispensed in the wells of a medium-binding strip. In wells A1 through E1, 5µl of each standard concentration of BSA in 33 mM MES pH 6.5 containing 4 mM $CaCl_2$ were added and mixed well. In F1, 5µl of N1 and N3 diluted 1:50 and 1:100 were added. The solutions were mixed well and the absorbance was recorded at 500 nm. The

recorded absorbance of the standard solutions was plotted as a function of BSA concentration to get a standard curve. The concentration of the sample was determined from this standard calibration curve.

3.4.2.2 Determination of Michelis-Menten constant for MUNANA

For the determination of Michealis constant (K_m), 25 µl of the diluted supernatant containing the recombinant neuraminidases (ten–fold for H7N1 and eighty-fold for H7N3) were incubated at 37 °C with an equal volume of MUNANA spanning the concentration range of 0-2000 µM. The reaction velocity was measured every 30 minutes for 2 hours. The enzyme kinetic data were fit to the Lineweaver-Burk plot in order to determine K_m of substrate conversion (Lineweaver, 1934).

3.4.2.3 Determination of *Ki* for oseltamivir carboxylate

To conveniently determine the *Ki* of oseltamivir carboxylate for neuraminidases H7N1 H7N3 and H5N1, a 96 (12 x 8) wells microtitre plate was used as an array of reaction vessels. The concentrations of enzyme and substrate were kept constant in all of the wells, while the concentration of the inhibitor was varied by performing a two-fold dilution along the vertical direction of the plate from wells A1••••G1. In well H1 the inhibitor was not added for a positive control. After the mixture was incubated for 2 hours, the substrate MUNANA was added in each well. The complete reaction mixtures were then stopped in a sequential manner of time course: 30 minutes for the vertical lanes A1-H1, 60 minutes for A2-H2, 90 minutes for A3-H3, etc. By proceeding in this way, the fluorescence reading of the wells A1, A2, A3,•••A12 plotted against time would give the kinetic of MUNANA cleavage in the presence of the highest inhibitor concentrations. The reading of the wells B1, B2, B3,•••B12 plotted against time would give the kinetic of MUNANA cleavage in the presence of a 2-fold diluted inhibitor concentration, and so on and so forth. The fluorescence reading of the wells H1, H2, H3,•••H12 plotted against time gives the kinetic of MUNANA cleavage in the absence of the inhibitor.

3.4.2.4 *Ki* determination for recombinant neuraminidases H7N1 H7N3 and inactivated H5N1

Ninety microlitres of 33 mM MES pH 6.5 containing 4 mM $CaCl_2$ were dispensed in each well of the plate except for the first well of each lane. In the first well of each vertical lane 18 µl of 0.01 mM oseltamivir for H7N1 and 0.1 µM for H7N3 and H5N1 were mixed with 162 µl of 33 mM MES pH 6.5 containing 4 mM $CaCl_2$, the solution was thoroughly mixed to obtain a solution of 5 µM for H7N1 assay and 0.05 µM for H7N3 and H5N1 assay. For each assay, a 90 µl aliquot of this solution was withdrawn from the first well and added to the second well in the same vertical lane obtaining a two-fold diluted solution of oseltamivir. The 2-fold dilution process was continued up to the seventh well, with the eighth well used as blank (no inhibitor was added). At the end of the dilution process each well contained 90 µl of solution. To each well, 25 µl of enzyme stock solution were added. After an incubation time of 2 hours, 25 µl of MUNANA were added to each well, the final concentrations of oseltamivir carboxylate spanned the range 10-643 nM for H7N1 assay and 0.1-6.43 nM for H7N3 and H5N1 assay. After 30 minutes of incubation, 50 µl of stop solution were added to the first vertical lane, and the fluorescence was recorded. After an additional 30 minutes (60 minutes total) the stop solution was added to the second vertical lane and the fluorescence recorded. After additional 30 minutes (90 minutes total) the stop solution was added to the third vertical lane and the fluorescence recorded etc. The experiment was performed in duplicate. The initial velocities of the reactions were plotted against the concentration of inhibitor and the data were analysed according to Dixon (Dixon, 1953)

3.4.3 Validation of neuraminidase inhibition assay

In a microtitre plate, 90 µl of 33 mM MES pH 6.5 containing 4 mM $CaCl_2$ were dispensed in a suitable number of wells. In the first well 10 µl of oseltamivir carboxylate solutions (1 mM for H7N1 inhibition assay and 10 µM for H7N3 and H5N1 inhibition assay) were added and the solution was thoroughly mixed obtaining a 0.1 mM (for H7N1) and 1 µM (for H7N3 and H5N1) oseltamivir concentrations. A 10 µl aliquot of this solution was transferred based on ten-fold dilution to obtain a 0.1 nM solution of

oseltamivir for the H7N1 assay and 0.001 nM for the H7N3 and H5N1 assay, the final volume in each well was 90 µl. To each well, 25 µl of the enzyme stock solution were mixed with the oseltamivir solution and incubated for 2 hours at 37 °C. After the incubation time, 25 µl of 20 µM MUNANA were added. In the reaction mixture the final concentration of oseltamivir carboxylate spanned in the ranges 0.064 nM-64.2 µM for H7N1 assay and 0.64 pM-642 nM for H7N3 and H5N1 assay. After incubating the plate for 5 hours at 37°C, 50 µl of stop solution (0.1 M glycine, pH 10.7 containing 25% ethanol) were added. The fluorescence of the solutions contained in each well was read with the Victor ^{3} multilabel counter. The 50% inhibitory concentration (IC_{50}) was determined from dose-response curve using GraphPad Prism 5; GraphPad, San Diego,CA).

3.4.4 Neuraminidase inhibitory activity of various test compounds

3.4.4.1 Synthesized oseltamivir analogs

3.4.4.1.1 Analysis of inhibition against recombinant H7N1

In a microtitre plate, 90 µl of 33 mM MES buffer pH 6.5 containing 4 mM $CaCl_2$ were dispensed in a suitable number of wells. Since PMC-35 was insoluble in 33 mM MES buffer pH 6.5, 10% DMSO was added in this case. 10 µl of 1 mM oseltamivir carboxylate and its analogues were added in the first well, and the solution was thoroughly mixed obtaining a 0.1 mM inhibitor concentration. A 10 µl aliquot of this solution was transferred in a second well and thoroughly mixed, reaching after dilution an inhibitor concentration of 0.01 mM. The process was continued until the seventh, 0.1 nM inhibitor concentration was obtained, at the end of the dilution process. Each well contained a final volume of 90 µl. 25 µl of enzyme stock solution were added to each well, and the mixtures were incubated for 2 hours at 37 °C; after the incubation time, 25 µl of a 20 µM MUNANA solution were added, with final concentrations of oseltamivir carboxylate or its analogs spanning the 0.064 nM - 64.2 µM range. After incubating the plate for 5 hours at 37°C, 50 µl of stop solution (0.1 M glycine in 25% aqueous EtOH, pH 10.7) were added. The fluorescence of the solutions contained in each well was read

with the Victor^3 multilabel counter. The 50% inhibitory concentration (IC_{50}) was determined from the dose-response curve using the GraphPad Prism 5 software (GraphPad, San Diego, CA). All measurements were replicated in three to five independent experiments.

3.4.4.1.2 Analysis of inhibition against recombinant H7N3

Procedure for PMC-34 (4), PMC-35 (5), PMC-36 (6) and oseltamivir free acid:

90 µl of 33 mM MES buffer pH 6.5 containing 4 mM $CaCl_2$ were dispensed in a suitable number of wells in a microtiter plate. Namely, 10 µl of 10 µM inhibitor solutions (PMC-34, PMC-35 and commercial oseltamivir) were added in the first well and the mixture was thoroughly mixed obtaining a 1 µM inhibitor concentration. A 10 µl aliquot of this solution was transferred in a second well and thoroughly mixed obtaining a 0.1 µM inhibitor solution. The process was continued until the seventh 0.001 nM solution was obtained, at the end of the dilution process. Each well contained a final volume of 90 µl. 25 µl of enzyme stock solution were added to each well, and the mixtures were incubated for 2 hours at 37 °C; after the incubation time, 25 µl of a 20 µM MUNANA solution were added, with final concentrations of oseltamivir carboxylate or its analogs spanning the 0.00064 nM - 642 nM range. After incubating the plate for 5 hours at 37°C 50 µl of stop solution (0.1 M glycine in 25% aqueous EtOH, pH 10.7) were added. The fluorescence of the solutions contained in each well was read with the Victor^3 multilabel counter. The 50% inhibitory concentration (IC_{50}) was determined from dose-response curve using a GraphPad Prism 5 software (GraphPad, San Diego, CA). All measurements were replicated in three to five independent experiments.

Procedure for PMC-31 (1), PMC-32 (2), PMC-33 (3):

For PMC-31 (1), PMC-32 (2), PMC-33 (3), the same procedure described for the N1 study was used. The 50% inhibitory concentration (IC_{50}) was determined from dose-response curves using the GraphPad Prism 5 software (GraphPad, San Diego, CA). All measurements were replicated in three to five independent experiments.

3.4.4.1.3 Analysis of inhibition against virus solution H5N1

In a microtitre plate, 90 µl of 33 mM MES buffer pH 6.5 containing 4 mM $CaCl_2$ were dispensed in a suitable number of wells. Since PMC-35 was insoluble in 33 mM MES buffer pH 6.5, 10% DMSO was added in this case.

PMC-31: 20 µl of 10 mM PMC-31 were added in a first well, and the solution was thoroughly mixed obtaining a 1.8 mM inhibitor concentration. A 20 µl aliquot of this solution was transferred in the second well and thoroughly mixed, reaching after dilution an inhibitor concentration of 0.3 mM. The process was continued until a seventh, 65 nM inhibitor concentration was obtained.

PMC-32, 33: 10 µl of 0.01 mM PMC-32, 33 were added in the first well and the solution was thoroughly mixed obtaining a 0.1 mM inhibitor concentration. A 10 µl aliquot of this solution was transferred in a second well and thoroughly mixed, reaching after dilution an inhibitor concentration of 0.01 mM. The process was continued until a seventh, 0.1 nM inhibitor concentration was obtained.

PMC-34, 35, 36 and oseltamivir: 10 µl of 0.01 mM PMC-34, 35, 36 and oseltamivir were added in the first well, and the solution was thoroughly mixed obtaining a 1 µM inhibitor concentration. A 10 µl aliquot of this solution was transferred in a second well and thoroughly mixed, reaching after dilution an inhibitor concentration of 0.1 µM. The process was continued until the seventh, 1 pM inhibitor concentration was obtained.

At the end of the dilution process, each well contained a final volume of 90 µl. 25 µl of enzyme stock solution were added to each well, and the mixtures were incubated for 2 hours at 37 °C; after the incubation time, 25 µl of a 20 µM MUNANA solution were added. After incubating the plate for 2 hours at 37°C, 50 µl of stop solution (0.1 M glycine in 25% aqueous EtOH, pH 10.7) were added. The fluorescence of the solutions contained in each well was read with the Victor^3 multilabel counter. The 50% inhibitory concentration (IC_{50}) was determined from the dose-response curve using the GraphPad Prism 5 software (GraphPad, San Diego, CA). All measurements were replicated in three independent experiments.

3.4.4.2 Flavonoids

3.4.4.2.1 Inhibition test of flavonoids at 714 μM

Ten microlitres of 10 mM flavonoids solution in methanol were mixed with 80 μl of 33 mM MES pH 6.5, 4 mM $CaCl_2$ in microtitre plate, 25 μl of enzyme solution were then added. This mixture was incubated for 2 hours at 37 °C, then 25 μl of 20 μM MUNANA were added to each well to initiate the enzymatic reaction. After incubating the plate at 37 °C for approximately 5 hours, the reaction was terminated by adding 50 μl of stop solution (0.1 M glycine, pH 10.7 containing 25% Ethanol). The fluorescence was measured by using the Victor^3 multilabel counter (Perkin Elmer) with excitation and emission wavelengths of 355 and 460 nm respectively.

3.4.4.2.2 Inhibition test of flavonoids at 142 μM

Flavonoids showed inhibitory activity more than 50 % from previous experiment [1mM] were tested for the inhibitory activity at 200 μM. For this, 10 μl of 2 mM flavonoid solution were mixed with 80 μl of 33 mM MES pH 6.5, 4 mM $CaCl_2$ in microtitre plate. 25 μl of enzyme solution were then added. This mixture was incubated for 2 hours at 37 °C, then 25 μl of 20 μM MUNANA were added to each well to initiate the enzymatic reaction. After incubating the plate at 37 °C for approximately 5 hours, the reaction was terminated by adding 50 μl of stop solution (0.1 M glycine, pH 10.7 containing 25% Ethanol). The fluorescence was measured by using the Victor^3 multilabel counter (Perkin Elmer) with excitation and emission wavelengths of 355 and 460 nm respectively.

3.4.4.2.3 Dose-response curves of flavonoids

In a microtitre plate, 20 μl of 10 mM flavonoids were added in the first well containing 160 μl of 33 mM MES buffer pH 6.5 containing 4 mM $CaCl_2$. The solution was thoroughly mixed obtaining a 1.1 mM flavonoids' concentration. A 90 μl aliquot of this solution was transferred in a second well containing 90 μl of 33 mM MES buffer pH 6.5 containing 4 mM $CaCl_2$, reaching after dilution a flavonoids' concentration of 0.55 mM. The process was continued until the seventh, 8.7 μM flavonoids' concentration was

obtained. At the end of the dilution process, each well contained a final volume of 90 µl. 25 µl of enzyme stock solution were added to each well, and the mixtures were incubated for 2 hours at 37 °C; after the incubation time, 25 µl of a 20 µM MUNANA solution were added. After incubating the plate for 2 hours at 37°C, 50 µl of stop solution (0.1 M glycine in 25% aqueous EtOH, pH 10.7) were added. The fluorescence of the solutions contained in each well was read with the Victor3 multilabel counter. The 50% inhibitory concentration (IC_{50}) was determined from the dose-response curve using the GraphPad Prism 5 software (GraphPad, San Diego, CA). All measurements were replicated in three independent experiments.

3.4.5 Quenching test of flavonoids on fluorescence intensity of 4-MU

Ninety microlitres of two-fold serial dilution of different flavonoids dissolved in 44 % methanol in 33 mM MES pH 6.5, 4 mM $CaCl_2$ with concentration in the range 0-1 mM were prepared in microtitre plate. 25 µl of 33 mM MES pH 6.5, 4 mM $CaCl_2$ and 25 µl of 20 µM 4-methylumbelliferone were added to each well. Finally, 50 µl of stop solution (0.1 M glycine, pH 10.7 containing 25% Ethanol) were added. The fluorescence was measured by using the Victor^3 multilabel counter (Perkin Elmer) with excitation and emission wavelengths of 355 and 460 nm respectively.

CHAPTER IV

RESULTS

4.1 Establishment of *in vitro* neuraminidase inhibition assay

4.1.1 Setting up of a standard neuraminidase assay

The assay set-up requires the study of various factors to obtain optimal experimental conditions. These include substrate concentration, limit of detection of the reaction product by using 4-MU and the signal to noise ratio for the 4-MU analysis. In the experiments, the minimum concentration of 4-MU that could be detected was found to be as low as 70 ± 15 nM corresponding to 14 ± 3 pmol of 4-MU per well (The limit of detection was set from the fluorescence intensity of 4-MU in which 3-fold higher than standard deviation of blank). The reaction mixture was then used as follows: 1 mg of 4-MU was dissolved in 1 ml of ethanol on eppendorf tube. A serial dilution of 4- MU with 33 mM MES pH 6.5 containing 4 mM $CaCl_2$ ranging from 17.3 nM to 141.9 mM in a total volume of 100 µl in a transparent, medium binding ELISA plate was carried out. 100 µl of stop solution were added in each well followed by reading the fluorescence intensity. The results showed that the fluorescence intensity increased linearly when the concentration of 4-MU did not exceed than 35 µM. After that the saturation of fluorescence intensity was then observed (**Figure 4**). The linear range for detection of fluorescence intensity of 4-MU was in the range of 70 nM to 35 µM. We also noticed that fluorescence intensity of 4-MU is high enough to allow the use of transparent plate instead of the black well plate normally used for fluorometric analysis without hampering the reliability of the assay.

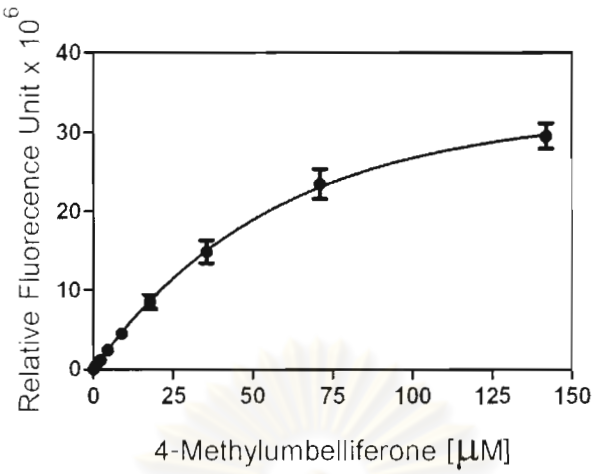

Figure 4 Fluorescence intensity of 4-MU in the range from 17.3 nM to 141.9 μM

In terms of pH dependence, the reaction mixture was determined at the concentration of 1 mg/ml using 6 different buffers: 0.1 M Glycine pH 2.5, 0.1 M Sodium acetate pH 4, 33 mM MES pH 6.5 containing 4 mM $CaCl_2$, PBS pH 7.2, 0.1 M Glycine pH 10.7 and 0.1 M $NaHCO_3$ pH 12.2. The results showed that the fluorescence intensity of 4-MU increased when increasing pH of buffers (Figure 5). Among 6 different buffers, 0.1 M Glycine pH 10.7 and 0.1 M $NaHCO_3$ pH 12.2 are the optimum buffers that fluorescence intensity of 4-MU reached the maximum intensity. From this experiment, we chose 0.1 M Glycine pH 10.7 as a stop solution for enhancing fluorescence intensity of 4-MU.

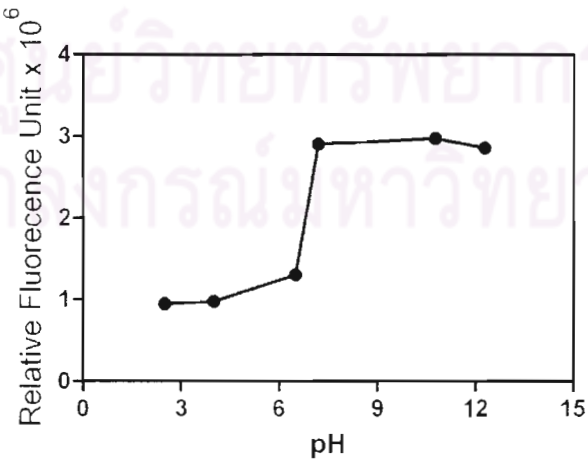

Figure 5 Effect of pH on the florescence intensity of 4-methylumbelliferone.

4.1.2 Characterization of neuraminidase from various sources

4.1.2.1 Recombinant H7N1 and H7N3 neuraminidases

The development of neuraminidase inhibitory screening assay required preliminary assessment of the presence of enzyme activity of the crude recombinant neuraminidase preparations. This could be carried out by determining fluorometrically using 2′-(4-methylumbelliferyl)-α-D-acetyl neuraminic acid (MUNANA) as the substrate. The amount of 4-MU released by the enzymatic reaction was then determined by comparison with the calibration curve obtained by plotting the fluorescence intensity of an authentic sample of 4-MU against its concentration. The results showed that the total protein concentration of H7N1 and H7N3 neuraminidases were in the same level (19.6 ± 1.8 mg/ml for H7N1 and 26.6 ± 4.1 mg/ml for H7N3) whereas the specific activities were quite different, with only 0.04 mU/mg for H7N1 and a ten fold high (0.4 mU/mg) for H7N3 (**Table 11**).

Table 11 Total protein concentration and specific activity of recombinant H7N1 and H7N3

Avian Influenza Type	Total protein ± SD (mg/ml)	Specific activity (mU/mg)*
H7N1	19.6 ± 1.8	0.04
H7N3	26.6 ± 4.1	0.4

* One unit of enzyme activity is defined as the amount of active neuraminidase enzyme required to release one micromole of 4-MU per minute at 37 °C.

The enzyme activities of H7N1 and H7N3 were further characterized by determining their Michaelis-Menten constant (*Km*) against MUNANA. The enzyme preparations were incubated with increasing amounts of substrate spanning the range 0-2000 μM. The initial rate of the enzymatic reaction was then plotted against the substrate concentrations. As shown in **Figures 6-7**, both neuraminidases preparations showed well behaved enzyme activities against substrate concentration band on both the normal and Lineweaver-Burk plots. The Michaelis-Menten constant obtained for

neuraminidase H7N1 appeared to be 400 ± 60 μM (**Figure 6, A-B,Table 12**), while the Michaelis constant for H7N3 was 87 ± 4 μM (**Figure 7, A-B, Table 12**).

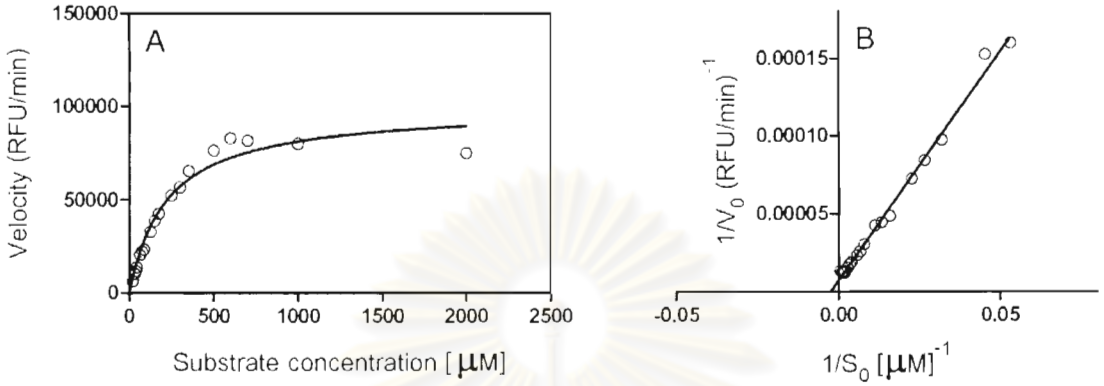

Figure 6 Neuraminidase kinetics (A) and Lineweaver-Burk plot (B) of the recombinant H7N1 neuraminidase

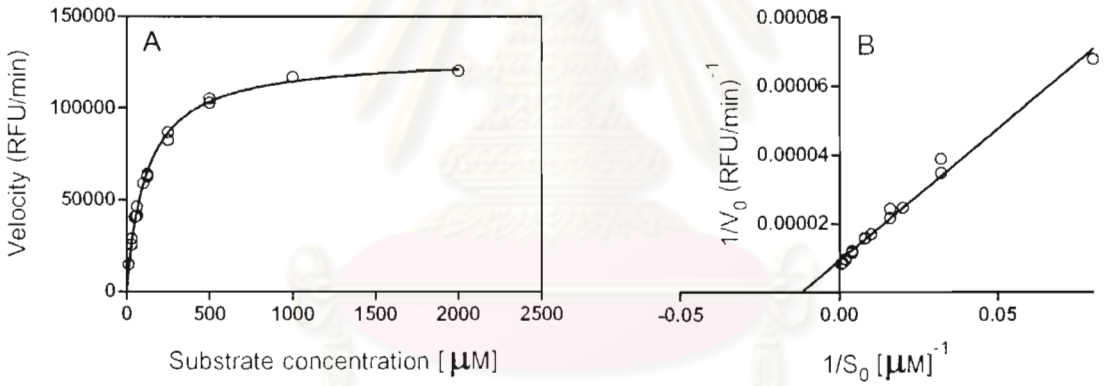

Figure 7 Neuraminidase kinetics (A) and Lineweaver-Burk plot (B) of the recombinant H7N3 neuraminidase

To further characterize the enzyme activity, a series of kinetic experiments were carried out in order to determine the inhibition constants, Ki, of oseltamivir carboxylate. By plotting the initial velocity of the reaction against the concentration of oseltamivir carboxylate at a fixed concentration of substrate, a linear Dixon plot was obtained for each of the enzymes. As shown in **Figures 8A-10A**, the Ki values for recombinant neuraminidase H7N1 and recombinant neuraminidase H7N3 were found to be 23.5 ± 7.2 nM and 0.12 ± 0.11 nM, respectively (**Table 12**). Based on these data the IC_{50} of oseltamivir carboxylate could be calculated using the following equation which was

found to be the values of 25 ± 4 nM for recombinant neuraminidase H7N1 and 0.2 ± 0.02 nM for recombinant neuraminidase H7N3.

Table 12 Enzymatic characterization of the recombinant H7N1, H7N3 neuraminidases, and the inactivated H5N1 virus solution

Recombinant protein	*Km* ± SD (μM)[a]	Mean IC_{50} ± SD (nM)[a,b]	*Ki* ± SD (nM)[a]
N1	400 ± 60	25 ± 4	23.5 ± 7.2
N3	87 ± 4	0.2 ± 0.02	0.12 ± 0.11
Inactivated H5N1	-	0.4 ± 0.1	-

[a] K_m, IC_{50} and *Ki* were obtained from three independent experiments.

[b] IC_{50} is a concentration of Oseltamivir which inhibit by 50% the neuraminidase activity.

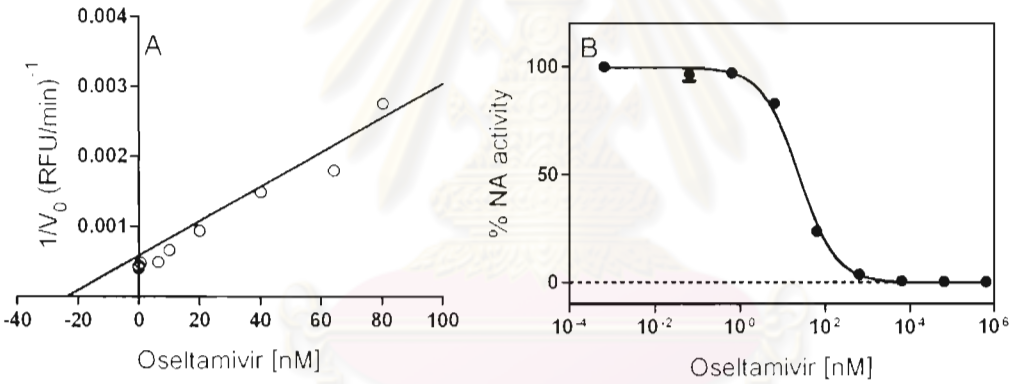

Figure 4 Dixon plots (A) and a dose-response curve (B) for inhibition of oseltamivir carboxylate on the recombinant H7N1 neuraminidase

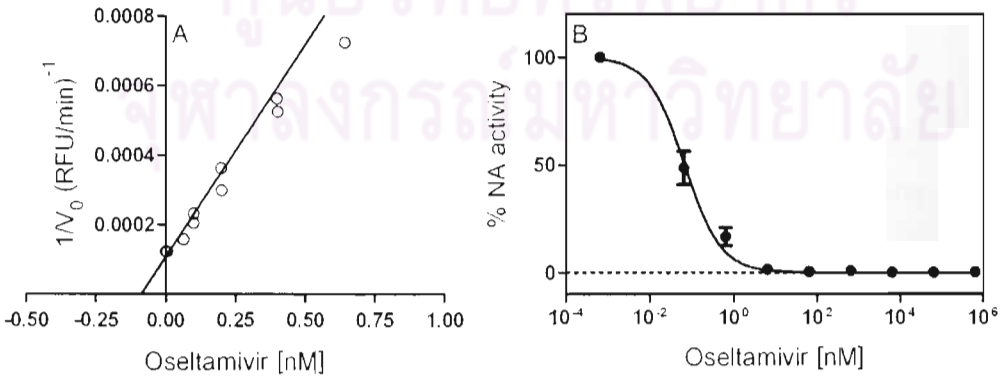

Figure 5 Dixon plots (A) and a dose-response curve (B) for inhibition of oseltamivir carboxylate on the recombinant H7N3 neuraminidase

4.1.2.2 Inactivated influenza H5N1 virus (A/turkey/turkey/1/2005)

For characterization of the inactivated avian influenza virus H5N1, 25 µl of this solution was incubated with 20 µM MU-NANA. A stop solution (0.1 M glycine, pH 10.7 containing 25% Ethanol) was then added after 2 hours of incubation time. The fluorescence was measured by using the Victor^3 multilabel counter (Perkin Elmer) with excitation and emission wavelengths of 355 and 460 nm respectively. The neuraminidase activity was plotted against the various amount of viral solution. It was found that neuraminidase activity still remained in this viral solution since enzymatic activity decreased when the viral solution was diluted (**Figure 10A**). An eighty-fold of inactivated H5N1 was further investigated for the inhibitory activity on oseltamivir. A well behavior of a dose-response curve was obtained (**Figure 10B**). The IC_{50} value was found to be 0.4±0.1 nM (**Table 12**).

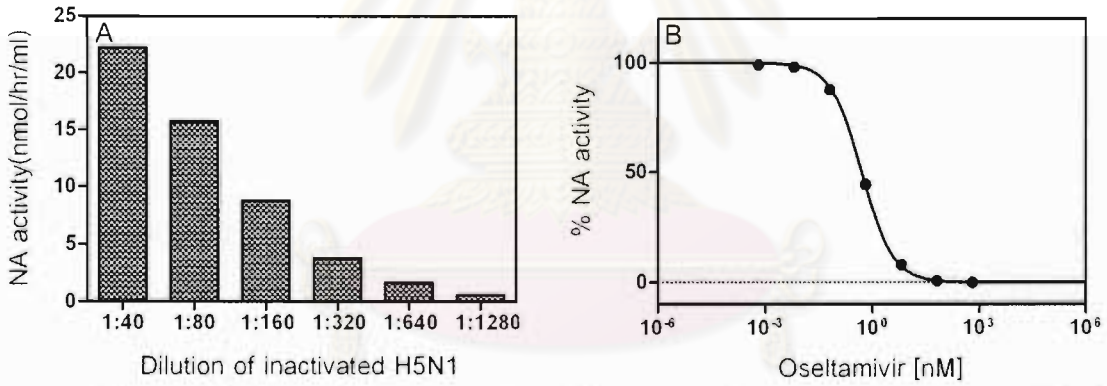

Figure 10 Neuraminidase activity (A) and a dose-response curve (B) of inactivated H5N1 virus

4.1.3 Screening assay set-up and validation

In setting up a screening neuraminidase inhibitory assay using the characterized neuraminidase preparations, a 96-well microtiter plate was employed as an array of reaction vessels. Each vessel could be used to test a single compound at a given concentration. Practically, each test compound is incubated for two hours in the presence of the neuraminidases (H7N1, H7N3 and H5N1), and afterwards the substrate is added. The reaction mixture is then incubated for 5 hours at 37 °C, followed by

stopping the reaction by addition the suitable amount of the stop solution. The fluorescence intensity in each well is read by using an excitation and emission wavelengths of 355 and 460 nm respectively.

To validate this assay set-up, we used the specific neuraminidase inhibitor oseltamivir carboxylate as a benchmark compound, with different concentrations in order to assess the sensitivity and the repeatability of the system. The reproducibility of the fluorescence reading was evaluated by determining the within- and between-assay coefficient of variations (CV) in the repeated analysis. It was found that the within-assay CV values were 4.6% for recombinant neuraminidase H7N1, 3.8% for recombinant neuraminidase H7N3 and 5.3% for inactivated virus H5N1, while the between-assay CV values were found to be 12%, 5 % and 11% for recombinant neuraminidase H7N1, H7N3 and inactivated virus H5N1 respectively, based on six replicate experiments. The IC_{50} values of oseltamivir against recombinant neuraminidase H7N1, H7N3 and inactivated virus H5N1 showed the values of 25 ± 4 nM and 0.2 ± 0.02 nM and 0.4 ± 0.1 nM respectively (**Table 12**). The dose-response curves obtained are shown in **Figures 8B-10B** which also gave the IC_{50} values for both enzymes in good agreement with the values obtained by the inhibition kinetics, and thus confirming the robustness of the assay.

4.3 Neuraminidase inhibitory activity of various test compounds

4.3.1 Synthesized oseltamivir analogs

Five synthesized oseltamivir analogs were tested for their neuraminidase inhibitory activity against H7N1, H7N3 and H5N1. Their chemical structures are shown in **Figure 11**.

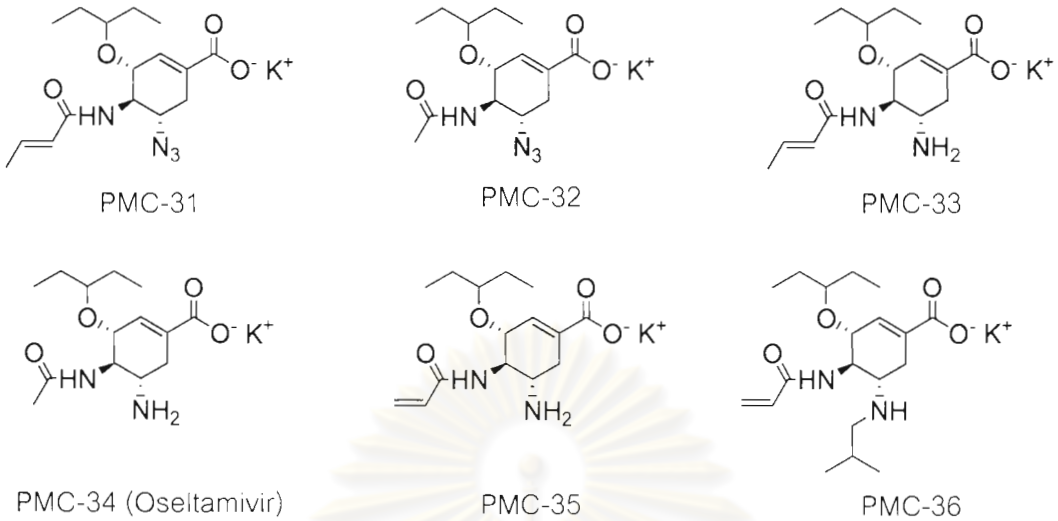

Figure 11 The chemical structures of oseltamivir (PMC-34) and oseltamivir analogs.

4.3.1.1 Neuraminidase inhibitory activity on recombinant H7N1 neuraminidase

All the inhibitors were tested at different concentrations, ranging from 0.064 nM to 64.2 μM. A dose-response curve was obtained for each compound. Fitting of the experimental data allowed the determination of the IC_{50} for each compound; the experimental data are shown in **Figure 12**. The inhibitory activity of the six compounds is also shown for two selected concentrations (64.3 nM and 642 nM) in **Figure 13**.

The analysis of the experimental data indicated that PMC-36 was the best inhibitor of N1 activity within the panel of tested compounds, displaying an IC_{50} of 14.6 ± 3.0 nM, while commercial oseltamivir displayed an IC_{50} of 24.9 ± 3.9 nM; a synthetically prepared sample of oseltamivir, PMC-34, was also included in this analysis and it displayed an IC_{50} of 39.3 ± 3.2 nM (**Table 13**). Compound PMC-35 displayed an IC_{50} of 31.8 ± 6.9 nM, while PMC-32 was less active with an IC_{50} of 84.4 ± 20 nM. Both PMC-33 and PMC-31 had a limited inhibitory activity with an IC_{50} of 138.9 ± 21 μM and 51.6 ± 3.0 μM respectively (**Table 13**).

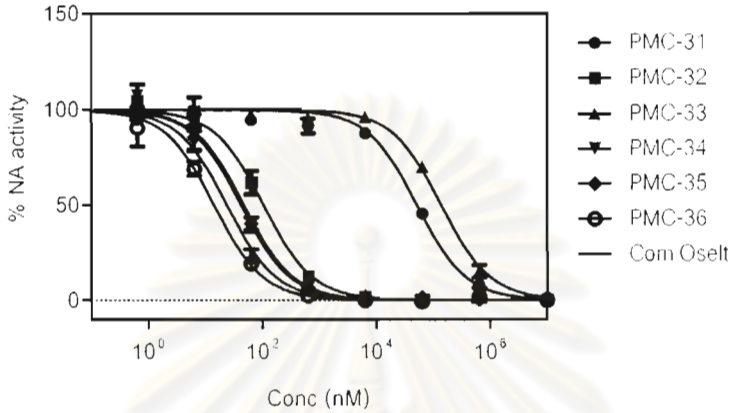

Figure 12 Dose-response curves of oseltamivir and its analogues against H7N1 neuraminidase

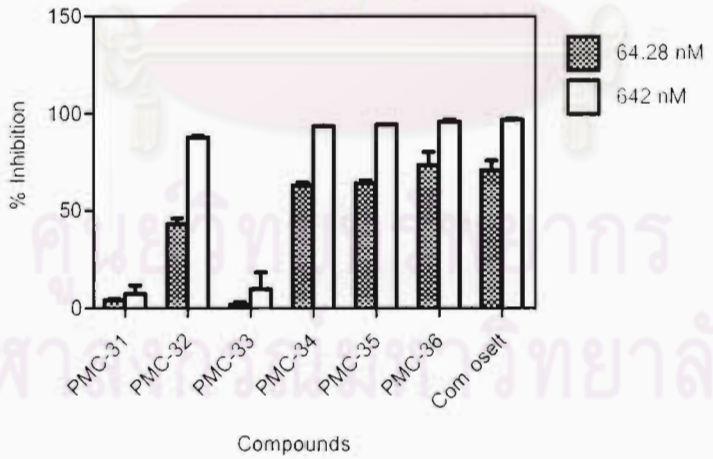

Figure 13 Inhibitory activity of the test compounds against H7N1 neuraminidase

ต้นฉบับไม่มีหน้านี้

NO THIS PAGE IN ORIGINAL

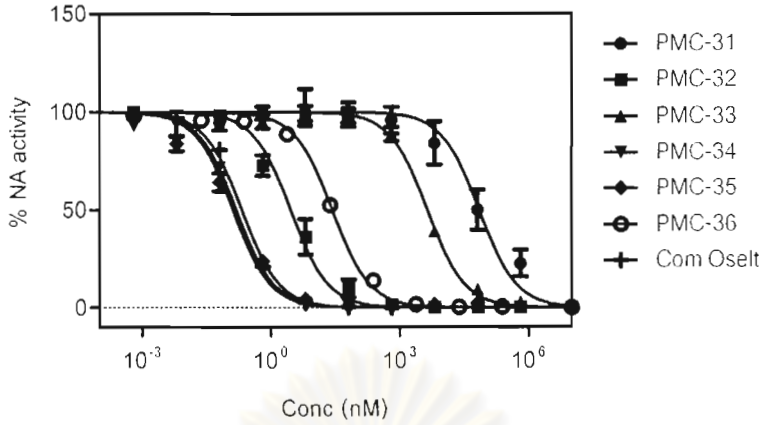

Figure 14 Dose-response curves of oseltamivir and its analogues against H7N3 neuraminidase

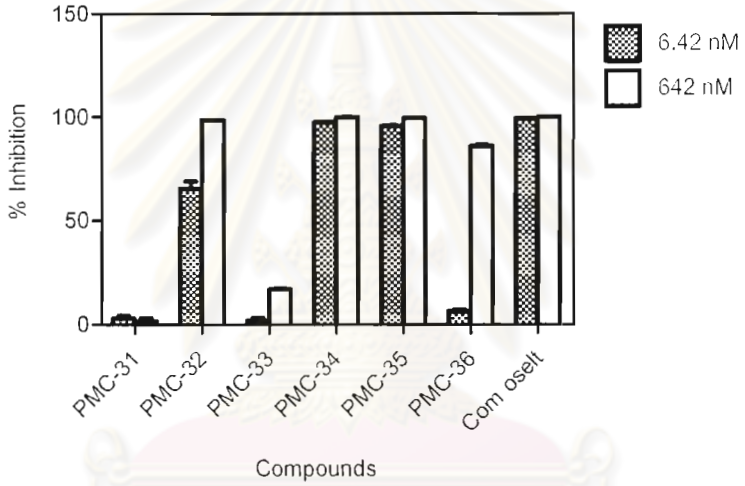

Figure 15 Inhibitory activity of the test compounds against H7N3 neuraminidase

Among the tested compounds PMC-35, PMC-34 and commercial oseltamivir showed a potent inhibitory activity on neuraminidase subtype 3 with IC_{50} of 0.1 ± 0.03, 0.1 ± 0.08 and 0.2 ± 0.02 nM respectively. All the other compounds displayed a lower inhibitory potency, with IC_{50} values ranging from 2.2 ± 1.4 nM for PMC-32 to 99.3 ± 32.4 μM for PMC-31. The data for the whole set of tested compounds is reported in **Table 14**.

Table 14 IC_{50} values of oseltamivir analogs against H7N3 avian influenza virus A

Compounds	IC_{50} ± SD on H7N3 (nM)
PMC-31	99,295 ± 32,416
PMC-32	2.2 ± 1.4
PMC-33	4,512 ± 1,172
PMC-34 (oseltamivir)	0.1 ± 0.08
PMC-35	0.1 ± 0.03
PMC-36	28.1 ± 9.7
Commercial oseltamivir	0.2 ± 0.02
Oseltamivir carboxylate	2.9[a] – 3.3[b]

[a] Influenza virus: A/duck/Singapore/3/97 (H5N3)

[b] Influenza virus: A/duck/Germany/1215/73 (H2N3)

4.3.1.3 Neuraminidase inhibitory activity on H5N1 neuraminidase

The concentration of oseltamivir analogs used in this study can be divided into 3 ranges. For PMC-31, the concentration started from 0.04 μM to 1.17 mM while PMC-32 and PMC-33, the concentration spanned the range of 0.06 nM to 64.28 μM. For PMC-34 (oseltamivir), PMC-35 and PMC-36, the concentration was in range of 0.64 pM to 642 nM. It was found that PMC-35 showed the inhibitory effect with the IC_{50} of 1.7 ± 0.2 nM which close to that of PMC-34 (oseltamivir carboxylate, IC_{50} = 1.2 ± 0.1 nM). PMC-36 also displayed good inhibitory activity with the IC_{50} of 2.5 ± 0.4 nM while PMC-32 (IC_{50} = 53.6 ± 4.3 nM) showed moderate inhibitory effect compared with PMC-35 and PMC-36. We also found that PMC-31 and PMC-32 showed less inhibitory activity among tested compounds with the IC_{50} of 24.1 ± 2.6 μM and 59.7 ± 5.6 μM respectively. The dose-response curves for each compound are reported in **Figure 16**. The inhibitory activity of the six compounds is also reported for two selected concentrations (6.42 nM and 642 nM) in **Figure 17**. The IC_{50} values of all the tested compounds on avian influenza A (H5N1) are reported in **Table 15**.

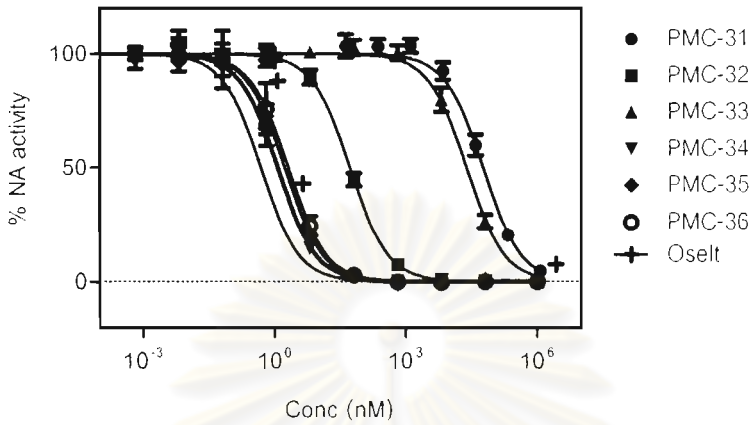

Figure 16 Dose-response curves of oseltamivir and its analogues against H5N1 neuraminidase

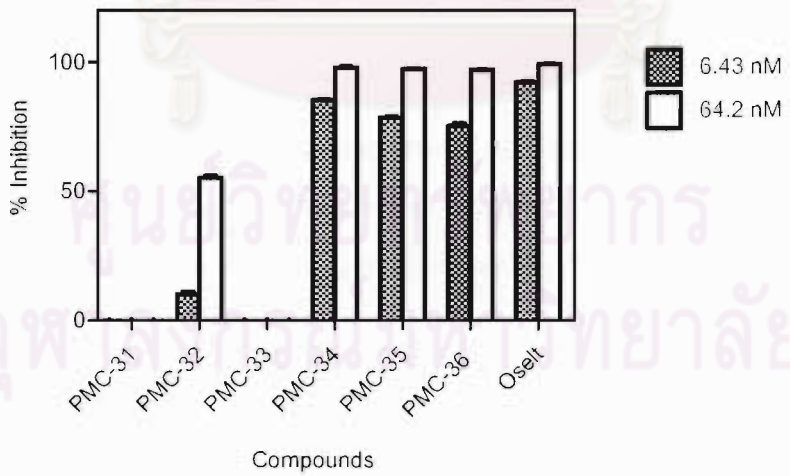

Figure 17 Inhibitory activity of the test compounds against H5N1 neuraminidase

Table 15 IC_{50} values of oseltamivir analogs against H5N1 avian influenza virus A

Compounds	IC_{50} ± SD on H5N1 (nM)
PMC-31	59,678 ± 5,651
PMC-32	53.6 ± 4.3
PMC-33	24,097 ± 2,651
PMC-34 (oseltamivir)	1.2 ± 0.1
PMC-35	1.7 ± 0.2
PMC-36	2.5 ± 0.4
Commercial oseltamivir	0.6 ± 0.1
Oseltamivir carboxylate	0.1[a]-1.5[b]

[a] Influenza virus: A/duck/Laos/25/06 (Govorkova *et al.*, 2009)

[b] Influenza virus: A/whooper swan/Mongolia/244/05(Govorkova *et al.*, 2009)

4.3.2 Flavonoids

Thirty three flavonoids (**Tables 16-20**, **Figure 18**) were tested for their inhibitory activity on neuraminidases H7N3 and H5N1. Initially, inhibitory properties of the flavonoids were screened using each compound at a concentration of 714 μM, after incubation with the enzyme the reaction was started by addition of MUNANA. The reaction mixture was incubated at 37°C for 5 hours and the reaction was stopped by adding the stop solution. The fluorescence intensity of 4-MU was recorded and compared to that of the reaction in the absence of flavonoids. The obtained results were displayed in **Table 21**.

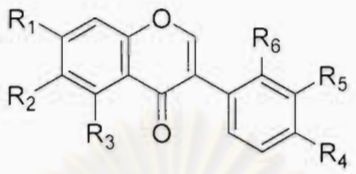

Table 16 Chemical structures of Isoflavones tested for avian neuraminidase inhibitory activity

No.	Chemical names	R1	R2	R3	R4	R5	R6
2	Genistein	OH	H	OH	OH	H	H
3	Calycosin	OH	H	H	OMe	OH	H
4	Biochanin A	OH	H	OH	OMe	H	H
5	Tectorigenin	OH	OMe	OH	OH	H	H
6	3'-*O*-Methylorobol	OH	H	OH	OH	OMe	H
7	Khrinone C	OH	H	OH	OMe	OH	OMe
8	Theralin	OH	H	OH	OH	H	OMe
9	2'-Methoxybiochanin A	OH	H	OH	OMe	H	OMe
10	Cajanin	OMe	H	OH	OH	H	OH
11	Irilin D	OH	OMe	OH	OH	OH	H

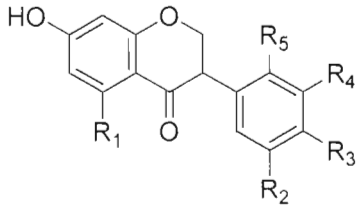

Table 17 Chemical structures of Isoflavanones tested for avian neuraminidase inhibitory activity

No.	Chemical names	R1	R2	R3	R4	R5
12	(3*R*)-7,3'-Dihydroxy-4'-methoxyisoflavanone	H	H	OMe	OH	H
13	(3*S*)-Sativanone	H	H	OMe	H	OMe
14	(3*RS*)-Violanone	H	H	OMe	OH	OMe
15	Dalparvin B	H	H	OMe	OMe	OH
16	Dalparvin	H	OH	OMe	H	OMe
17	Secundiflorol H	OH	H	OMe	OH	OMe
18	(3*RS*)-Onogenin	H	$O-CH_2-O$		H	OMe
19	Dalparvin A	OH	OH	OH	H	OMe

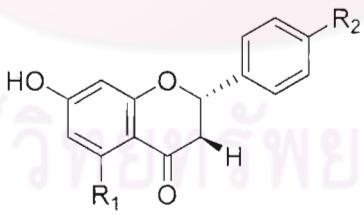

Table 18 Chemical structures of Flavanones tested for avian neuraminidase inhibitory activity

No.	Chemical names	R1	R2
21	(2*S*)- Liquiritigenin	H	OH
22	(2*S*)-Pinocembrin	OH	H
23	Alpinetin	OMe	H
24	(2*S*)-Naringenin	OH	OH

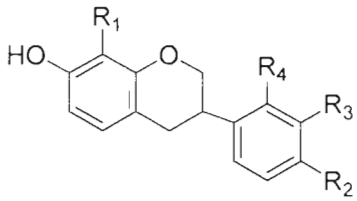

Table 19 Chemical structures of Isoflavans tested for avian neuraminidase inhibitory activity

No.	Chemical names	R1	R2	R3	R4
25	Duartin	OMe	OMe	OH	OMe
26	(3*R*)(+)-Mucronulatol	H	OMe	OH	OMe
27	(3*S*)-8-Demethylduartin	OH	OMe	OH	OMe
28	(3*RS*)-3'-Hydroxy-8-methoxyvestitol	OMe	OMe	OH	OH
29	Sativan	H	OMe	H	OMe

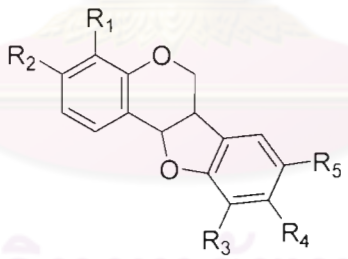

Table 20 Chemical structures of Pterocarpans tested for avian neuraminidase inhibitory activity

No.	Chemical names	R1	R2	R3	R4	R5
30	(6αR, 11αR)-3,8-Dihydroxy-9-methoxy pterocarpan	H	OH	H	OMe	OH
31	Melilotocarpan D	OH	OMe	OH	OMe	H

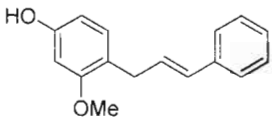

Obustyrene (32)

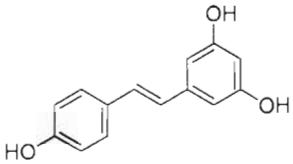

Resveratrol (33)

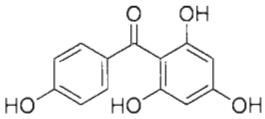

Iriflophenone (35)

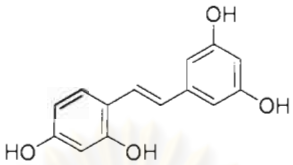

Oxyresveratrol (36)

Figure 18 Chemical structures of miscellaneous compounds used for screening of neuraminidase inhibitors

Table 21 Inhibitory activity of flavonoids (714 μM) on various types of avian influenza neuraminidases

ID	Class	Chemical Name	% inhibition at a concentration of 714 μM	
			H7N3	H5N1
2	Isoflavones	Genistein	53.1 ± 10.7	44.1 ± 5.1
3		Calycosin	40.1 ± 3.4	37.7 ± 8.5
4		Biochanin A	68.2 ± 5.0	40.1 ± 7.7
5		Tectorigenin	51.4 ± 19.3	20.5 ± 6.2
6		3-*O*-Methylorobol	33.2 ± 2.0	41.3 ± 8.4
7		Khrinone C	45.2 ± 14.9	83.6 ± 5.1
8		Theralin	37.6 ± 20.5	81.7 ± 1.8
9		2'-Methoxybiochanin A	45.8 ± 10.2	41.9 ± 3.6
10		Cajanin	45.9 ± 11.1	35.2 ± 8.8
11		Irilin D	59.7 ± 2.0	82.4 ± 2.5
12	Isoflavanones	(3*R*)-7,3'-Dihydroxy-4-methoxyisoflavanone	75.2 ± 0.4	81.2 ± 1.8
13		(3*S*)-Sativanone	47.2 ± 2.7	40.1 ± 9.5

Table 21 (continued)

ID	Class	Chemical Name	% inhibition at a concentration of 714 μM	
			H7N3	H5N1
14	Isoflavanones	(3*RS*)-Violanone	48.9 ± 3.1	55.5 ± 6.6
15		Darparvin B	58.3 ± 0.3	71.6 ± 1.8
16		Darparvin	68.9 ± 0.4	76.0 ± 4.0
17		(3*S*)-Secundiflorol H	45.7 ± 0.3	56.4 ± 8.3
18		(3*RS*)-Onogenin	58.2 ± 3.3	64.3 ± 3.2
19		Dalparvin A	55.7 ± 2.5	60.2 ± 2.7
21	Flavanones	(2*S*)-Liquiritigenin	66.9 ± 6.6	84.7 ± 1.5
22		(2*S*)-Pinocembrin	36.1 ± 13.2	62.3 ± 5.7
23		Alpinetin	44.8 ± 3.8	30.6 ± 5.1
24		(2*S*)-Naringenin	30.0 ± 14.4	67.6 ± 1.3
25	Isoflavans	Duartin	5.3 ± 5.0	30.2 ± 13.1
26		Mucronulatol	4.5 ± 2.0	5.8 ± 2.4
27		(3*S*)-8-Demethylduartin	67.9 ± 1.4	81.9 ± 1.5
28		(3*RS*)-3'-Hydroxy-8-methoxy vestitol	59.1 ± 0.4	58.5 ± 0.3
29		Sativan	46.0 ± 4.4	79.1 ± 5.9
30	Pterocarpans	3-8-Dihydroxy-9-methoxypterocarpan	40.1 ± 16.1	74.8 ± 1.8
31		Melilotocarpan D	16.3 ± 8.9	47.2 ± 6.8
32	Miscellaneous	Obustyrene	39.6 ± 4.9	30.6 ± 5.1
33		Resveratrol	87.2 ± 7.4	96.9 ± 1.8
35		Iriflophenone	49.5 ± 2.6	42.7 ± 4.3
36		Oxyresveratrol	-	99.6 ± 4.5

The phenolic structures shown in this study can be divided into 6 groups: isoflavones, isoflavanones, flavanones, isoflavans, pterocarpans and miscellaneous. The analysis of the data reported in **Table 21** indicated that at the concentration of 714 μM, Irilin D (**11**) showed the highest neuraminidase inhibitory activity among 2 subtypes within the Isoflavones class. Most of flavonoids in the Isoflavanones class showed a significant neuraminidase inhibition for both neuraminidase subtypes at this concentration. In the flavanones class, there was only (2*S*)-Liquiritigenin (**21**) that showed potent inhibitory activity especially on neuraminidase H5N1. For Isoflavans class, (3*S*)-8-Demethylduartin (**27**) showed high inhibitory activity against all neuraminidase subtypes whereas Sativan (**29**) showed potent inhibitory activity only on neuraminidase H5N1. For pterocarpans, the significant reduction of fluorescence intensity of 4-MU on H5N1 was found only on 3-8-Dihydroxy-9-methoxypterocarpan (**30**). In the miscellaneous class, Resveratrol (**33**) showed potent inihibitory activity against all neuraminidase subtypes whereas Oxyresveratrol (**36**) also exhibited potent inihibitory activity against H5N1 neuraminidase. However, those phenolic compounds causing a significant reduction of the fluorescence intensity of 4-MU were also re-tested at lower concentration (142 μM). The obtained results were displayed in **Table 22**.

Table 22 Inhibitory activity of flavonoids (142 μM) on H7N3 and H5N1 neuraminidases

ID	Class	Chemical Name	% inhibition at a concentration of 142 μM	
			H7N3	H5N1
7	Isoflavones	Khrinone C	-	54.9 ± 2.8
8		Theralin	-	48.9 ± 2.2
11		Irilin D	38.5 ± 3.5	51.2 ± 6.4
12	Isoflavanones	(3*R*)-7,3'-Dihydroxy-4-methoxyisoflavanone	43.5 ± 3.2	50.2 ± 5.2
14		(3*RS*)-Violanone	-	28.2 ± 4.6
15		Darparvin B	37.4 ± 0.4	44.8 ± 5.9
16		Darparvin	46.0 ± 2.8	36.8 ± 6.4

Table 22 (continued)

ID	Class	Chemical Name	% inhibition at a concentration of 142 μM	
			H7N3	H5N1
18	Isoflavanones	(3*RS*)-Onogenin	29.0 ± 4.6	33.2 ± 0.5
19		Dalparvin A	22.4 ± 2.0	28.3 ± 3.4
21	Flavanones	(2*S*)-Liquiritigenin	37.8 ± 6.4	57.9 ± 3.5
22		(2*S*)-Pinocembrin	-	32.2 ± 4.4
24		(2*S*)-Naringenin	-	36.9 ± 4.6
27	Isoflavanes	(3*S*)-8-Demethylduartin	35.7 ± 7.8	52.7 ± 3.0
28		(3*RS*)-3'-Hydroxy-8-methoxy vestitol	40.3 ± 7.1	42.2 ± 2.0
29		Sativan	-	42.1 ± 4.4
30	Pterocarpan	3-8-Dihydroxy-9-methoxypterocarpan	-	50.5 ± 8.2
31		Melilotocarpan D	-	25.1 ± 3.8
33	Miscellaneous	Resveratrol	80.3 ± 1.4	62.5 ± 3.4
36		Oxyresveratrol	-	80.6 ± 8.9

For neuraminidase H5N1, Khrinone C (**7**), Irilin D (**11**), (2*S*)-Liquiritigenin (**21**), (3*S*)-8-Demethylduartin (**27**), Resveratrol (**33**) and Oxyresveratrol (**36**) showed more than 50% inhibition on neuraminidase H5N1 at the concentration of 142 μM while neuraminidase inhibitory activity on neuraminidase H7N3, it was found that only Resveratrol (**33**) showed more than 50% inhibition at the concentration of 142 μM (**Table 22**). Neuraminidase inhibitory activity of Oxyresveratrol (**36**) was greatest (80.6±8.9% for H5N1 at the concentration of 142 μM) among tested compounds. We also further investigated the 50 % neuraminidase inhibitory (IC_{50}) on H5N1 of Khrinone C (**7**), Irilin D (**11**), (3*R*)-7,3'-Dihydroxy-4-methoxyisoflavanone (**12**), (2*S*)-Liquiritigenin (**21**), (3*S*)-8-Demethylduartin (**27**), 3-8-Dihydroxy-9- methoxypterocarpan (**30**) Resveratrol (**33**) and

Oxyresveratrol (**36**). The IC_{50} values of those flavonoids were observed by plotting the concentration of flavonoids against neuraminidase activity. The Titration curves showed in **Figure 19**. Our results showed that all tested flavonoids had the IC_{50} values on neuraminidase H5N1 more than 100 μM (**Table 23**) except Oxyresveratrol (**36**) showed the lowest IC_{50} value (66.1 ± 6.8 μM). Resveratrol (**33**) and (2*S*)-Liquiritigenin (**21**) showed the IC_{50} value (129.2 ± 32.0 μM and 137.0 ± 9.3 μM, respectively) grater than that of Oxyresveratrol (**36**). Khrinone C (**7**) and (3S)-8-Demethylduartin (**27**) showed moderate neuraminidase inhibitory activity (IC_{50} = 155.6 ± 0.3 μM and 153.6 ± 22.0 μM, respectively). Irilin D (**11**) and 3-8-Dihydroxy-9-methoxypterocarpan (**30**) had less inhibitory activity on neuraminidase H5N1 with the IC_{50} values of 182.7 ± 71.2 and 186.5±11.9 μM, respectively.

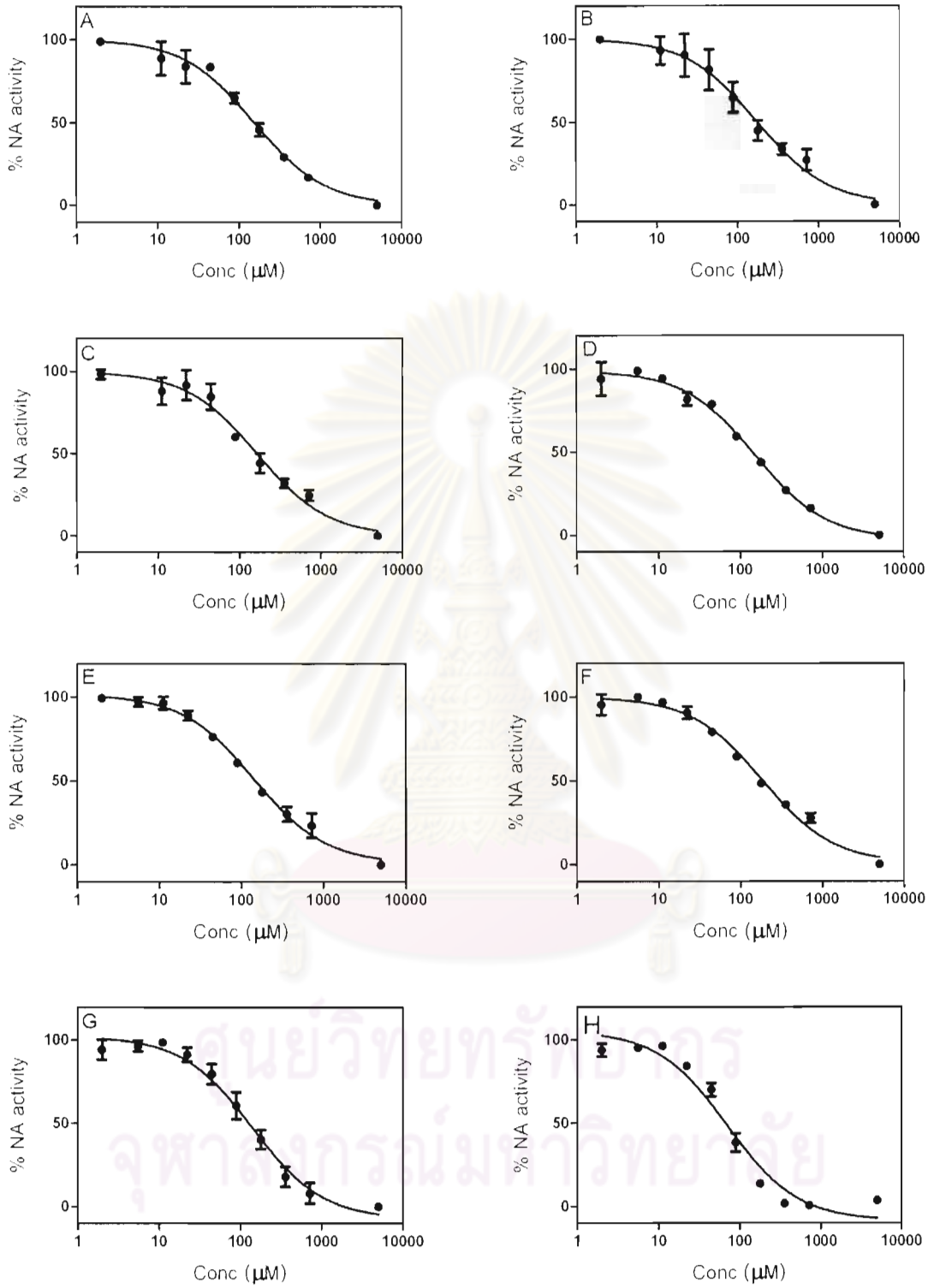

Figure 19 Dose-response curves of Khrinone C (A), Irilin D (B), (3*R*)-7,3'-Dihydroxy-4-methoxyisoflavanone (C), (2*S*)-Liquiritigenin (D), (3*S*)-8-Demethylduartin (E), 3-8-Dihydroxy-9-methoxypterocarpan (F), Resveratrol (G) and Oxyresveratrol (H) on H5N1 neuraminidase

Table 23 IC_{50} values of tested flavonoids on H5N1 neuraminidase

ID	Class	Chemical Name	$IC_{50} \pm$ SD (μM)
7	Isoflavones	Khrinone C	155.6 ± 0.3
11		Irilin D	182.7 ± 71.2
12	Isoflavanones	(3R)-7,3'-Dihydroxy-4-methoxyisoflavanone	166.5 ± 32.6
21	Flavanones	(2S)-Liquiritigenin	137.0 ± 9.3
27	Isoflavans	(3S)-8-Demethylduartin	153.6 ± 22.0
30	Pterocarpan	3-8-Dihydroxy-9-methoxypterocarpan	186.5 ± 11.9
33	Miscellaneous	Resveratrol	129.2 ± 32.0
36		Oxyresveratrol	66.1 ± 6.8
		Oseltamivir	0.0006 ± 0.0001

4.3.3 Quenching effect of flavonoids on neuraminidase inhibition assay

From a general point of view the concentration dependence of the fluorescence quenching exerted by a given species on a fluorescent molecule (probe) can be described by the Stern-Volmer equation as follows:

$$\frac{I_0}{I} = 1 + k_q \tau_0 [Q] = 1 + Ksv[Q] \quad (1)$$

where I_0 and I are the fluorescence intensities of the probe in the absence and presence of the quencher respectively, k_q is the quenching constant and τ_0 is the fluorophore lifetime in the absence of quencher. The quencher concentration is represented by $[Q]$ and *Ksv* is the pertinent Stern-Volmer constant which is a measure of the ability of a given compound to act as a quencher. In this study, fluorescence quenching analyses were carried out by varying the concentrations of the different flavonoids in the range 0-1 mM in a solution containing a fixed amount of 4-methylumbelliferone (the probe) and monitoring its fluorescence as a function of the flavonoids' concentration. By plotting the I_0/I ratio versus the flavonoids' concentration a

well behaved linear plot could be obtained in all of the cases, **Figures 21-27**, thus confirming that a real fluorescence quenching was taking place into solution. The *Ksv* of all tested compounds were calculated by linear fitting of the experimental data and are reported in **Table 29**, in this case the analysis was possible for the complete set of 35 flavonoids (**Tables 24-28, Figure 20**).

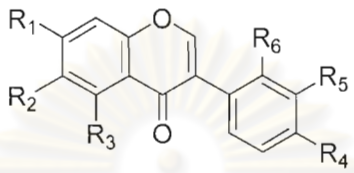

Table 24 Chemical structures of Isoflavones tested for quenching effect on 4-methylumbelliferone (4-MU)

No.	Chemical names	R1	R2	R3	R4	R5	R6
1	Daidzein	OH	H	H	OH	H	H
2	Genistein	OH	H	OH	OH	H	H
3	Calycosin	OH	H	**H**	OMe	OH	H
4	Biochanin A	OH	H	OH	OMe	H	H
5	Tectorigenin	OH	OMe	OH	OH	H	H
6	3'-*O*-Methylorobol	OH	H	OH	OH	OMe	H
7	Khrinone C	OH	H	OH	OMe	OH	OMe
8	Theralin	OH	H	OH	OH	H	OMe
9	2'-Methoxybiochanin A	OH	H	OH	OMe	H	OMe
10	Cajanin	OMe	H	OH	OH	H	OH
11	Irilin D	OH	OMe	OH	OH	OH	H

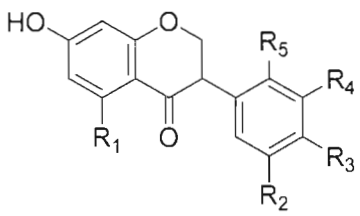

Table 25 Chemical structures of Isoflavanones tested for quenching effect on 4-methylumbelliferone (4-MU)

No.	Chemical names	R1	R2	R3	R4	R5
12	(3*R*)-7,3'-Dihydroxy-4'-Methoxyisoflavanone	H	H	OMe	OH	H
13	(3*S*)-Sativanone	H	H	OMe	H	OMe
14	(3*RS*)-Violanone	H	H	OMe	OH	OMe
15	Dalparvin B	H	H	OMe	OMe	OH
16	Dalparvin	H	OH	OMe	H	OMe
17	Secundiflorol H	OH	H	OMe	OH	OMe
18	(3*RS*)-Onogenin	H	O-CH_2-O		H	OMe
19	Dalparvin A	OH	OH	OH	H	OMe

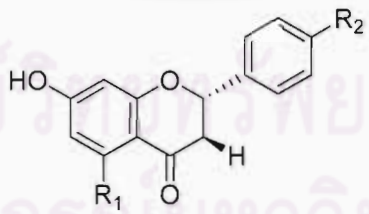

Table 26 Chemical structures of Flavanones tested for quenching effect on 4-methylumbelliferone (4-MU)

No.	Chemical names	R1	R2
21	(2*S*)- Liquiritigenin	H	OH
22	(2*S*)-Pinocembrin	OH	H
23	Alpinetin	OMe	H
24	(2*S*)-Naringenin	OH	OH

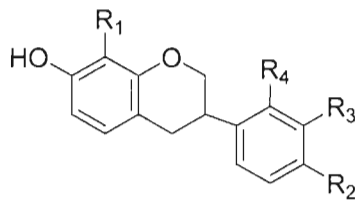

Table 27 Chemical structures of Isoflavans tested for quenching effect on 4-methylumbelliferone (4-MU)

No.	Chemical names	R1	R2	R3	R4
25	Duartin	OMe	OMe	OH	OMe
26	(3*R*)(+)-Mucronulatol	H	OMe	OH	OMe
27	(3*S*)-8-Demethylduartin	OH	OMe	OH	OMe
28	(3*RS*)-3'-Hydroxy-8-methoxyvestitol	OMe	OMe	OH	OH
29	Sativan	H	OMe	H	OMe

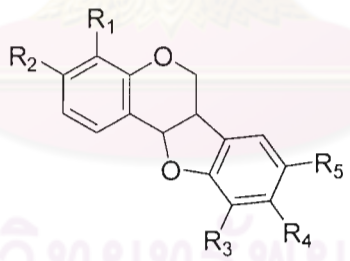

Table 28 Chemical structures of Pterocarpans tested for quenching effect on 4-methylumbelliferone (4-MU)

No.	Chemical names	R1	R2	R3	R4	R5
30	(6αR, 11αR)-3,8-dihydroxy-9-methoxy pterocarpan	H	OH	H	OMe	OH
31	Melilotocarpan D	OH	OMe	OH	OMe	H

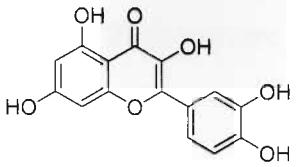

Quercetin (20)

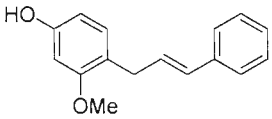

Obustyrene (32)

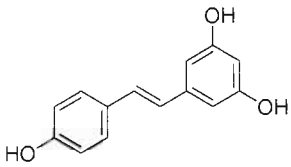

Resveratrol (33)

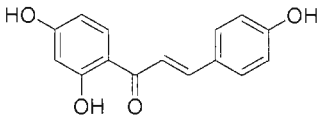

Isoliquiritigenin (34)

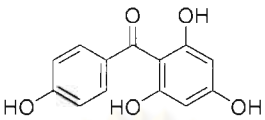

Iriflophenone (35)

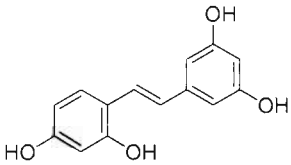

Oxyresveratrol (36)

Figure 6 Chemical structures of other flavonoids and miscellaneous compounds tested for quenching effect on 4- methylumbelliferone (4-MU)

Table 29 The values of Stern-Volmer quenching constant (K_{sv}) of various flavonoids on 4-MU

ID	Class	Chemical Name	*Ksv* (x 10^3 M^{-1})
1	Isoflavones	Daidzein	0.06 ± 0.03
2		Genistein	2.81 ± 0.10
3		Calycosin	1.04 ± 0.06
4		Biochanin A	2.34 ± 0.14
5		Tectorigenin	4.38 ± 0.13
6		3-*O*-Methylorobol	0.92 ± 0.06
7		Khrinone C	3.66 ± 0.08
8		Theralin	3.22 ± 0.12
9		2'-Methoxy biochanin A	2.31 ± 0.09
10		Cajanin	2.76 ± 0.12
11		Irilin D	5.15 ± 0.11
12	Isoflavanones	(3*R*)-7,3'-Dihydroxy-4-methoxyisoflavanone	2.72 ± 0.12
13		(3*S*)-Sativanone	0.96 ± 0.07

Table 29 (continued)

ID	Class	Chemical Name	*Ksv* (x 10^3 M^{-1})
14	Isoflavanones	(3*RS*)-Violanone	1.26 ± 0.06
15		Darpavin B	1.73 ± 0.06
16		Darpavin	2.93 ± 0.11
17		(3*S*)-Secundiflorol H	1.13 ± 0.04
18		(3*RS*)-Onogenin	1.35 ± 0.07
19		Dalparvin A	1.21 ± 0.13
20	Flavones	Quercetin	10.46 ± 0.46
21	Flavanones	(2*S*)-Liquiritigenin	4.04 ± 0.05
22		(2*S*)-Pinocembrin	1.15 ± 0.05
23		Alpinetin	0.51 ± 0.05
24		(2*S*)-Naringenin	0.93 ± 0.07
25	Isoflavans	Duartin	0.11 ± 0.05
26		(3*R*)-Mucronulatol	0.26 ± 0.07
27		(3*S*)-8-Demethoxyduartin	3.07 ± 0.25
28		(3*RS*)-3'-Hydroxy-8-methoxy vestitol	1.63 ± 0.12
29		Sativan	0.77 ± 0.08
30	Pterocarpan	(6a*R*, 11a*R*)-3-8-Dihydroxy-9-methoxypterocarpan	0.85 ± 0.03
31		Melilotocarpan D	0.44 ± 0.05
32	Miscellaneous	Obustyrene	0.77 ± 0.04
33		Resveratrol	1.49 ± 0.08
34		Isoliquiritigenin	47.43 ± 1.48
35		Iriflophenone	0.92 ± 0.05
36		Oxyresveratrol	2.50 ± 0.03

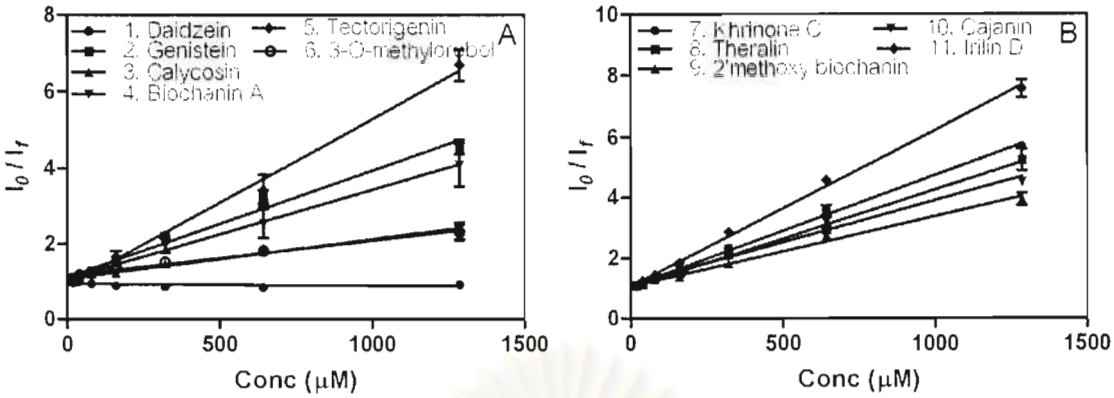

Figure 21 Stern-Volmer plot showing fluorescence quenching of 4-methylumbelliferone by isoflavones

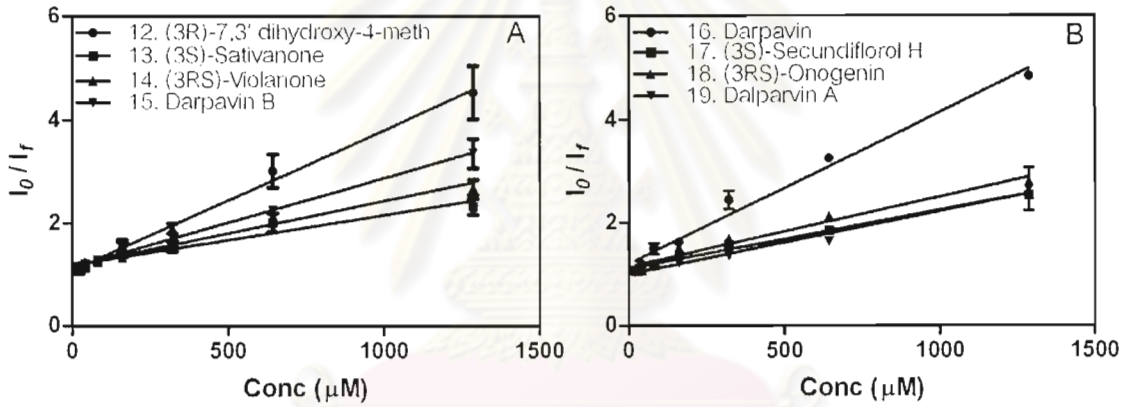

Figure 22 Stern-Volmer plot showing fluorescence quenching of 4-methylumbelliferone by isoflavanones

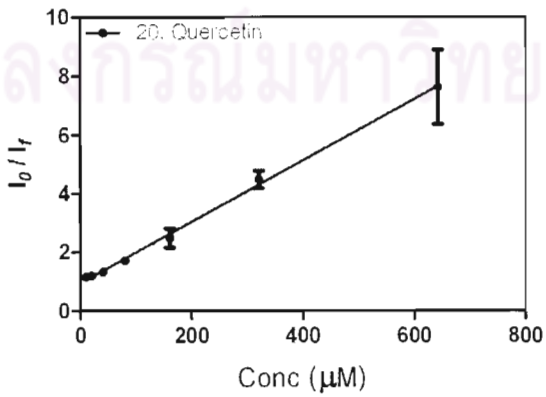

Figure 23 Stern-Volmer plot showing fluorescence quenching of 4-methylumbelliferone by flavones

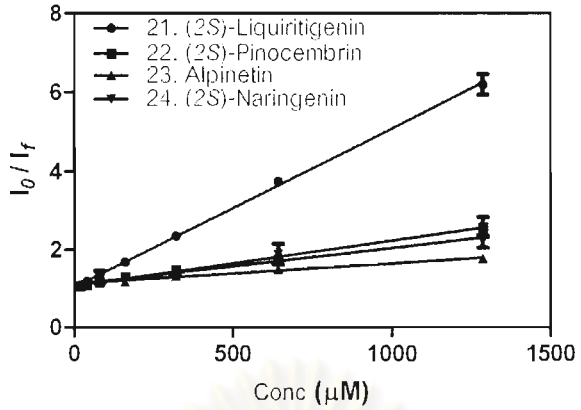

Figure 24 Stern-Volmer plot showing fluorescence quenching of 4-methylumbelliferone by flavanones

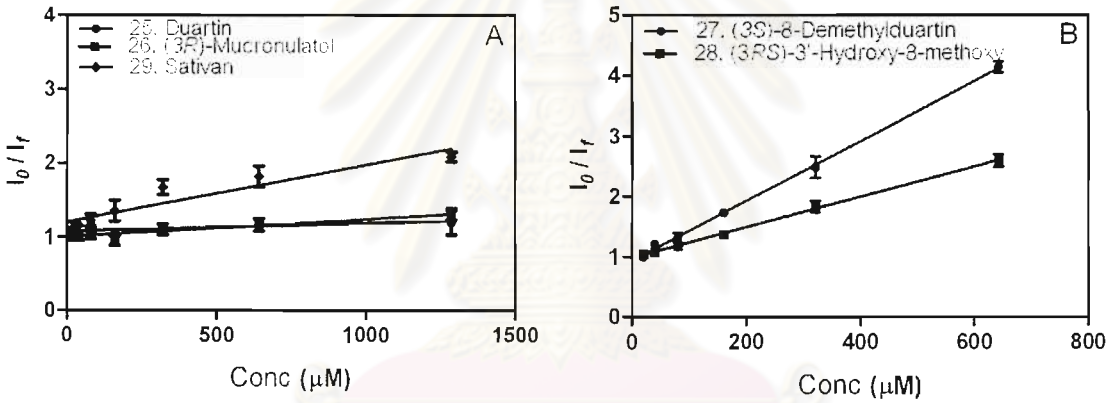

Figure 25 Stern-Volmer plot showing fluorescence quenching of 4-methylumbelliferone by isoflavans

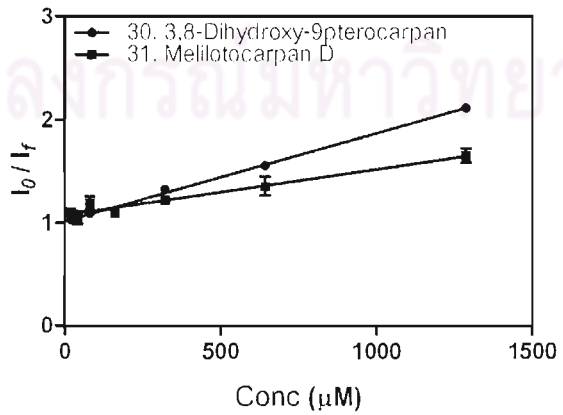

Figure 26 Stern-Volmer plot showing fluorescence quenching of 4-methylumbelliferone by pterocarpans

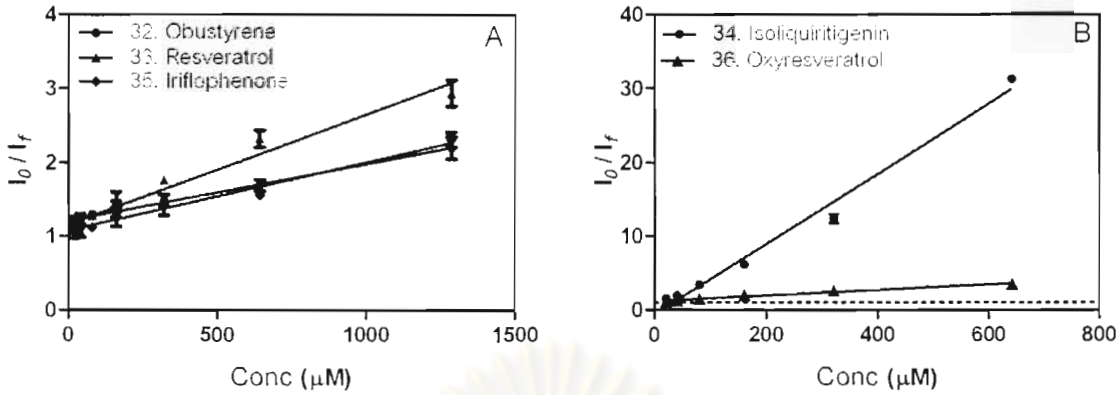

Figure 27 Stern-Volmer plot showing fluorescence quenching of 4-methylumbelliferone by miscellaneous flavonoids

As a result, flavonoids presenting high *Ksv* were found to be a good quencher for 4-MU since it can drastically decrease the fluorescence intensity of 4-MU. In contrast, flavonoids presenting low *Ksv* were found to be a weak quencher for 4-MU. From this study, only a few flavonoids showed less effect on 4-MU (*Ksv* < 0.5 x 10^3 M^{-1}), these flavonoids are Daidzein (**1**), Duartin (**25**), (3R)-Mucronulatol (**26**) and Melilotocarpan D (**31**). Other flavonoids had a significant effect on decreasing of fluorescence intensity of 4-MU. We also noticed that the degree of quenching was varying among the same class of flavonoids. For example, Daidzein (**1**) did not quench the fluorescence intensity of 4-MU (*Ksv* = 0.06 ± 0.03 x 10^3 M^{-1}) whereas Irilin D (**11**) had a high effect on 4-MU (*Ksv* = 5.15 ± 0.11 x 10^3 M^{-1}). Duartin (**25**) and (3*S*)-8-Demethylduartin (**27**) are in the isoflavans class but (3S)-8-Demethylduartin (**27**) showed high *Ksv* (3.07 ± 0.25 x 10^3 M^{-1}) compared with Duartin (**25**) (*Ksv*= 0.11 ± 0.05 x 10^3 M^{-1}). In this study, we also found that Isoliquiritigenin (**34**) was a strong quencher for 4-MU since the *Ksv* was highest among tested flavonoids. The *Ksv* of Isoliquiritigenin (**34**) was found to be 47.43 ± 1.48 x 10^3 M^{-1}). These findings proved that the structure of flavonoids affect directly on the fluorescence intensity of 4-MU which of course leading to a false positive result when this phenomena occurs in the same reaction with neuraminidase inhibition assay using MUNANA as a fluorogenic substrate.

CHAPTER V

DISCUSSION

5.1 Establishment of *In vitro* neuraminidase inhibition assay

Highly pathogenic avian influenza H5N1 remains a problematic issue in certain regions of the world and the development of reliable methods for screening of new antiviral compounds with potent inhibitory activity on the neuraminidase is in an urgent need. To this aim, the availability of cheap sources of enzymatically active neuraminidase is mandatory. Among various sources, inactivated avian influenza virus H5N1, recombinant H7N1 and H7N3 neuraminidases obtained from a baculovirus carrying the neuraminidase gene, propagated in insect cells and expressed as fused neuraminidase with the baculovirus surface glycoproteins are of particular interest and readily available. These virus particles were originally used to elicit protecting antibodies in poultry through the development of a N1-N3 discriminatory test (Cattoli *et al.*, 2003) which could be applied in the program of DIVA vaccination strategy for the control of avian Influenza (Cattoli *et al.*, 2006). Although the success of vaccination strategy does not require the presence of enzyme activity of the recombinant neuraminidases, our preliminary study showed, interestingly, that the preparations of H7N1, H7N3 and H5N1 used for the vaccination remained enzymatically active. This opened a possibility of obtaining a cheap source of the neuraminidases for supplying the work of enzyme-based bioassay, and thus prompted us to develop an effective screening assay for potent neuraminidase inhibitors.

Using recombinant H7N1 and H7N3 neuraminidases as enzyme sources, our results showed that the supernatants consisting of baculovirus particles carrying the recombinant neuraminidases N1 and N3 contained the specific enzyme activities of 0.04 and 0.4 mU/mg protein, respectively. Although these values are not as high as those reported for the enzyme preparations from other sources, (Dalakouras *et al.*, 2006, Tanimoto *et al.*, 2004, Yongkiettrakul *et al.*, 2009), the obtained neuraminidase activity levels were quite sufficient for the assay set-up using the sensitive fluorimetric method. The developed enzyme assay system allowed the three neuraminidase

preparations being characterized. As summarized in **Table 12**, the recombinant H7N1 preparation possesses its *Km* value of 400 ± 60 μM which is almost 5 times higher than the *Km* of H7N3, 87 ± 4μM, suggesting that N3 can catalyze the reaction under low substrate concentration whereas N1 needs high substrate concentration.

For the inhibition constants (*Ki*) based on oseltamivir free acid, N1 (23.5 nM) showed its *Ki* value about 200 times higher than the *Ki* of N3 (0.12 nM). This suggests that oseltamivir free acid is much more potent in inhibiting the activity of N3 than that of N1. These enzyme properties reflected well the results of the inhibition experiment using oseltamivir carboxylate as the inhibitor (**Table 12**). It can be seen that the obtained IC_{50} values (25 ± 4 nM and 0.2 ± 0.02 nM for the N1 and N3, respectively) are in good agreement with the results from the kinetic studies. In addition, further validation of the assay system showed that the intra-assay coefficients of variation on the recorded fluorescence data were lower than 5% for both N1 and N3, and the corresponding inter-assay coefficients of variation were lower than 10%, suggesting good reproducibility of the assay system.

Comparatively, the values of *Km* and IC_{50} (oseltamivir) of N1 obtained from this study appear to be higher than those reported previously (Rameix-Welti *et al.*, 2006, Yen *et al.*, 2007, Yongkiettrakul *et al.*, 2009). These differences may be due to the different strains (clades) of avian influenza viruses used in the various studies. In fact, the values of *Km* of neuraminidase N1 against MUNANA have been reported to span in the range 15-359 μM (Rameix-Welti *et al.*, 2008, Yen *et al.*, 2007, Yongkiettrakul *et al.*, 2009), depending on the specific nature of the neuraminidase considered. For the IC_{50} values, The observed higher sensitivity of N3 than N1 towards oseltamivir might be explained by the fact that the original design of the oseltamivir molecule was against the neuraminidase subgroup 2 structures (comprising N2, N3, N6, N7 and N9), not the subgroup 1 structures (comprising N1, N4, N5 and N8) (Russell *et al.*, 2006). In addition, it has been reported that the clade 1 H5N1 (China, South East Asia) is intrinsically more sensitive to oseltamivir than the clade 2 H5N1 (Europe, Africa, Indonesia, China, South East Asia) (Taylor *et al.*, 2010).

For inactivated influenza H5N1 (A/turkey/turkey/1/2005), we found that neuraminidase activity was also present in this viral solution. Similar findings have been reported in inactivated human influenza A (H3N2), avian A (H7N3) and seasonal and pandemic A (H1N1) virus isolates (Jonges *et al.*, 2010).This allowed us to use the viral solution readily as the source of H5N1 neuraminidase. Although without full characterization of the viral solution, optimization of its neuraminidase activity is sufficient for the assay set-up. Therefore, the use of the recombinant H7N1 and H7N3 neuraminidases and the inactivated H5N1 viral solution are considered covering a reasonable range of neuraminidase inhibition assay. Importantly, these neuraminidase sources are considered cheap, safe to work with and readily available for the medium to high throughput of screening.

5.2 Neuraminidase inhibitory activity of various test compounds

5.2.1 Synthesized oseltamivir analogs

5.2.1.1 Inhibitory activity of oseltamivir analogues on recombinant H7N1 neuraminidase

The variations in the measured inhibition for the different compounds revealed that an isopropyl group linked to the 5-amino group site to form a secondary amine is well tolerated and appears to increase the affinity for the enzyme, as shown in the case of **PMC-36** (**6**). This might be because the alkyl group affects the strengths of hydrogen bonds of the amine group with acidic residues of the N1 neuraminidase, and/or it fills and makes favourable contacts in the 150-loop cavity, which is located in the vicinity and interacts with the amino and acetamido groups of bound oseltamivir(Russell *et al.*, 2006). Moreover, a small increase in size for the acid residue on the 4-amido group from the original acetyl group of oseltamivir also seems to enhance the inhibitory activity of the novel species, as observed in the case of **PMC-36** (**6**) and **PMC-35** (**5**). However, this position seems to be intolerant to the introduction of larger groups, since the presence of a 2-butenyl amide dramatically reduces the affinity of compound **PMC-33** (**3**) with respect to the oseltamivir benchmark. The IC_{50} of commercial oseltamivir on N1

did not perfectly match that of synthesized oseltamivir (**PMC-34**), but its variability is well within the acceptable limits. Interestingly, 5-azido and 5-amino pairs (i.e., **PMC-31** and **32**, **PMC-33** and **34**) showed comparable IC_{50} values, although both the electronic properties and the reactivity profiles of the two chemical functions are quite different. The titration curves and the IC_{50} values of all the tested compounds on N1 are reported in **Figure 12** and **Table 13**, respectively.

5.2.1.2 Inhibitory activity of oseltamivir analogues on recombinant H7N3 neuraminidase

The differences in the observed inhibitory properties of the investigated species indicated that the primary 5-amino group is essential for inhibitory activity on neuraminidase subtype 3. Modification of the amine seems to decrease the activity, as shown for **PMC-32** (**2**) and **PMC-36** (**6**); this observation infers a different trend in comparison with N1, where **PMC-36** (**6**) outperformed **PMC-35** (**5**). Adding a small group on the 4-amido function as for **PMC-35** (**5**) does not affect the activity. In contrast, the presence of a bulky group on the amide as in **PMC-31** (**1**) and **PMC-33** (**3**) greatly decreases the ability to inhibit the N3 neuraminidase. The IC_{50} of commercial oseltamivir is similar to that of synthesized oseltamivir (**PMC-34**). Higher inhibitory potency of oseltamivir towards the group-2 neuraminidase N3 over the group-1 neuraminidase subtype N1 was reported also by other groups (Govorkova *et al.*, 2001).

5.2.1.3 Inhibitory activity of oseltamivir analogues on inactivated H5N1 avian influenza neuraminidase

The screening of neuraminidase inhibitory activity on oseltamivir analogs allowed a preliminary assessment of a structure-activity relationship for the modification of the 4-amido and 5-amino groups of oseltamivir carboxylate. We found that modification of 5-amino groups with an isopropyl group to form a secondary amine as in **PMC-36** (**6**) slightly decreases on inhibitory activity compared with **PMC-34** (**4**). However, the decreasing of inhibitory activity is not greater than substitution with an azide group as in **PMC-32** (**2**). Interestingly, modification of 4-amido side chain with a propenylamido

group as showed in **PMC-35 (5)** does not affect on the observed activity compared with **PMC-34 (4)** meanwhile substitution with a 2-butenylamido moiety as in **PMC-31 (1)** and **PMC-33 (3)** significantly reduced the inhibitory activity. Nevertheless, modification 5-amino groups with an isopropyl group in the oseltamivir structure while remaining 5-amino group should be further investigated.

Overall, the effect of structure modification of oseltamivir analogs on neuraminidase inhibitory activity can be divided into 2 groups. Group-1 neuraminidase (H7N1 and H5N1) and Group-2 neuraminidase (H7N3): For group-1 neuraminidase, we found that modification of 5-amino groups with an isopropyl group (**PMC-36**) increased the inhibitory activity especially on H7N1 neuraminidase whereas this modification did not effect on that of H7N3. Since modification of these oseltamivir analogs subjected to developed for group-1 neuraminidase thus the increasing of neuraminidase activity on group-2 neuraminidase such as H7N3 compared with oseltamivir was not observed. However, H7N3 neuraminidase was found to be more sensitive to the oseltamivir analogues, while neuraminidase N1 was less sensitive; this is probably the result of the original design of oseltamivir which was rationally designed on the structure of group-2 neuraminidases. These data was shown in **Table 30**.

Table 30 IC_{50} values of oseltamivir analogs on various types of neuraminidases

Compounds	IC_{50} ± SD on H7N1 (nM)	IC_{50} ± SD on H7N3 (nM)	IC_{50} ± SD on H5N1 (nM)
PMC-31	51,576 ± 2,904	99,295 ± 32,416	59,678 ± 5,651
PMC-32	84.4 ± 20	2.2 ± 1.4	53.6 ± 4.3
PMC-33	138,962 ± 21,589	4,512 ± 1,172	24,097 ± 2,651
PMC-34 (oseltamivir)	39.3 ± 3.2	0.1 ± 0.08	1.2 ± 0.1
PMC-35	31.8 ± 6.9	0.1 ± 0.03	1.7 ± 0.2
PMC-36	14.6 ± 3.0	28.1 ± 9.7	2.5 ± 0.4
Commercial oseltamivir	24.9 ± 3.9	0.2 ± 0.02	0.6 ± 0.1

5.2.2 Flavonoids

Thirty three flavonoids extracted from *Dalbergia parviflora* and *Belamcanda chinensis* were tested for their inhibitory activity on H7N3 and H5N1 neuraminidases. The H7N1 was excluded in this study due to run out of enzyme preparation. Firstly, we screened for their inhibitory activity at the concentration of 714 μM. Flavonoids showed more than 50% inhibition were also re-tested at the concentration of 142 μM. From our findings, almost tested flavonoids had an inhibitory activity on neuraminidase H5N1 over H7N3 at the concentration of 142 μM. There was only Resveratrol (**33**) that seemed to have an inhibitory activity on H7N3 over H5N1. Seven flavonoids were chosen for determination of the IC_{50} on neuraminidase H5N1 since these flavonoids exhibited more than 50% inhibition at the concentration of 142 μM. Whereas there was only Resveratrol (**33**) exhibited more than 50% inhibition on neuraminidase H7N3 at the concentration of 142 μM. The results showed that all tested flavonoids had the IC_{50} on H5N1 more than 100 μM which can be interpreted that these flavonoids are weak inhibitors (Liu *et al.*, 2008b) against avian influenza neuraminidase H5N1. Several studies (Jeong *et al.*, 2009, Liu *et al.*, 2008b, Nguyen *et al.*, 2010a, Nguyen *et al.*, 2010b, Ryu *et al.*, 2008, Ryu *et al.*, 2009b) have been reported good inhibitory activity of various classes of flavanoids on neuraminidase but none of them has been mentioned their inhibitory activity on avian influenza neuraminidase H5N1 and H7N3. The structure-activity relationship of flavonoids as influenza neuraminidase inhibitor has been revealed that for good inhibitory effect, the 4'-OH, 7-OH, C4=O, and C2=C3 functionalities were essential (Liu *et al.*, 2008b). This finding could not be applied for avian influenza neuraminidase H7N3 and H5N1 since the observed inhibition was rather low (>100 μM).

5.3 Quenching effect of flavonoids on neuraminidase inhibition assay

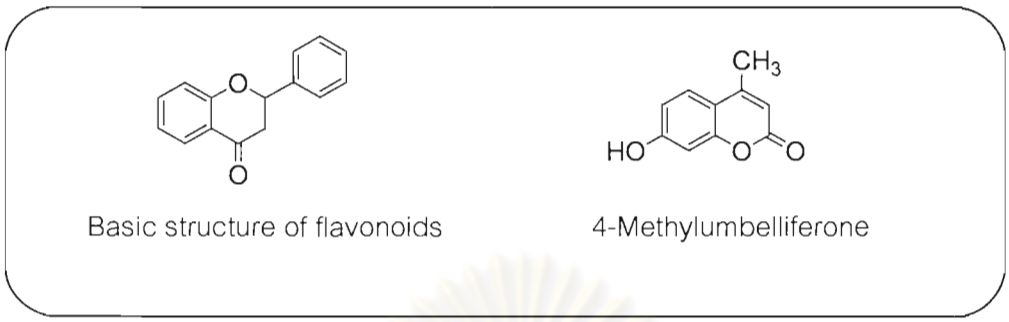

Figure 28 Chemical structures of flavonoids and 4-methylumbelliferone

Since a part of flavonoids structures is similar with 4-MU (Figure 28), the fluorescence product obtained from neuraminidase catalytic reaction with MUNANA. It may be possible that the structure of flavonoids can affect on the fluorescence intensity of 4-MU leading to the interference of neuraminidase inhibition assay. In order to observe this effect, the Stern-Volmer equation was used for evaluation of the quenching effect on 4-MU. A preliminary comparative analysis of the data reported in Table 29 highlighted that almost flavonoids displaying pronounced quenching effect on 4-MU which can be reported by a high *Ksv* value. To gain further insight on the magnitude of the flavonoids' interference in the fluorimetric neuraminidase inhibition assay, we computed the magnitude of the fluorescence decrease ($1-I/I_0$) which could be ascribed solely to quenching for each flavonoid considered. This is possible because by rearranging (1), one obtains:

$$1-\frac{I}{I_0}=1-\frac{1}{1+Ksv[Q]} \qquad (2)$$

and either *Ksv* and $[Q]$ are known, the obtained data, expressed as percentages, are reported in Tables 31-32. These values can be compared to the decrease in fluorescence intensity obtained in the inhibition experiments, Tables 31-32. These data demonstrated that the values observed from inhibition effect were similar with the values observed from quenching effect especially at a high concentration of flavonoids (Table 31). This finding points out that the observed neuraminidase inhibition of flavonoids was partially interfered by the quenching effect of its own structure on 4-MU.

Table 31 Comparison between the observed inhibition values of various flavonoids (714 μM) and the calculated contribution to the decrease of fluorescence intensity due to quenching

ID	Class	Chemical Name	% Quenching contribution[a]	% inhibition at a concentration of 714 μM	
				H7N3	H5N1
2	Isoflavones	Genistein	66.8	53.1 ± 10.7	44.1 ± 5.1
3		Calycosin	42.6	40.1 ± 3.4	37.7 ± 8.5
4		Biochanin A	62.6	68.2 ± 5.0	40.1 ± 7.7
5		Tectorigenin	75.8	51.4 ± 19.3	40.5 ± 6.2
6		3-*O*-Methylorobol	39.7	33.2 ± 2.0	41.3 ± 8.4
7		Khrinone C	72.3	45.2 ± 14.9	83.6 ± 5.1
8		Theralin	69.7	37.6 ± 20.5	81.7 ± 1.8
9		2'- Methoxy biochanin A	62.2	45.8 ± 10.2	41.9 ± 3.6
10		Cajanin	66.3	45.9 ± 11.1	35.2 ± 8.8
11		Irilin D	78.6	59.7 ± 2.0	82.4 ± 2.5
12	Isoflavanones	(3*R*)-7,3'-Dihydroxy-4-methoxy isoflavanone	66.0	75.2 ± 0.4	81.2 ±1.8
13		(3*S*)-Sativanone	40.7	47.2 ± 2.7	40.1 ± 9.5
14		(3*RS*)-Violanone	47.4	48.9 ± 3.1	55.5 ± 6.6
15		Darparvin B	55.3	58.3 ± 0.3	71.6 ± 1.8
16		Darparvin	67.7	68.9 ± 0.4	76.0 ± 4.0
17		(3*S*)-Secundiflorol H	44.7	45.7 ± 0.3	56.4 ± 8.3
18		(3*RS*)-Onogenin	49.1	58.2 ± 3.3	64.3 ± 3.2
19		Dalparvin A	46.4	55.7 ± 2.5	60.2 ± 2.7

[a] The contribution due to quenching was calculated according to the following equation:

$$100\left(1-\frac{I}{I_0}\right)=100\left(1-\frac{1}{1+Ksv[Q]}\right)$$

Table 31 (Continued)

ID	Class	Chemical Name	% Quenching contribution[a]	% inhibition at a concentration of 714 μM	
				H7N3	H5N1
21	Flavanones	(2*S*)-Liquiritigenin	74.3	66.9 ± 6.6	84.7 ± 1.5
22		(2*S*)-Pinocembrin	45.1	36.1 ± 13.2	62.3 ± 5.7
23		Alpinetin	26.7	44.8 ± 3.8	30.6 ± 5.1
24		(2*S*)-Naringenin	40.0	30.0 ± 14.4	67.6 ± 1.3
25		Duartin	7.3	5.3 ± 5.0	30.2 ± 13.1
26		Mucronulatol	15.7	4.5 ± 2.0	5.8 ± 2.4
27	Isoflavanes	(3*S*)-8-Demethyl duartin	68.7	67.9 ± 1.4	81.9 ± 1.5
28		(3*RS*)-3'-Hydroxy-8-methoxy vestitol	53.8	59.1 ± 0.4	58.5 ± 0.3
29		Sativan	35.5	46.0 ± 4.4	79.1 ± 5.9
30	Pterocarpan	3-8-Dihydroxy-9-methoxy-pterocarpan	37.8	40.1 ± 16.1	74.8 ± 1.8
31		Melilotocarpan D	23.9	16.3 ± 8.9	47.2 ± 6.8
32	Miscellaneous	Obustyrene	35.5	39.6 ± 4.9	30.6 ± 5.1
33		Resveratrol	51.5	87.2 ± 7.4	96.9 ± 1.8
35		Iriflophenone	39.7	49.5 ± 2.6	42.7 ± 4.3
36		Oxyresveratrol	64.1	-	99.6 ± 4.5

[a] The contribution due to quenching was calculated according to the following equation:

$$100\left(1-\frac{I}{I_0}\right)=100\left(1-\frac{1}{1+Ksv[Q]}\right)$$

Table 32 Comparison between the observed inhibition values of various flavonoids (142 μM) and the calculated contribution to the decrease of fluorescence intensity due to quenching

ID	Class	Chemical Name	% Quenching contribution[a]	% inhibition at a concentration of 142 μM	
				H7N3	H5N1
7	Isoflavones	Khrinone C	34.2	-	54.9 ± 2.8
8		Theralin	31.4	-	48.9 ± 2.2
11		Irilin D	24.7	38.5 ± 3.5	51.2 ± 6.4
12	Isoflavanones	(3*R*)-7,3'-Dihydroxy-4-methoxyisoflavanone	28.2	43.5 ± 3.2	50.2 ± 5.2
14		(3*RS*)-Violanone	15.2	-	28.2 ± 4.6
15		Darparvin B	19.7	37.4 ± 0.4	44.8 ± 5.9
16		Darparvin	29.4	46.0 ± 2.8	36.8 ± 6.4
18		(3*RS*)-Onogenin	16.1	29.0 ± 4.6	33.2 ± 0.5
19		Dalparvin A	14.7	22.4 ± 2.0	28.3 ± 3.4
21	Flavanones	(2*S*)-Liquiritigenin	36.4	37.8 ± 6.4	57.9 ± 3.5
22		(2*S*)-Pinocembrin	14.1	-	32.2 ± 4.4
24		(2*S*)-Naringenin	11.7	-	36.9 ± 4.6
27	Isoflavans	(3*S*)-8-Demethylduartin	30.3	35.7 ± 7.8	52.7 ± 3.0
28		(3*RS*)-3'-Hydroxy-8-methoxy vestitol	18.8	40.3 ± 7.1	42.2 ± 2.0
29		Sativan	9.9	-	42.1 ± 4.4

[a] The contribution due to quenching was calculated according to the following equation:

$$100\left(1-\frac{I}{I_0}\right)=100\left(1-\frac{1}{1+Ksv[Q]}\right)$$

Table 32 (Continued)

ID	Class	Chemical Name	% Quenching contribution[a]	% inhibition at a concentration of 142 μM	
				H7N3	H5N1
30	Pterocarpans	3-8-Dihydroxy-9-methoxypterocarpan	10.8	-	50.5 ± 8.2
31		Melilotocarpan D	5.9	-	25.1 ± 3.8
33	Miscellaneous	Resveratrol	17.4	80.3 ± 1.4	62.5 ± 3.4
36		Oxyresveratrol	26.2	-	80.6 ± 8.9

[a] The contribution due to quenching was calculated according to the following equation:

$$100\left(1-\frac{I}{I_0}\right)=100\left(1-\frac{1}{1+Ksv[Q]}\right)$$

The quenching effect by a variety of compounds on species structurally related to 4-methylumbelliferone has been reported in the literature. As representative examples: the fluorescence of 7-ethoxycoumarin is quenched by halide ions (Moriya, 1984), the fluorescence of 3-methyl 7-hydroxyl coumarin is quenched in the presence of acetone (Sharma *et al.*, 2007), and that of 3-carboxy-5,6-benzocoumarin by aromatic amines(Tablet and Hillebrand, 2007). On the other hand, there have also been reports on the quenching effect of flavonoids on the fluorescence of many compounds with no structural relationship to 4-methylumbelliferone such as 1,6-diphynyl-1,3,5-hexatriene (DPH) (Schoefer *et al.*, 2001), human salivary r-amylase (HSA) (Soares *et al.*, 2007), bovine serum albumin (BSA)(Papadopoulou *et al.*, 2005, Soares *et al.*, 2007, Wang *et al.*, 2007) and 2,3-diazabicyclo[2.2.2]oct-2-ens(DBO) (Anbazhagan *et al.*, 2008).

Since we proved that the structure of phenolic compounds can reduce the fluorescence intensity of 4-MU directly. It is important to perform the quenching assay along with the neuraminidase inhibition assay for avoiding the misinterpreting of the real efficacy of flavonoids in neuraminidase inhibition. In this experiment, 8 flavonoids showed significant reduction of fluorescence intensity of 4-MU in neuraminidase H5N1 inhibition assay at the concentration of 142 μM were chosen for determining the IC_{50}

values before and after subtraction with quenching effect. These data reported in **Figures 29-32** and **Table 33**. For neuraminidase H7N3, we excluded the determination of the IC_{50} values before and after subtraction with quenching effect because we found that there was only Resveratrol (**33**) showed inhibitory activity more than 50% at the concentration of 142 μM.

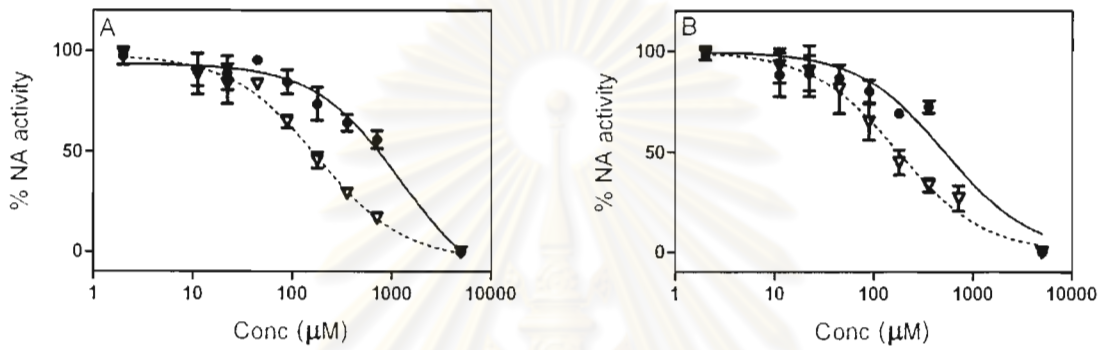

Figure 29 Dose-response curves of Khrinone C (A) and Irilin D (B) showing before and after subtraction of quenching [● After subtraction, ▽ Before subtraction]

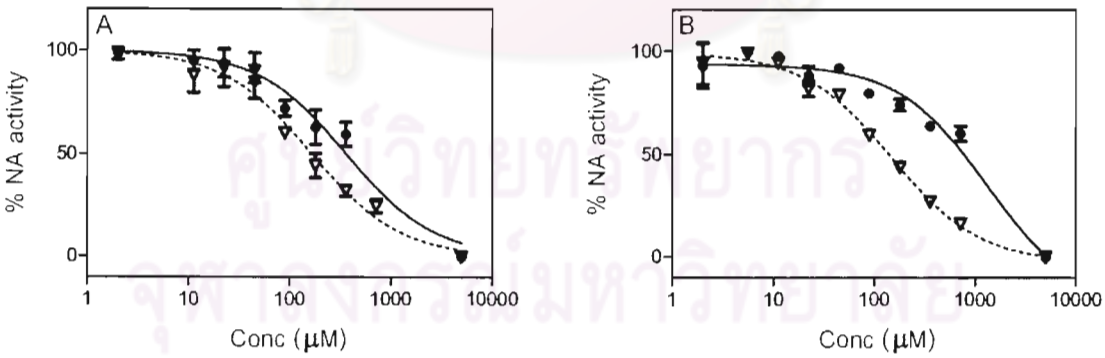

Figure 30 Dose-response curves of (3*R*)-7,3'-Dihydroxy-4-methoxyisoflavanone (A) and (2*S*)-Liquiritigenin (B) showing before and after subtraction of quenching [● After subtraction, ▽ Before subtraction]

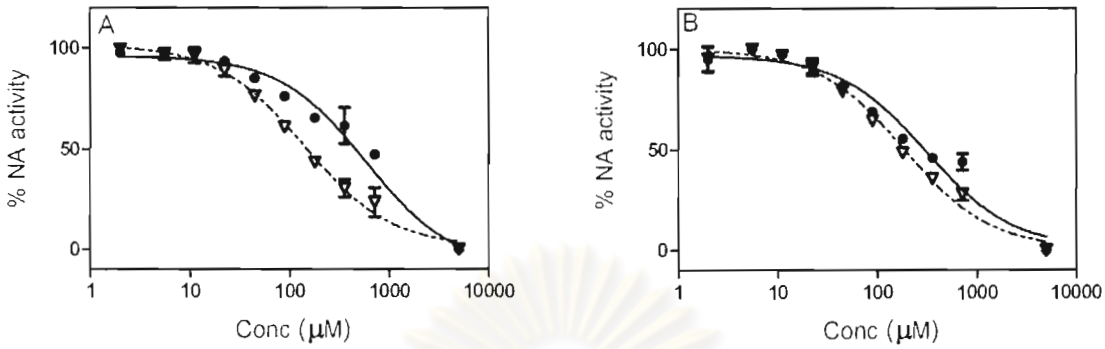

Figure 31 Dose-response curves of (3*S*)-8-Demethylduartin (A) and 3-8-Dihydroxy-9-methoxy pterocarpan (B) showing before and after subtraction of quenching [● After subtraction, ▽ Before subtraction]

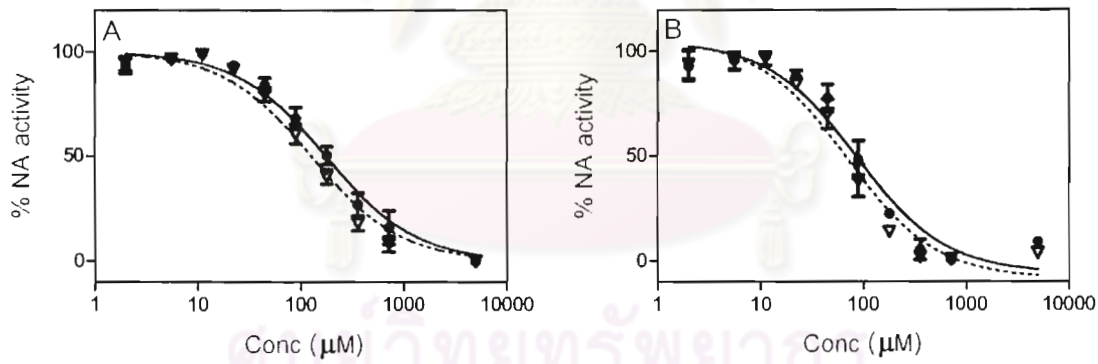

Figure 32 Dose-response curve of Resveratrol (A) and Oxyresveratrol (B) showing before and after subtraction of quenching [● After subtraction with quenching, ▽ Before subtraction]

Table 33 IC_{50} values of 6 flavonoids and 2 stilbenes on H5N1 neuraminidase

ID	Class	Chemical Name	$IC_{50} \pm SD$ (μM) on H5N1	
			After subtraction	Before subtraction
7	Isoflavanones	Khrinone C	> 500	155.6 ± 0.3
11		Irilin D	> 500	182.7 ± 71.2
12	Isoflavones	(3*R*)-7,3'-Dihydroxy-4-methoxyisoflavanone	> 500	166.5 ± 32.6
21	Flavanones	(2*S*)-Liquiritigenin	> 500	137.0 ± 9.3
27	Isoflavans	(3*S*)-8-Demethylduartin	418.0 ± 35.2	153.6 ± 22.0
30	Pterocarpans	3-8-Dihydroxy-9-methoxy pterocarpan	284.4 ± 24.8	186.5 ± 11.9
33	Miscellaneous	Resveratrol	185.1 ± 68.2	129.2 ± 32.0
36		Oxyresveratrol	84.6 ± 10.6	66.1 ± 6.8

The results showed that IC_{50} values of 8 flavonoids after subtraction with quenching were higher than that of before subtraction (**Table 33**). Moreover, 4 flavonoids including: Khrinone C (**7**), Irilin D (**11**), (3*R*)-7,3'-Dihydroxy-4-methoxyisoflavanone (**12**) and (2*S*)-Liquiritigenin (**21**) exhibited inhibitory activity more than 500 μM. Among tested flavonoids, Osyresveratrol (**36**) (IC_{50} = 84.6 ± 10.6 μM) was found to retain some neuraminidase inhibitory activity against H5N1 neuraminidase whereas resveratrol (**33**), in this study, did not show a significant inhibitory activity on H5N1 (IC_{50} = 185.1 ± 68.2 μM). This might be because the 2-OH group presents on oxyresveratrol's structure plays an important role on inhibitory activity.

Fluorescence quenching and enzyme inhibition are completely different and mechanistically independent phenomena. In facts enzyme inhibition reflects the property of a given species (the inhibitor) to somehow hinder the normal activity of the enzyme against its natural substrates. On the contrary fluorescence quenching does not require interaction with neither the enzyme nor the substrate, the only requirement is the

interaction with the fluorescent product of the reaction. The only explanation for the observed behaviour is that quenching may indeed largely contribute to the magnitude of the signals obtained in fluorimetric assays aimed to test the inhibitory properties of flavonoids generating false positive results. Since quenching and inhibition are not mechanistically mutually exclusive phenomena, they occur at the same time. If flavonoids are effective inhibitors, the amounts of 4-MU released in the neuraminidase catalysed reaction will be of course lower than those expected in absence of inhibitors; however the excess flavonoids present in solution will quench the fluorescence of the released 4-MU resulting in an apparently higher inhibitory effect. Because of the above considerations it might be possible, as a first approximation, to subtract the contribution of the quenching effect from the data obtained in the inhibition experiments. From this experiment, the collected data point out that when the quenching effect is not taken into account, flavonoids may produce false positive results in generating misleading interpretation of their effects on viral neuraminidase.

CHAPTER 6

CONCLUSION

In summary, the findings of this work suggest that the crude preparations of recombinant enzyme could be safely used to set up cost-effective throughput screening assays to analyze the potency of various putative neuraminidase inhibitors. The crude preparations can be used readily without the need of expensive purification of recombinant neuraminidases or the costs associated to the safety standards related to the use of avian influenza viruses. In fact, those materials containing baculovirus particles are safer to work with than most mammalian viruses since they are noninfectious to vertebrates.

Based on the established enzyme-based assay system, we could report the results of preliminary screening of some novel putative neuraminidase inhibitors obtained by rational design on the basis of the oseltamivir structure and obtained from the isolated natural flavonoid compounds. The collected data suggest that the introduction of small substituent on the 5-amino group of oseltamivir increases the affinity of the new analogs against N1, but it seems to be rather ineffective with respect to N3. In addition, the introduction of large substituent on the 4-amino group of oseltamivir carboxylate decreases the affinity of the compounds for N1 while this structural modification seems to be somewhat better tolerated by N3. Although the investigated analogues present an activity similar to that of oseltamivir carboxylate, among the panel of analyzed compounds two different species, namely **PMC-36** (6) and **PMC-35** (5), displayed a promising activity as inhibitors of neuraminidase N1 and N3 respectively. In general, neuraminidase N3 was found to be more sensitive to the structural modifications of the oseltamivir analogues, while neuraminidase N1 was less sensitive; this is probably the result of the original design of oseltamivir which was rationally designed on the structure of group-2 neuraminidases.

With the natural flavonoids isolated from Thai medicinal plants: *Dalbergia parviflora* and *Belamcanda chinensis*. The results of the screening, unexpectedly, led to the findings that the structure of flavonoids can directly quench the fluorescence intensity of 4-MU. The quenching constant of each flavonoid was determined by using the Stern-Volmer approach in order to compare the fluorescence quenching effect among the panel of flavonoids considered. Almost of all flavonoids classes can produce a false positive to neuraminidase inhibition assay which using 4-MUNANA as a substrate. Therefore, our findings suggest that the accuracy of neuraminidase inhibition assay should be improved by analyzing the quenching properties of flavonoids on 4-MU prior to test the inhibition effect Moreover, It also might be possible, as a first approximation, to subtract the contribution of the quenching effect from the data obtained in the inhibition experiments in order to get accurate neuraminidase inhibitory activity.

REFERENCES

Anbazhagan, V., Kalaiselvan, A., Jaccob, M., Venuvanalingam, P., and Renganathan, R. 2008. Investigations on the fluorescence quenching of 2,3-diazabicyclo[2.2.2]oct-2-ene by certain flavonoids. Journal of Photochemistry and Photobiology B-Biology 91: 143-150.

Aymard-Henryn, M., *et al.* 1973. Influenza virus neuraminidase and neuraminidase-inhibition test procedures. Bulletin of the World Health Organization 48: 199–202.

Barnett, J.M., *et al.* 2000. Zanamivir susceptibility monitoring and characterization of influenza virus clinical isolates obtained during phase II clinical efficacy studies. Antimicrobial Agents and Chemotherapy 44: 78-87.

Buxton, R.C., *et al.* 2000. Development of a sensitive chemiluminescent neuraminidase assay for the determination of influenza virus susceptibility to zanamivir. Analytical Biochemistry 280: 291-300.

Cattoli, G., *et al.* 2006. Development and validation of an anti-N3 indirect immunofluorescent antibody test to be used as a companion diagnostic test in the framework of a "DIVA" vaccination strategy for avian influenza infections in poultry. Avian Pathology 35: 154-U123.

Cattoli, G., Terregino, C., Brasola, V., Rodriguez, J.F., and Capua, I. 2003. Development and preliminary validation of an ad hoc N1-N3 discriminatory test for the control of avian influenza in Italy. Avian Diseases 47: 1060-1062.

Connor, R.J., Kawaoka, Y., Webster, R.G., and Paulson, J.C. 1994. Receptor specificity in human, avian, and equine H2 and H3 influenza virus isolates. Virology 205: 17-23.

Couceiro, J.N., Paulson, J.C., and Baum, L.G. 1993. Influenza virus strains selectively recognize sialyloligosaccharides on human respiratory epithelium; the role of the host cell in selection of hemagglutinin receptor specificity. Virus Research 29: 155-165.

Dalakouras, T., Smith, B.J., Platis, D., Cox, M.M.J., and Labrou, N.E. 2006. Development of recombinant protein-based influenza vaccine expression and affinity purification of H1N1 influenza virus neuraminidase. Journal of Chromatography A 1136: 48-56.

Dao, T.T., *et al.* 2011. Chalcones as novel influenza A (H1N1) neuraminidase inhibitors from *Glycyrrhiza inflata*. Bioorganic & Medicinal Chemistry Letters 21: 294-298.

Davis, G.A. 1973. Quenching of aromatic hydrocarbons by alkylpyridinium halides. Journal of the Chemical Society - Chemical Communications 728-729.

De Clercq, E. 2004. Antivirals and antiviral strategies. Nature Reviews Microbiology 2: 704-720.

De Clercq, E. 2006. Antiviral agents active against influenza A viruses. Nature Reviews Drug Discovery 5: 1015-1025.

de Jong, M.D., *et al.* 2005. Brief report - Oseltamivir resistance during treatment of influenza A (H5N1) infection. New England Journal of Medicine 353: 2667-2672.

de Jong, M.D., and Hien, T.T. 2006. Avian influenza A (H5N1). Journal of Clinical Virology 35: 2-13.

Earhart, K.C., *et al.* 2009. Oseltamivir resistance mutation N294S in human influenza A(H5N1) virus in Egypt. Journal of Infection and Public Health 2: 74-80.

Eftink, M.R., and Ghiron, C. 1981. Fluorescence quenching studies with proteins. Analytical Biochemistry 114: 199-227.

Eftink, M.R. 1991a. Fluorescence quenching reactions: probing biological macromolecular structures. ed., Biophysical and biochemical aspects of fluorescence spectroscopy, pp. 1-41. New York: Plenum Press.

Eftink, M.R. 1991b. Fluorescence spectroscopy. Lakowicz JR, ed., Fluorescence quenching: theory and applications, Vol. 2 pp. 53-126. New York: Plenum Press.

Eichelberger, M.C., Hassantoufighi, A., Wu, M., and Li, M. 2008. Neuraminidase activity provides a practical read-out for a high throughput influenza antiviral screening assay. Virology Journal 5: 109.

Federspiel, M., *et al.* 1999. Industrial synthesis of the key precursor in the synthesis of the anti-influenza drug oseltamivir phosphate (Ro 64-0796/002, GS-4104-02): Ethyl (3R,4S,5S)-4,5-epoxy-3-(1-ethyl-propoxy)-cyclohex-1-ene-1-carboxylate. Organic Process Research & Development 3: 266-274.

Gambaryan, A.S., *et al.* 1997. Specification of receptor-binding phenotypes of influenza virus isolates from different hosts using synthetic sialylglycopolymers: non-egg-adapted human H1 and H3 influenza A and influenza B viruses share a common high binding affinity for 6'-sialyl(N-acetyllactosamine). Virology 232: 345-350.

Govorkova, E.A., *et al.* 2009. Susceptibility of Highly Pathogenic H5N1 Influenza Viruses to the Neuraminidase Inhibitor Oseltamivir Differs In Vitro and in a Mouse Model. Antimicrobial Agents and Chemotherapy 53: 3088-3096.

Govorkova, E.A., Leneva, I.A., Goloubeva, O.G., Bush, K., and Webster, R.G. 2001. Comparison of efficacies of RWJ-270201, zanamivir, and oseltamivir against H5N1, H9N2, and other avian influenza viruses. Antimicrobial Agents and Chemotherapy 45: 2723-2732.

Gubareva, L.V., Robinson, M.J., Bethell, R.C., and Webster, R.G. 1997. Catalytic and framework mutations in the neuraminidase active site of influenza viruses that are resistant to 4-guanidino-Neu5Ac2en. Journal of Virology 71: 3385-3390.

Gubareva, L.V., Webster, R.G., and Hayden, F.G. 2002. Detection of influenza virus resistance to neuraminidase inhibitors by an enzyme inhibition assay. Antiviral Research 53: 47-61.

Guo, C.T., Takahashi, T., Bukawa, W., Takahashi, N., Yagi, H., Kato, K., Hidari, K.I.P.J., Miyamoto, D., Suzuki, T., Suzuki, Y. 2006. Edible bird's nest extract inhibits influenza virus infection. Antiviral Research 70: 140-146.

Ito, T., *et al.* 1998. Molecular basis for the generation in pigs of influenza A viruses with pandemic potential. Journal of Virology 72: 7367-7373.

Jeong, H.J., *et al.* 2009. Neuraminidase inhibitory activities of flavonols isolated from *Rhodiola rosea* roots and their *in vitro* anti-influenza viral activities. Bioorganic & Medicinal Chemistry 17: 6816-6823.

Jonges, M., *et al.* 2010. Influenza virus inactivation for studies of antigenicity and phenotypic neuraminidase inhibitor resistance profiling. Journal of Clinical Microbiology 48: 928-940.

Kasha, M. 1952. Collisional perturbation of spin-orbital coupling and the mechanism of fluorescence quenching: a visual demonstration of the perturbation. The Journal of chemical physics 20: 71-74.

Kautsky, H. 1939. Quenching of luminescence by oxygen. Transactions of the Faraday Society 35: 216-219.

Knibbe, H., Rehm, D., and Weller, A. 1968. Intermediates and kinetics of fluorescence quenching by electron transfer. Berichte der Bunsen-Gesellschaft für Physikalische Chemie 72: 257-263.

Knipe, D.M., and Howley, P.M. 2007. Orthomyxoviridae: The virus and Their replication. ed., Fields' virology, Vol. 1 pp. 1487-1524. Philadelphia: Lippincott Williams & Wilkins.

Lakowicz, J.R. 2006. Quenching of Fluorescence. ed., Principles of fluorescence spectroscopy, pp. 277-330. New York: Springer.

Le, Q.M., *et al.* 2005. Avian flu - Isolation of drug-resistant H5N1 virus. Nature 437: 1108-1108.

Liu, A.L., *et al.* 2008a. Anti-influenza virus activities of flavonoids from the medicinal plant *Elsholtzia rugulosa*. Planta Medica 74: 847-851.

Liu, A.L., Wang, H.D., Lee, S.M.Y., Wang, Y.T., and Du, G.H. 2008b. Structure-activity relationship of flavonoids as influenza virus neuraminidase inhibitors and their in vitro anti-viral activities. Bioorganic & Medicinal Chemistry 16: 7141-7147.

Matrosovich, M.N., *et al.* 1997. Avian influenza A viruses differ from human viruses by recognition of sialyloligosaccharides and gangliosides and by a higher conservation of the HA receptor-binding site. Virology 233: 224-234.

Matrosovich, M.N., Matrosovich, T.Y., Gray, T., Roberts, N.A., and Klenk, H.D. 2004. Human and avian influenza viruses target different cell types in cultures of human airway epithelium. Proceedings of the National Academy of Sciences of the United States of America 101: 4620-4624.

McSharry, J.J., McDonough, A.C., Olson, B.A., and Drusano, G.L. 2004. Phenotypic drug susceptibility assay for influenza virus neuraminidase inhibitors. Clinical and Diagnostic Laboratory Immunology 11: 21-28.

Mercader, A.G., and Pomilio, A.B. 2010. QSAR study of flavonoids and biflavonoids as influenza H1N1 virus neuraminidase inhibitors. European Journal of Medicinal Chemistry 45: 1724-1730.

Miki, K., *et al*. 2007. Anti-influenza virus activity of biflavonoids. Bioorganic & Medicinal Chemistry Letters 17: 772-775.

Monthakantirat, O., *et al*. 2005. Phenolic constituents of the rhizomes of the Thai medicinal plant *Belamcanda chinensis* with proliferative activity for two breast cancer cell lines. Journal of natural products 68: 361-364.

Moriya, T. 1984. Excited-state reactions of coumarins in aqueous solutions. II. The fluorescence quenching of 7-Ethoxycoumarins by halide ions. Bulletin of the Chemical Society of Japan 57: 1723-1730.

Moscona, A. 2005. Drug therapy - Neuraminidase inhibitors for influenza. New England Journal of Medicine 353: 1363-1373.

Nakao, Y., Takada, K., Matsunaga, S., and Fusetani, N. 2001. Calyceramides A-C: neuraminidase inhibitory sulfated ceramides from the marine sponge *Discodermia calyx*. Tetrahedron 57: 3013-3017.

Nayak, D.P., and Reichl, U. 2004. Neuraminidase activity assays for monitoring MDCK cell culture derived influenza virus. Journal of Virological Methods 122: 9-15.

Nguyen, P.H., *et al*. 2010a. New stilbenoid with inhibitory activity on viral neuraminidases from *Erythrina addisoniae*. Bioorganic & Medicinal Chemistry Letters 20: 6430-6434.

Nguyen, P.H., *et al*. 2010b. Prenylated pterocarpans as bacterial neuraminidase inhibitors. Bioorganic & Medicinal Chemistry 18: 3335-3344.

Nguyen, T.N.A., *et al*. 2011. Influenza A (H1N1) neuraminidase inhibitors from *Vitis amurensis*. Food Chemistry 124: 437-443.

Papadopoulou, A., Green, R.J., and Frazier, R.A. 2005. Interaction of flavonoids with bovine serum albumin: A fluorescence quenching study. Journal of Agricultural and Food Chemistry 53: 158-163.

Potier, M., Mameli, L., Belisle, M., Dallaire, L., and Melancon, S.B. 1979. Fluorometric assay of neuraminidase with a sodium (4-methylumbelliferyl-alpha-D-N-acetylneuraminate) substrate. Analytical Biochemistry 94: 287-296.

Rameix-Welti, M.A., *et al.* 2006. Natural variation can significantly alter the sensitivity of influenza A (H5N1) viruses to oseltamivir. Antimicrobial Agents and Chemotherapy 50: 3809-3815.

Rameix-Welti, M.A., Enouf, V., Cuvelier, F., Jeannin, P., and van der Werf, S. 2008. Enzymatic properties of the neuraminidase of seasonal H1N1 influenza viruses provide insights for the emergence of natural resistance to oseltamivir. Plos Pathogens 4: -.

Rogers, G.N., *et al.* 1983. Single amino acid substitutions in influenza haemagglutinin change receptor binding specificity. Nature 304: 76-78.

Rogers, G.N., and Paulson, J.C. 1983. Receptor determinants of human and animal influenza virus isolates: differences in receptor specificity of the H3 hemagglutinin based on species of origin. Virology 127: 361-373.

Rogers, G.N., and D'Souza, B.L. 1989. Receptor binding properties of human and animal H1 influenza virus isolates. Virology 173: 317-322.

Rohloff, J.C., *et al.* 1998. Practical total synthesis of the anti-influenza drug GS-4104. Journal of Organic Chemistry 63: 4545-4550.

Romero, E.L., Pardo, M.F., Porro, S., and Alonso, S. 1997. Sialic acid measurement by a modified Aminoff method: a time-saving reduction in 2-thiobarbituric acid concentration. Journal of biochemical and biophysical methods 35: 129-134.

Rungrotmongkol, T., Frecer, V., De-Eknamkul, W., Hannongbua, S., and Miertus, S. 2009. Design of oseltamivir analogs inhibiting neuraminidase of avian influenza virus H5N1. Antiviral Research 82: 51-58.

Russell, R.J., *et al*. 2006. The structure of H5N1 avian influenza neuraminidase suggests new opportunities for drug design. Nature 443: 45-49.

Ryu, H.W., *et al*. 2010a. Xanthones with neuraminidase inhibitory activity from the seedcases of *Garcinia mangostana*. Bioorganic & Medicinal Chemistry 18: 6258-6264.

Ryu, Y.B., *et al*. 2008. Pterocarpans and flavanones from *Sophora flavescens* displaying potent neuraminidase inhibition. Bioorganic & Medicinal Chemistry Letters 18: 6046-6049.

Ryu, Y.B., *et al*. 2009a. Characteristic of neuraminidase inhibitory xanthones from *Cudrania tricuspidata*. Bioorganic & Medicinal Chemistry 17: 2744-2750.

Ryu, Y.B., *et al*. 2010b. Inhibition of neuraminidase activity by polyphenol compounds isolated from the roots of *Glycyrrhiza uralensis*. Bioorganic & Medicinal Chemistry Letters 20: 971-974.

Ryu, Y.B., *et al*. 2009b. Structural characteristics of flavanones and flavones from *Cudrania tricuspidata* for neuraminidase inhibition. Bioorganic & Medicinal Chemistry Letters 19: 4912-4915.

Schoefer, L., Braune, A., and Blaut, M. 2001. A fluorescence quenching test for the detection of flavonoid transformation. Fems Microbiology Letters 204: 277-280.

Schunemann, H.J., *et al*. 2007. WHO rapid advice guidelines for pharmacological management of sporadic human infection with avian influenza A (H5N1) virus. Lancet Infectious Diseases 7: 21-31.

Scott, T.G., Spencer, R.D., Leonard, N.J., and Weber, G. 1970. Emission propertiesof NADH: studies of fluorescence lifetimes and quantum efficiencies of NADH, AcPyADH, and simplified synthetic models. Journal of the American Chemical Society 92: 687-695.

Sharma, V.K., Mohan, D., and Sahare, P.D. 2007. Fluorescence quenching of 3-methyl 7-hydroxyl Coumarin in presence of acetone. Spectrochimica Acta Part a-Molecular and Biomolecular Spectroscopy 66: 111-113.

Shinitzky, M., and Rivnay, B. 1977. Degree of exposure of membrane proteins determined by fluorescence quenching. Biochemistry 16: 982-986.

Skehel, J.J., and Schild, G.C. 1971. The polypeptide composition of influenza A viruses. Virology 44: 396-408.

Soares, S., Mateus, N., and De Freitas, V. 2007. Interaction of different polyphenols with bovine serum albumin (BSA) and human salivary alpha-amylase (HSA) by fluorescence quenching. Journal of Agricultural and Food Chemistry 55: 6726-6735.

Song, H., Wang, Q., Li, Y., Zhang, D., and Cheng, J. 2010. Expression of neuraminidase protein of H1N1 swine-origin influenza A virus (S-OIV) in insect cells with a baculovirus expression system. International Journal of Infectious Diseases 14: S47-S48.

Song, J.M., Lee, K.H., and Seong, B.L. 2005. Antiviral effect of catechins in green tea on influenza virus. Antiviral Research 68: 66-74.

Spencer, R.D., and Weber, G. 1972. Thermodynamics and kinetics of the intramolecular complex in flavin-adenine dinucleotide. Akeson A & Ehrenberg A, ed., In Structure and function of oxidation reduction enzymes, pp. 393-399. New York: Pergamon Press.

Steiner, R.F., and Kirby, E.P. 1969. The interaction of the ground and excited states of indole derivatives with electron scavengers. The Journal of Physical Chemistry 73: 4130-4135.

Tablet, C., and Hillebrand, M. 2007. Quenching of the fluorescence of 3-carboxy-5,6-benzocoumarin by aromatic amines. Journal of Photochemistry and Photobiology a-Chemistry 189: 73-79.

Takada, K., Nakao, Y., Matsunaga, S., van Soest, R.W., and Fusetani, N. 2002. Nobiloside, a new neuraminidase inhibitory triterpenoidal saponin from the marine sponge *Erylus nobilis*. Journal of natural products 65: 411-413.

Tanimoto, T., *et al.* 2004. Expression of influenza neuraminidase in CHO-K1 cells International Congress Series 1263: 568-572

Taylor, W.R., *et al.* 2010. Avian influenza--a review for doctors in travel medicine. Travel Medicine and Infectious Disease 8: 1-12.

Umehara, K., *et al.* 2008. Estrogenic constituents of the heartwood of *Dalbergia parviflora*. Phytochemistry 69: 546-552.

Verma, R., Boleti, E., and George, A.J. 1998. Antibody engineering: comparison of bacterial, yeast, insect and mammalian expression systems. Journal of Immunological Methods 216: 165-181.

von Itzstein, M. 2007. The war against influenza: discovery and development of sialidase inhibitors. Nature Reviews Drug Discovery 6: 967-974.

Wang, Y.Q., Zhang, H.M., Zhang, G.C., Tao, W.H., and Tang, S.H. 2007. Interaction of the flavonoid hesperidin with bovine serum albumin: A fluorescence quenching study. Journal of Luminescence 126: 211-218.

Wetherall, N.T., *et al.* 2003. Evaluation of neuraminidase enzyme assays using different substrates to measure susceptibility of influenza virus clinical isolates to neuraminidase inhibitors: Report of the neuraminidase inhibitor susceptibility network. Journal of Clinical Microbiology 41: 742-750.

White, D.O., and Fenner, F.J. 1994. Medical virology 4th ed. San Diego Academic Press.

WHO 2011. Cumulative Number of Confirmed Human Cases of Avian Influenza A/(H5N1) Reported to WHO[Online]. World Health Organization: Available from http://www.who.int/csr/disease/avian_influenza/country/cases_table_2011_01_13/en/index.html [16 January 2011]

Woods, J.M., *et al.* 1993. 4-Guanidino-2,4-Dideoxy-2,3-Dehydro-N-Acetylneuraminic Acid is a highly effective inhibitor both of the sialidase (Neuraminidase) and of growth of a wide-range of influenza A and influenza B viruses *in vitro*. Antimicrobial Agents and Chemotherapy 37: 1473-1479.

Yen, H.L., *et al.* 2007. Neuraminidase inhibitor-resistant recombinant A/Vietnam/1203/04 (H5N1) influenza viruses retain their replication efficiency and pathogenicity *in vitro* and *in vivo*. Journal of Virology 81: 12418-12426.

Yongkiettrakul, S., *et al.* 2009. Avian influenza A/H5N1 neuraminidase expressed in yeast with a functional head domain. Journal of Virological Methods 156: 44-51.

Appendices

Appendix A

Preparation of the 10% SDS-PAGE gel

1. The glass plates and spacer were cleaned with ethanol prior to use. The gel plate was set up by clamping with casting stand.

2. Resolving gel which contains the solutions below was prepared in beaker and loaded into gel plate.

Milli Q water	2809	µl
1.5M Tris HCl pH 8.8	1750	µl
10% SDS	70	µl
Acrylamide 30% bis 0.8 %	2333	µl
TEMED	2.3	µl
10% APS	35	µl

4. Ultra pure water was added into gel plate to replace the stacking gel. Gel plate was stand for a while for polymerization.

5. Ultra pure water was poured off after resolving gel was polymerized.

6. Stacking gel which contains the solutions below was prepared in beaker and loaded into gel plate.

Milli Q water	2405	µl
0.5 M Tris HCl pH 6.8	1000	µl
10% SDS	40	µl
Acrylamide 30% bis 0.8 %	533.2	µl
TEMED	3	µl
10% APS	30	µl

7. Dry comb was introduced into the stacking gel. Leave it until gel was polymerized.

8. SDS electrophoresis buffer 1X was prepared by adding 80 ml of 10x SDS electrophoresis buffer into 720 ml water.

Appendix A (Continued)

9. Comb was removed slowly. The gel plate was washed with SDS electrophoresis buffer 1X and clamped it with electrode stand. This stand was placed in the tank filled with SDS electrophoresis buffer 1X.

10. Supernatant neuraminidase diluted 1:10, 7 ul each (total amount of protein = 2 ug) was mixed with equal volume of STB 2X NO DTT. These samples were boiled for 5 minutes.

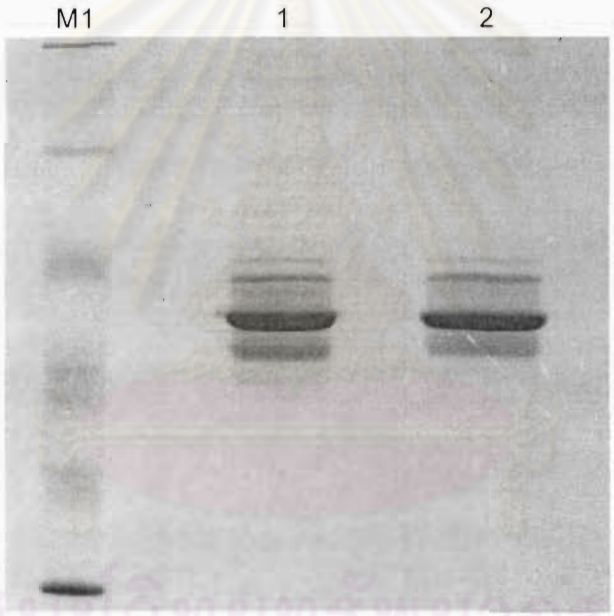

Total protein isolated from recombinant neuraminidase

Lane MARKER = PageRuler™ Plus Prestained Protein ladder, Fermentas

Lane 1= Total Protein isolated from recombinant neuraminidase H7N1

Lane 2 = Total Protein isolated from recombinant neuraminidase H7N3

Appendix A (Continued)

Preparation of 10x SDS electrophoresis buffer (250 mM Tris, 1.92 M Glycine, 1% SDS)

Tris (Hydroxymethyl)-aminomethane	30.0	g
Glycine	144.0	g
SDS	10.0	g

Dissolved and adjusted to volume 1 liter with distilled water

Appendix B

Preparation of enzyme assay buffer solutions

33 mM MES pH 6.5, 4 mM $CaCl_2$

MES	1.61	g
$CaCl_2$	110.99	mg

Adjusted pH to 6.5 and adjusted volume to 250 ml with distilled water

0.1M Glycine pH 10.7 containing 25% Ethanol

Glycine	750.7	mg
Distilled water	75	ml

Adjusted pH to 10.7 and added 25 ml of ethanol

0.1M Glycine pH 2.5

Glycine	750.7	mg

Adjusted pH to 2.5 and adjusted volume to 100 ml with distilled water

0.1M Sodium acetate pH 4.0

Sodium acetate

Adjusted pH to 4.0 and adjusted volume to 100 ml with distilled water

PBS pH 7.2

NaCl	8	g
KCl	0.2	g
Na_2HPO_4	1.44	g
KH_2PO_4	0.2	g

Adjusted pH to 7.2 and adjusted volume to 1000 ml with distilled water

Appendix B (Continued)

0.1M $NaHCO_3$ pH 12.2

$NaHCO_3$ 0.84 g

Adjusted pH to 12.2 and adjusted volume to 100 ml with distilled water

20 μM MUNANA in 33 mM MES pH 6.5, 4 mM $CaCl_2$

MUNANA 1 mg/ml in 33 mM MES pH 6.5, 4 mM $CaCl_2$ 120 ul

Adjusted volume to 12 ml with 33 mM MES pH 6.5, 4 mM $CaCl_2$

20 μM 4-methylumbelliferone

4-MU 1 mg/ml in ethanol 35 ul

Adjusted volume to 10 ml with 33 mM MES pH 6.5, 4 mM $CaCl_2$

Appendix C

Enzymatic reaction of neuraminidase

There are several methods for determination of neuraminidase activity. One of the most commonly used methods is fluorometric assay which has many advantages over the others. This fluorometric assay is simple, high sensitivity and less time consuming.

Principle:

4-methylumbelliferyl-α-D-N-acetylneuraminic acid (MUNANA) is used as a fluorogenic substrate. 4-methylumbelliferone (4-MU) is presented after neuraminidase cleavage from MU-NANA. Therefore, neuraminidase activity can be measured by quantification of their fluorogenic products, 4-MU. The fluorescence intensity was recorded at excitation wavelength of 355 nm and emission wavelength of 460 nm.

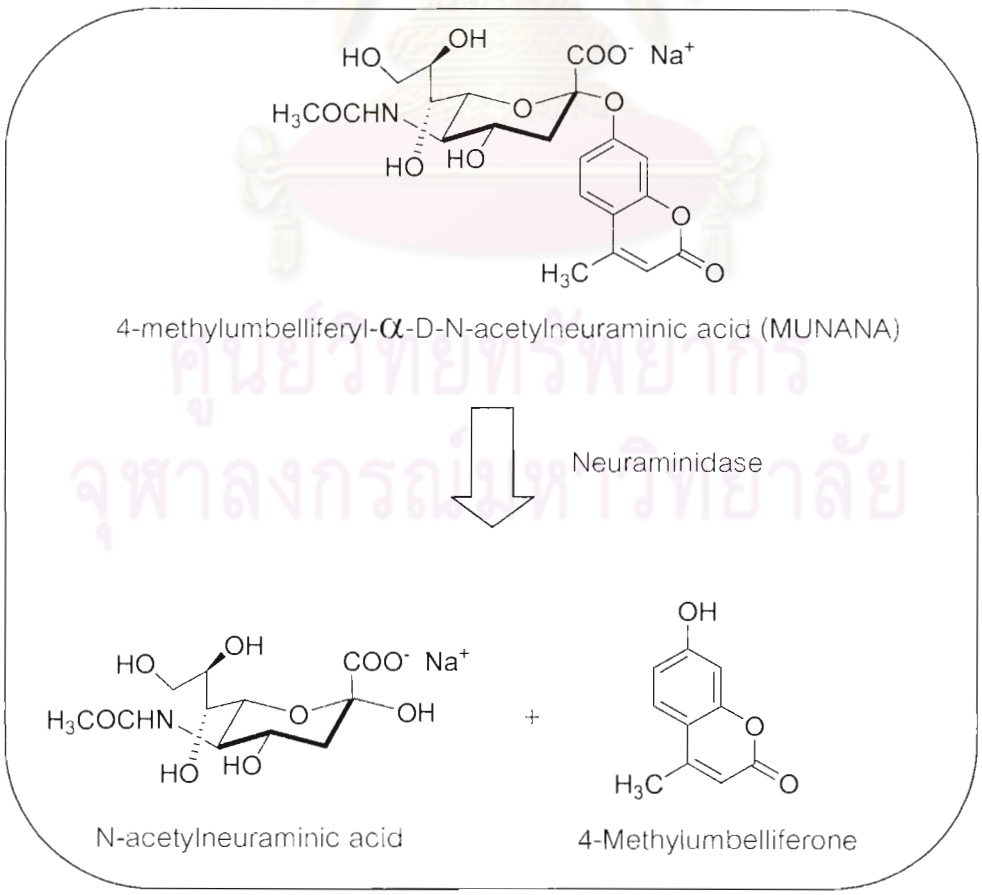

Enzymatic mechanism of influenza virus sialidase (von Itzstein, 2007)

It was originally proposed that the solution-dominant α-sialoside $^{2}C_{5}$ conformer binds to the influenza virus sialidase and is distorted by the active-site environment from this chair conformation into an α-boat conformer (**Figure 33**). X-ray crystallographic studies of sialidase–Neu5Ac (N-acetylneuraminic acid) complexes confirmed both distortion of the substrate upon binding and the formation of a salt bridge between the substrate's negatively charged carboxyl group and highly conserved triarginyl cluster. The departure of the aglycon residue would appear to be facilitated by the resulting conformational strain through the formation of an oxocarbocation ion intermediate, a sialosyl cation, that has been identified by kinetic isotope effect measurements and molecular modelling studies. The negatively charged environment within that region of the sialidase catalytic site is thought to stabilize the charged intermediate. A water molecule then reacts in a stereoselective manner with the sialosyl cation intermediate to afford α-Neu5Ac(compound 1a) as the first product of release that then mutarotates to the thermodynamically more favourable β-anomer (compound 1b). Alternatively, it has been proposed that all sialidases, irrespective of origin, may trap the cation to form a glycosyl-enzyme covalent intermediate, a common feature of retaining glycohydrolases, that is stereospecifically hydrolysed to afford compound 1a (**Figure 33**).

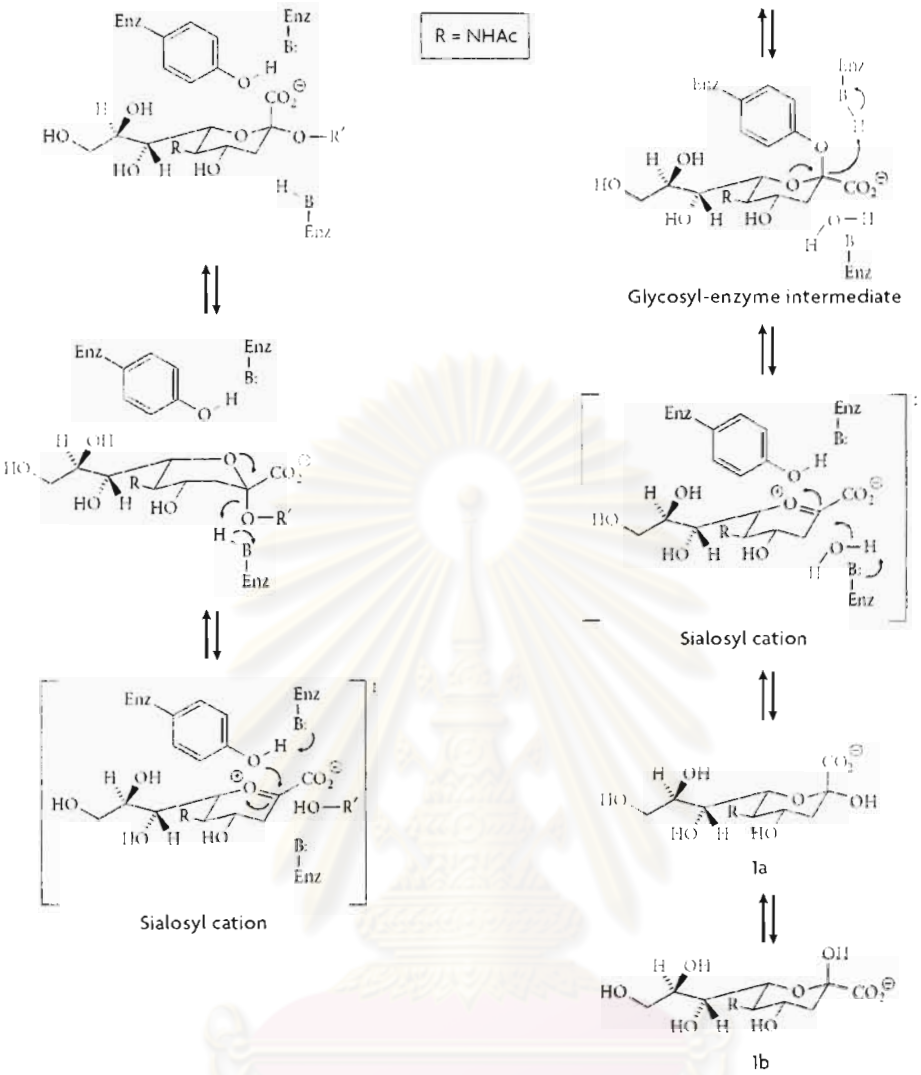

Figure 33 Enzymatic mechanism of influenza virus neuraminidase

VITA

Miss Jarinrat Kongkamnerd was born on 26 August 1983 in Chiang Mai Province, Thailand. She received her Bachelor's degree of Pharmacy from Faculty of Pharmacy, Chiang Mai University in 2006. After that, she enrolled in the Doctor of Philosophy Program in Pharmacognosy, Faculty of Pharmaceutical Sciences, Chulalongkorn University from May 2006 until May 2011. During her studies, she was granted by International Centre for Science and High Technology (ICS-UNIDO) within a collaborative framework of activities with the Chulalongkorn University. Her work was also partially supported by Italian Ministry of Foreign Affairs and Graduate school, Chulalongkorn University.

Publications:

Jarinrat Kongkamnerd, Adelaide Milani, Giovanni Cattoli, Calogero Terregino, Ilaria Capua, Luca Beneduce, Andrea Gallotta, Paolo Pengo, Giorgio Fassina, Stanislav Miertus, Wanchai De-Eknamkul. A Screening Assay for Neuraminidase Inhibitors Using Neuraminidases N1 and N3 from a Baculovirus Expression System. Journal of Enzyme Inhibition and Medicinal Chemistry. (Accepted)

Jarinrat Kongkamnerd, Adelaide Milani, Giovanni Cattoli, Calogero Terregino, Ilaria Capua, Luca Beneduce, Andrea Gallotta, Paolo Pengo, Giorgio Fassina, Kaoru Umehara, Wanchai De-Eknamkul, Stanislav Miertus. The quenching effect of flavonoids on 4-methylumbelliferone, a potential pitfall in fluorimetric neuraminidase inhibition assays. Journal of Biomolecular Screening. (Accepted)

Jarinrat Kongkamnerd, Luca Cappelletti, Adolfo Prandi, Pierfausto Seneci, Thanyada Rungrotmongkol, Nutthapon Jongaroonngamsang, Vladimir Frecer, Adelaide Milani, Giovanni Cattoli, Calogero Terregino, Ilaria Capua, Luca Beneduce, Andrea Gallotta, Paolo Pengo, Giorgio Fassina, Stanislav Miertus, Wanchai De-Eknamkul. *In vitro* study of novel neuraminidase inhibitors against avian influenza virus. (In preparation)

Jarinrat Kongkamnerd, Adelaide Milani, Giovanni Cattoli, Calogero Terregino, Ilaria Capua, Luca Beneduce, Andrea Gallotta, Paolo Pengo, Giorgio Fassina, Kaoru Umehara, Orawan Monthakantirat, Wanchai De-Eknamkul, Stanislav Miertus. Neuraminidase inhibitory activity of avian influenza virus H5N1 on flavonoids from Thai medicinal plants. (In preparation)